DEVELOPMENTAL DETERMINANTS OF NEURONAL IDENTITY IN THE DROSOPHILA EMBRYO

by

AUSTIN P. SEROKA

A DISSERTATION

Presented to the Department of Biology
and the University of Oregon Division of Graduate Studies
in partial fulfillment of the requirements
for the degree of
Doctor of Philosophy

March 2022

DISSERTATION APPROVAL PAGE

Student: Austin P. Seroka

Title: Developmental Determinants of Neuronal Identity in the Drosophila Embryo

This dissertation has been accepted and approved in partial fulfillment of the requirements for the Doctor of Philosophy degree in the Department of Biology by:

Adam Miller	Chairperson
Chris Doe	Advisor
Phil Washbourne	Core Member
Kryn Stankunas	Core Member
Adrianne Huxtable	Institutional Representative

and

Krista Chronister	Vice Provost for Graduate Studies

Original approval signatures are on file with the University of Oregon Division of Graduate Studies.

Degree awarded March 2022.

DISSERTATION ABSTRACT

Austin P. Seroka

Doctor of Philosophy

Department of Biology

March 2022

Title: Developmental Determinants of Neuronal Identity in the Drosophila Embryo

The complex function of the nervous system is dependent on precise connections between hundreds of thousands of diverse neurons. During development, a small pool of neural progenitors is tasked with quickly generating this diverse set of molecularly and morphologically distinct neuronal subtypes. These neurons are then required to navigate a complex environment to locate the appropriate synaptic partners, and establish the circuitry required for behavior. For this reason, identifying the mechanisms used by neural progenitors to generate the correct neural subtypes is critical to understanding circuit formation, and behavior itself. During Drosophila development, each neural progenitor cell, or neuroblast (**NB**), generates a characteristic set of diverse neuronal progeny over time. This is accomplished through the process of temporal patterning, in which each NB sequentially expresses a cascade of temporal transcription factors (**tTFs**), giving rise to molecularly distinct neuronal progeny in each expression window. These tTFs are only transiently expressed; little is known about their downstream effectors and how they specify and maintain the unique molecular and morphological properties of each neuronal subtype throughout larval life. Our central hypothesis, is that each tTF induces or represses a combinatorial set of downstream identity transcription factors

(**iTFs**), which in turn drive the expression of mature neuronal genes such as those encoding neurotransmitter machinery, ion channels, cell-surface protein expression and higher-order morphological features. Investigating the downstream targets of tTFs in a distinct embryonic lineage through single-cell sequencing will resolve this gap in understanding.

This dissertation includes previously published, co-authored material.

CURRICULUM VITAE

NAME OF AUTHOR: Austin P. Seroka

GRADUATE AND UNDERGRADUATE SCHOOLS ATTENDED:

University of Oregon, Eugene OR
New College of Florida, Sarasota FL

DEGREES AWARDED:

Doctor of Philosophy, Biology, 2022, University of Oregon
Bachelor of Arts, Chemistry/Biology, 2016, New College of Florida

AREAS OF SPECIAL INTEREST:

Developmental neuroscience

Stem cell biology

PROFESSIONAL EXPERIENCE:

Research Intern, Roskamp Institute, 2015-2016

GRANTS, AWARDS, AND HONORS:

National Institutes of Health (NIH) Developmental Biology Training Program (DBTP) Appointee, University of Oregon, 2017-2019

Co-Chair, DBTP Single-cell RNA Sequencing Symposium, University of Oregon, 2019

PUBLICATIONS:

Austin Q. Seroka, Chris Q. Doe; The Hunchback temporal transcription factor determines motor neuron axon and dendrite targeting in *Drosophila*. *Development* 1 April 2019; 146 (7): dev175570. doi: https://doi.org/10.1242/dev.175570

Seroka, A., Yazejian, R.M., Lai, SL., Doe, CQ; A novel temporal identity window generates alternating $Eve^{+}/Nkx6^{+}$ motor neuron subtypes in a single progenitor lineage. Neural Dev 15, 9 (2020). https://doi.org/10.1186/s13064-020-00146-6

ACKNOWLEDGMENTS

This work would not exist without the guidance and support I have received from mentors throughout my career. I am grateful to Dr. Alfred Beulig and Dr. Amy Clore for sparking my interest in research early in my undergraduate career, and guiding me towards graduate school. I also thank Dr. Laila Abdullah for accepting me into her lab at the Roskamp Institute and giving me crucial exposure to research techniques that I otherwise would not have had the resources to experience.

I am incredibly grateful to my graduate mentor Dr. Chris Doe for pushing me to the best of my abilities to help me succeed, and for his kindness and understanding during personal struggles. The Doe lab has truly felt like a second home. I also want to thank Dr. Sarah Ackerman, Dr. Sen-Lin Lai, Keiko Hirono and Dr. Mubarak Hussain Syed for their kindness, guidance and friendship. You have both taught me so much and provided support when I was struggling, and I am grateful.

I appreciate the support and guidance I have received from my graduate committee: Dr. Adam Miller, Dr. Adrianne Huxtable, Dr. Kryn Stankunas and Dr. Phil Washbourne. You have all inspired me, and helped me to see science from a different perspective.

For my family: Pam Seroka, Pete Seroka, Adam Seroka and Miranda Riley. You have shown me the value of hope and perseverance, and this work would not have been possible without you.

TABLE OF CONTENTS

Chapter Page

LIST OF FIGURES

LIST OF FIGURES

CHAPTER I

GENERATION OF NEURONAL DIVERSITY

Introduction:

During neurogenesis across species, a small pool of neural progenitor cells is tasked with generating diverse populations of neurons required for behavior. One of the ways this is accomplished is through the process of temporal patterning, in which each progenitor (or neuroblast (**NB**)) undergoes a series of asymmetric divisions, sequentially expressing a cascade of key temporal transcription factors (**TTFs**) which diversify the neuronal progeny born during each expression window (Isshiki et al. 2001, Doe, 2017). Recent work in the *Drosophila* ventral nerve cord (**VNC**) and central brain has demonstrated the ability of TTFs to regulate high-order features of neuronal identity in post-mitotic neurons, including molecular identity, morphology, axon and dendrite targeting (Sullivan et al. 2019, Seroka and Doe, 2019; Meng et al. 2019, Seroka et al 2020, Meng et al. 2020, Mark et al. 2021). These results suggest temporal patterning as a powerful mechanism for generating diversity, and that the genetic programs which instruct neurogenesis also create a blueprint for circuit formation and neural function. While this phenomenon has been well characterized in the VNC, temporal patterning is employed in other key brain regions as well, including the central brain and visual processing centers (optic lobes). This chapter will summarize recent advances in the understanding of how temporal patterning generates not just molecular diversity but also complex higher-order neuronal features in the developing embryo and larvae, and how this corresponds to circuit wiring and function.

Neurogenesis in the ventral nerve cord:

The ventral nerve cord (**VNC**), analogous to the mammalian spinal cord, is located in the thorax and forms a feedback network with the central brain in order to receive sensory input and integrate it into locomotor output (Allen et al. 2020). The structure of the adult VNC is established in the embryo, where pioneering neurons born early in neurogenesis set up networks of tracts followed by other neurons later in development (Hartenstein, 2008; Allen et al. 2020). The VNC arises from the delamination of a sheet of neuroectoderm in the early embryo, which is subdivided into regions by the expression of spatially restricted patterning genes (Skeath and Thor, 2003). This spatial patterning process generates a stereotyped array of 30 molecularly-distinct neuronal precursor cells, neuroblasts (**NBs**), per bilateral hemisegment. Each NB then undergoes sequential asymmetric divisions to produce a series of ganglion mother cells (**GMCs**) which terminally divide to generate a pair of neurons or glia. (Hartenstein et al. 1994, Broadus et al. 1995, Bossing et al. 1996, Doe, 2017). As each NB gives rise to progeny, earlier-born neurons are subsequently pushed deeper into the VNC, while later born-neurons are positioned in more superficial layers, leading to birth-ordered spatial lineage architectures. Using this mechanism, each NB contributes a distinct and stereotyped lineage of progeny to the structures of the VNC (Bossing et al. 1996, Schmidt et al. 1997, Schmid et al. 1999, Mark et al. 2021). How does each NB reliably generate its stereotyped lineage of neuronal or glial subtypes at the correct place and time during development? The following section will focus on the identification of temporal patterning as a robust mechanism for the generation of neuronal diversity in individual NB lineages.

Discovery of temporal patterning:

Early studies of neuronal identity in the embryonic VNC identified three transcription factors expressed in mutually-exclusive layers of developing neurons: the zinc-finger transcription factor Hunchback (Hb) is expressed in only the deepest layer neurons, the POU domain TFs Pdm1/Pdm2 are expressed in middle layer neurons, and the zinc-finger TF Castor (Cas) is expressed in the most superficial neurons (Kambadur et al. 1998, Cui and Doe 1992, Pearson and Doe 2004). Observation of dividing NBs demonstrated that the earliest-born neurons from each lineage are displaced towards the deepest layers of the VNC by the generation of newer-born neurons, which are consequently located in more superficial layers of the cortex (Bossing et al. 1996, Schmid et al. 1999, Schmidt et al. 1997, Pearson and Doe 2004). The correlation of Hb, Kr, Pdm and Cas expression with the early to late-born organization of the VNC cortex suggested that these transcription factors might not just be correlated with neuronal birth-order, but also play an important role in specifying identity.

To further understand the role of these temporal transcription factors (TTFs) in specifying neuronal identity, Isshiki et al. (2001) examined the expression of Hb, Pdm and Cas in three distinct NB lineages: NB7-1, NB7-3 and NB2-4. They identified an additional TTF candidate Kruppel (Kr), defining a deep-layer of neurons located in between the Hb^+ and Pdm^+ layers, and demonstrated that each distinct NB goes through an invariant temporal pattern of Hb $\rightarrow$ Kr $\rightarrow$ Pdm $\rightarrow$ Cas expression which is transient in the NB itself, but persists in the neuronal progeny born in each expression window (Isshiki et al. 2001). The function of TTFs was examines in, the well-defined NB7-1 lineage. NB7-1 gives rise to five distinct Eve^+ motor neuron subtypes, the U1-U5 motor

neurons, through five distinct GMCs. Recent work has demonstrated that NB7-1 gives rise to a sole Nkx6^{+} VO motoneuron through a Kr^{+}/Pdm^{+} GMC, although this fate was not detected at the time of earlier studies (Fig. 1.1)

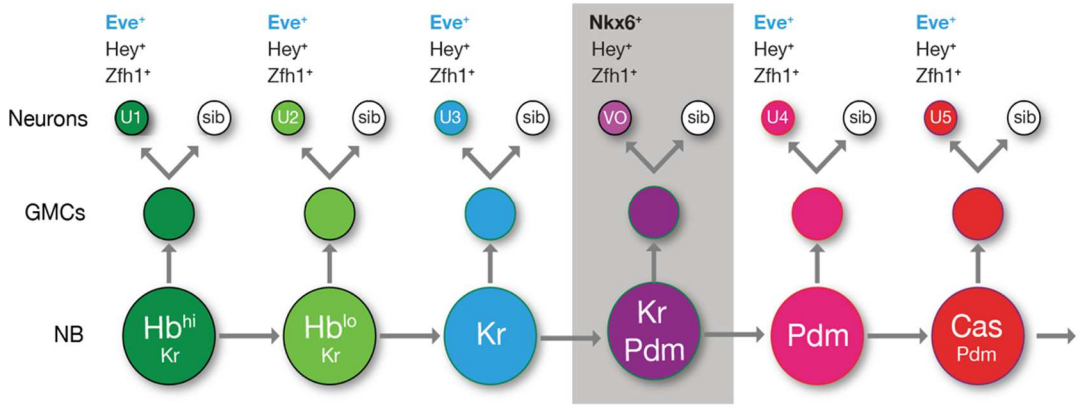

Fig. 1.1 Updated temporal patterning schematic for the NB7-1 lineage
NB7-1 sequentially expresses Hb → Kr → Pdm → Cas over time, giving rise to unique GMCs which undergo terminal divisions to generate neurons. The early-born cohort of NB7-1 is comprised of the Hb^{hi}/Kr^{+} U1 and Hb^{Lo}/Kr^{+} U2 motoneurons, which project to dorsal muscle targets. The later-born cohort is comprised of the Kr^{+} U3, Pdm^{+} U4 and Cas/Pdm^{Lo} U5 motoneurons projecting to more ventral muscle targets. The newly-described VO motorneuron (grey box) is generated from a novel Kr^{+}/Pdm^{+} GMC (Seroka et al. 2020), and had not yet been identified at the time of previous studies. All U motoneurons express the molecular identity marker even-skipped (Eve), with the exception of the VO fate which is Nkx6^{+}/Eve^{-}.

Examination of Hb expression in the NB7-1 lineage showed that the first two progeny of the lineage, the U1 and U2 motoneurons, are Hb^{+} while the later-born U3-U5 motoneurons do not express Hb (Kambadur et al. 1998, Pearson and Doe, 2003). Using a *hb* CNS mutant, Isshiki et al. demonstrated the loss of the first two GMCs in the lineage, and the corresponding U1 and U2 motoneuron progeny derived from these GMCs.

Alternatively, continual misexpression of Hb in NB7-1 induces the generation of up to 19 ectopic U1-U2 motoneuron fates based on known molecular markers. These transformations affect not only molecular identity, but also mature neuronal features such as axon targeting: Hb misexpression in all NBs results in the generation of ectopic motoneurons projecting to early-born dorsal muscle targets. Conversely, expression of the *hb* null allele in all NBs showed an overall decrease in motoneuron number and loss of dorsal muscle targeting (Isshiki et al. 2001, Novotny et al. 2002). These showed that Hb is necessary and sufficient for the generation of early-born cell fates in the NB7-1 lineage. The second TTF in the cascade, Kr, was shown to be necessary and sufficient for second-born neuronal fates across all three lineages. Hb, Kr, Pdm and Cas misexpression assays revealed complex regulatory interactions between the TTFs, in which each activates the next gene in the cascade while repressing the "next plus one" (Isshiki et al. 2001). Overexpression of Hb resulted in the activation of Kr and Pdm repression, while driving Kr resulted in the activation of Pdm and repression of Cas, although Hb expression was not affected (Isshiki et al. 2001). This network of cross-repression establishes a robust mechanism for carefully timing TTF expression. Collectively, these results introduced the model of temporal patterning, in which each VNC NB sequentially expresses a cascade of TTFs in the order Hb → Kr → Pdm → Cas, diversifying the GMCs born in each expression window and subsequently the neuronal progeny born from each GMC.

Neuroblast competence:

The NB7-1 lineage has been thoroughly characterized as a model for temporal patterning (Isshiki et al. 2001, Pearson and Doe 2003, Kohwi et al. 2013, Seroka and Doe 2019, Meng et al. 2019, Seroka et al. 2020) (Fig. 1.1). Previous studies showed that Hb misexpression in the 1-1 and 4-2 lineages was unable to fully transform every cell-type to an early-born fate, with only the first 2-3 GMCs in the lineage being fully converted (Isshiki et al. 2001). This raised the possibility that a "competence window" restricts the ability of the NB to respond to TTF manipulations over time, preventing fate transformations of neuronal progeny after a certain number of asymmetric divisions. This hypothesis was addressed in the NB7-1 lineage, in which the competence window to generate early-born Hb^{+} fates ends after five cell divisions. Constitutive misexpression of Hb in NB7-1 extends the early-born competence window, allowing for the generation of large clones of early-born fates before the NB resumes its normal lineage (Pearson and Doe, 2003). Conversely, Hb misexpression in the post-mitotic NB7-1 neurons showed no effect on cell fate, demonstrating that it is TTF function in the NB that determines fate in neuronal progeny (Pearson and Doe, 2003; Cleary and Doe, 2006). These results demonstrate that within the first five division of the NB Kr, Pdm and Cas misexpression is sufficient to generate ectopic copies of each respective U motorneuron fate, and that the early competence window of NB7-1 is not only specific to Hb, but shared with the other TTFs. Additionally, the competence of NB7-1 to respond to Hb or Kr manipulation is progressively restricted across the first five NB divisions, misexpression of either Hb or Kr generating fewer ectopic U fates if induced towards the middle or end of the competence window (Cleary and Doe, 2006).

Recent work by Kohwi et al. (2013) demonstrates the mechanism by which the early competence window of NB7-1 is progressively restricted. As the NB ages across its sequential divisions, the *hb* genomic locus is physically repositioned to the periphery of the nucleus and is no longer accessible. This repositioning of the *hb* locus has been shown to correlate with downregulation of the Pipsqueak-motif nuclear protein, Distal Antenna Protein (Dan) in the NB (Kohwi et al. 2011). This led to the hypothesis that Dan could be acting through its N-terminal DNA binding domain to bring distal DNA elements together across the nucleus, and consequently reposition the *hb* locus. When Dan was misexpressed in all NBs, movement of *hb* to the nuclear lamina was lost. In parallel, prolonged Hb misexpression did not alter the timing of *hb* repositioning. When Hb and Dan misexpression were performed simultaneously and the ability of the NB to generate ectopic early U1 and U2 fates was assessed, there was a significant increase in the number of ectopic early fates. Taken together, these results demonstrate that NB competence is regulated independently from temporal identity, and restricts the ability of the NB to generate early-cell fates at progressively later timepoints in development. This provides a robust developmental network for not only ensuring the generation of diversity within the nervous system, but also that each neuronal subtype is born in the correct spatial location at the appropriate time.

Temporal identity and connectivity:

Although NB lineage is a key organizational unit for the development of the nervous system, the relationship between the temporal identity of a neuron and its synaptic partner choice / circuit function remains poorly understood. While temporal

patterning is a robust mechanism for generating neurons with tightly regulated molecular fates, recent work has demonstrated the role of temporal identity in establishing circuit function. Using the eve^{+} interneurons of the NB3-3 lineage, Wreden et al. (2017) demonstrate that subsets of neuronal progeny born at different times within the lineage contribute to circuits processing distinct modalities of sensory information. Using connectivity data reconstructed from an EM volume of the larval *Drosophila* CNS, the authors demonstrated that the late-born interneurons of the 3-3 lineage contribute to a proprioceptive processing circuit: each late-born interneuron receives direct upstream inputs from proprioceptors while receiving few to no inputs from other types of sensory neurons. On the other hand, early-born eve^{+} 3-3 interneurons receive direct input from mechanosensitive chordotonal sensory neurons while receiving few inputs from neurons of other sensory modalities. The authors used calcium imaging to record the responses of early and late-born 3-3 interneurons to sound exposure, showing that early-born neurons displayed an induced calcium response while late-born neurons displayed no response (Wreden et al. 2017). These results lead to a model in which each NB produces many diverse neurons which are distributed into different circuits based of temporal identity.

Another recently-identified determinant of neuronal identity is hemilineage: the further diversification of each NB temporal identity window into Notch$^{ON/OFF}$ sub-windows. As each NB undergoes temporal patterning, it sequentially gives rise to distinct GMC which undergo a terminal division to generate a pair of neurons/glia. During this terminal asymmetric GMC division, the Notch inhibitor Numb (Nb) is restricted to one neuron (Notch^{OFF} neuron), while the other sibling neuron receives active notch signaling (Notch^{ON} neurons) (Mark et al. 2021). This process produces two hemilineages within

each NB lineage, however how this feature contributes to connectivity is only recently described. Using a Notch^{ON} reporter in several NB lineages, Mark et al. (2021) determined that the Notch^{ON} hemilineage neurons of each of these NBs project preferentially to the dorsal motor neuropil. Constitutive activation of Notch in the NB1-2, 5-2, 7-1 and 7-4 lineages, resulted in a complete loss of ventral projections and a significant increase in dorsal projections, confirming the role of hemilineage in synaptic partner choice and circuit contribution (Mark et al. 2021). Additionally, previous work demonstrates that Notch^{ON} and Notch^{OFF} hemilineages typically adopt different neurotransmitter fates in addition to contacting distinct synaptic partners (Lacin and Truman, 2016). This differential response between NB related neurons of different hemilineages suggests that each of these sets of neurons responds in a distinctive manner to global pathfinding cues, as respective dorsal/ventral hemilineage projections corresponds to regionalized expression of guidance cues such as Slit and Netrin within the VNC.

Temporal patterning ensures that neurons are born in the correct spatial location and time:

The studies described above elaborate on the mechanisms which tightly-regulate the hierarchical determination of neuronal fate over time. First, each NB is made distinct from one another by spatial patterning. Secondly, each NB lineage undergoes temporal patterning to sequentially generate a set of diverse neuronal progeny. Temporal identity determines the molecular identity and higher-order morphological and connective features of neuronal progeny, specifying them for participation in diverse circuit motifs.

Lastly, neuronal progeny are further subset into Notch $^{ON/OFF}$ hemilineages which allows each NB to contribute two distinct sets of neuronal progeny to the developing nervous system. Together, this robust regulatory network ensures that each neuronal fate is generated at the correct spatial location and the appropriate time during development.

While decades of work have revealed the complexities of temporal patterning, many open questions remain. What is the mechanism by which each TTF encodes a complex morphology and identity in each neuronal progeny? How did temporal patterning emerge evolutionarily? Is hemilineage a generalizable feature of CNS expression across species? Chapters II and II of this dissertation describe our recent efforts to understand how temporal identity shapes the complex morphologies and connective choices of neurons in the developing CNS.

Neurogenesis in the optic lobe:

In addition to the VNC, the Drosophila optic lobe (**OL**) provides a powerful model for understanding the contribution of developmental specification programs to the connective and morphological features of mature post-mitotic neurons. The OL is comprised of four distinct regions: the lamina, medulla, lobula and lobula plate. (Egger et al. 2007, Yasugi et al. 2008, Li et al. 2013). These structures are derived from two primary regions of the OL: the superficially located outer proliferation center (**OPC**) which gives rise to the neurons of the lamina and medulla, and the inner proliferation center (**IPC**) which generates the lobula and lobula plate neurons (Hofbauer and Campos-Ortega, 1990; Apitz and Salecker, 2014). Additionally, a specialized region at the tips of

the OPC (**tOPC**) uses Notch-dependent mechanisms to contribute a subset of neurons to the medulla, lobula and lobula plate (Bertet et al. 2014). Neurogenesis in the OL differs from the VNC. In the central brain and VNC, neurons are produced during two phases of neurogenesis by NBs derived from embryonic neuroectoderm, while OL neurons are derived from the two post-embryonically active NE domains that give rise to the OPC/IPC (Apitz and Salecker, 2014, Neriec and Desplan, 2016). Beginning in the second larval instar, optic lobe neuroepithelial (**NE**) cells sequentially express the proneural gene *l(1)sc* across a mediolateral axis, which locally upregulates other proneural genes such as *Delta* and *ase* and results in a conversion from a NE to NB fate, including a switch to rapid asymmetric division and the production of neurons (Campos-Ortega, 1993, Yasugi et al. 2008, Ngo et al. 2010, Egger et al. 2010). Progression of this proneural wave is regulated by JAK/STAT 11orpholog, in which expression of the ligand Upd shifts laterally across the NE domain, sequentially releasing medial NE cells from negative regulation, and allowing the NE/NB conversion to progress (Egger et al. 2007, Yasugi et al. 2008).

Following the NE/NB conversion, each OPC derived medulla NB generates a set of postmitotic neurons which are arranged by birth-order in a linear and radial orientation along two temporal axes. Each medulla NB gives rise to a column of neuronal progeny in a "beads on a string" arrangement in which the youngest columns of neurons are located close to the OPC neuroepithelium, displacing older neurons to more medial locations adjacent to the central brain. Additionally, within each column the youngest neurons are located next to their NBs at the superficial surface of the medulla cortex, while the oldest neurons are pushed deeper towards the neuropil (Hasegawa et al. 2011, Morante et al.

2011, Apitz and Salecker, 2014). This spatial orientation results in the arrangement of neuron subtypes expressing TF combinations corresponding with birth-order in concentric rings within the medulla cortex, and allows for the simultaneous observation of NBs at different temporal stages in their lineage progression (Hasegawa et al. 2011). Investigation of the developmental determinants producing this arrangement revealed six key temporal transcription factors (TTFs) that are sequentially expressed in medulla NBs as they age, in the order: Homothorax (Hth) → Klumpfuss (Klu) → Eyeless (Ey) → Sloppy paired 1 and 2 (Slp) → Dichaete (D) → Tailless (Tll), and control the downstream expression of the concentric subtype TFs that had been previously observed (Li et al. 2013, Suzuki et al. 2013). Similar to the temporal patterning cascade in the VNC, these TTF exhibit cross-regulatory interactions to specify neuronal fate (Doe, 2017). In an *Ey* mutant background the *Slp* window is lost but Hth expression is not affected in the earliest-born neurons, demonstrating that Ey is required to activate the next TTF Slp, but not to repress earlier TFs (Li et al 2013). Other TTFs in the cascade have different cross-repressive roles: *Ey*, *Slp* and *D* are required to activate the next TTF in the cascade, while slp and D are uniquely required to turn off the preceding TTF (Li et al. 2013). As seen in the VNC, the OL also uses a notch-ON/noth-OFF mechanism to further diversify each lineage into hemilineages with unique features: for example, about half of the neurons born during the Ey window maintain Ey expression, while the other half are Ey-/Apterous^{+} (**Ap**). In animals mutant for Su(H), the transcriptional effector on N 12orpholog, all of the neuronal progeny of the Ey window are converted to an Ey^{+} identity, with complete loss of Ap expression. Overall, the combined action of the TTF cascade, and Notch-dependent hemilineage generate remarkable diversity in the OL in

parallel to the function of these mechanisms in the VNC (Li et al. 2013, Suzuki et al. 2013, Mark et al. 2021). In the next section, I will explore the evidence that these neurogenic mechanisms not only generate diversity, but also specify higher-order neuronal features and contribute to circuit formation.

Specification of morphology and targeting by temporal patterning:

Evidence from these landmark studies also supports a role for the OL TTF cascade in specifying higher-order features of neuronal identity, such as morphology and connectivity. Prior to the identification of the TTf cascade in the OL, TTFs such as Hth had previously been described to regulate complex features of identity through the regulation of intermediate identity TFs. The iTF *Bsh,* both necessary and sufficient to specify the Mi1 celltype, is expressed in the N-ON hemilineage of GMCs derived from the Hth^+ temporal identity window. Ectopic expression of Hth in later-born NBs is sufficient to generate ectopic Bsh^+ neurons (although there is a competence in which the NB window responds to this manipulation). In a *hth/Su(H)* background Bsh^+ progeny are lost, demonstrating the requirement for both Hth and Notch in the specification of the Bsh^+ Mi1 fate (Hasegawa et al. 2011, Li et al. 2013). Bsh is required for the morphology and synaptic targeting of the Mi1 fate: in MARCM clones generated using bsh-Gal4, the majority of neurons are converted from Mi1 local interneurons arborizing at the M1, M5 and M9-10 layers of the medulla to Tm-type projection neurons which arborize in both the medulla and lamina (Hasegawa et al. 2013). Conversely, when drf-Gal4 is used to overexpress Bsh ectopic medulla intrinsic neurons appear that have correct arborizations in the M1, M5 and M9-10 layers, however these arborizations did not look wildtype.

Dual overexpression of Bsh and Hth is required to generate Mi1 neurons with wildtype arborization, not accomplishable by Hth overexpression alone although transformations from local interneurons to projections neurons have been described in hth mutant clones. Additionally, both Hth and Bsh contribute to the regulation of Ncad expression in Mi1 neurons, which plays an important regulatory role in the correct formation of Mi1 arborizations (Hasegawa et al. 2011, Morante and Desplan, 2008, Hasegawa et al. 2013). Together, these data paint a picture of a regulatory hierarchy in which the Hth TTF window gives rise to Bsh^{+} Mi1 neuron fates, the morphology and targeting of which is specified by Bsh (although the coordinate function of Hth and Bsh is required to specify the correct levels of Ncad).

Another example within the medulla, the specification of T1 neuron morphology is accomplished through combinatorial TF action downstream of temporal patterning in the NB (Naidu et al. 2020). T1 neurons are unicolumnar and connect the lamina and medulla, with cell bodies located in the medulla and characteristic "T" shaped axon branches. These neurons are distinguishable from all others in the medulla by a combinatorial code of three TFs expressed in mature T1 neurons and not in their NBs: Ocelliless (oc), Sox102F and Ets65A (Naidu et al. 2020). CRISPR-mediated knockdown of each of these iTFs in T1 neurons impacts different aspects of connectivity and morphogenesis. In an oc-CRISPR background T1 neurons have disorganized arborizations in the medulla while their axon projections still target the lamina as seen in wildtype, and loss of oc does not affect Sox102F expression. Loss of Sox102F causes overexpansion of T1 medulla arborizations, and eliminates wildtype axon projections to the lamina without affecting oc expression. Lastly, loss of Ets65A does not affect the

shape of medulla arborizations, but accuses these projections to overextend to the M6 layer without affecting either Sox201F or Oc expression. These results suggest a mechanism similar to the combinatorial codes identified in *C.elegans*, in which distinct TFs act in a combinatorial fashion to specify different aspects of morphology and targeting (Hobert, 2016, Naidu et al. 2020). How does expression of these TFs in T1 neurons relate to the temporal patterning axis? Utilizing Gal4 lines that label neurons generated in different medulla TTF windows reveals that the generation of Sox102F or Oc neurons begins in the Slp window, while neurons expressing Ets65A are largely generated in the D window. This suggests that the overlap of D and Slp during the transition between TTF windows specifies the generation of the T1 fate. In D mutant clones, Ets65A expression is lost without affecting Sox102F or Oc expression. Expression of Sox102F, however, is lost in slp mutant clones. Oc expression in neurons is lost in ey RNAi condition, demonstrating that ey is required for neuronal expression of OC in late-born progeny of the Ey window. Overall, each of the three TFs that coordinately determine T1 neuron identity initiate their expression in different TTF windows, span multiple TTF windows and are combinatorially active in the latest-born neurons of the D window, in which they specify the T1 identity (Naidu et al. 2020). Taken together, these results support a model in which temporal patterning in NBs sequentially activates the expression of three key iTFs in neuronal progeny, of which the latest born express all three in a combinatorial code. In this code each iTF regulates different key aspects of neuronal morphology and targeting.

The role of temporal patterning in the specification of circuit connectivity in the Ol is not limited to the medulla. Another key example of hierarchical temporal regulation

of morphological and connective features is found in the role of Dac and Ato in specifying T4/T5 lobula neuron fates derived from the IPC. Ato is a proneural gene that is expressed in a subset of IPC progenitors in the late larvae, and is downregulated prior to progenitor division. Generation of single-cell clones using IPC-gal4 revealed that Ato^{+} NB give rise to two distinct subtypes of direction selective neurons: the T4 and T5 neurons whose dendrites arborize within medulla layer 10 and Lo1 respectively, and axons projecting to one of four lobula plate layers (Apitz and Salecker, 2018, Hofbauer and Campos-Ortega, 1990). IPC NBs utilize a TTF cascade distinct from the VNC or OPC: D and Tll expression define the early and late stages of d-IPC neurogenesis. The combined effect of the D/Ase window gives rise C/T neurons, followed by D activating the expression of Tll (which simultaneously represses D, controlling the switch to the Tll window) which subsequently upregulates Ato and Dac in the NB to specify T4/T5 progeny. (Apitz and Salecker, 2015, Mora et al, 2018). The function of Dac in the specification of T4/T5 fates was tested using a Dac MARCM approach, demonstrating that in the absence of Dac T4/T5 neurons are converted to a T2/T3 morphology, with altered dendritic localization to medulla layer M9, and axons in Lo2 and Lo3. Simultaneous knockdown of Dac and Ato resulted in complete absence of T4/T5 fates (Apitz and Salecker, 2018). Examination of Ato mutants in the IPC reveals that Ato is not required for neurogenesis, as Ato^{+} NBs still give rise to neurons, however *Ato* mutant neurons demonstrate severe morphological and connective defects (Oliva et al. 2014). These results suggest that Ato and Dac are expressed in the Tll window of d-IPC NBs, where they act as identity TFs to specify higher-order features of the T4/T5 lobula neurons. In order to understand how Ato regulates these complex neuronal features,

CHIP experiments using Ato-GFP reveal that Ato binds to regulatory elements of the cell-fate determinant Brat, a result supported by Ato manipulations: In Ato overexpression condition in lower IPC NBs Brat is upregulated, while ato-null clones show a large reduction in Brat expression (Mora et al. 2018). Interestingly, when dual ato and Brat Rnai was performed, ectopic Dpn expression was detected in T4/T5 neurons, suggesting a pathway in which Ato regulates Brat in order to maintain a differentiated neural state in T4/T5 neurons.

How does Dac/Ato function downstream of the Tll window in d-IPC NBs to specify the complex properties of the T4/T5 direction selective neurons? In order to identify identity TFs that instruct these mature morphological properties, Schilling et al. performed a RNAi screen against known TFs expressed in T4/T5 neurons, using the optomotor response as an output for the screen. RNAi against either SoxN or Sox102F resulted in a severely disrupted optomotor response, implicating these factors in the function of the T4/T5 neurons although their expression was only detected in T4/T5 neurons themselves and not in their progenitor populations. When T4/T5 neurons were visualized during developing in a SoxN-RNAi background the T4/T5 dendrites overextended into ectopic medulla layers and showed greatly disrupted axon targeting demonstrating a regulatory role for these genes in specifying targeting and connectivity (Schilling et al. 2019). In order to determine whether these genes play a ubiquitous or cell-type specific role in the development of T4/T5 neurons, SoxN and Sox102F were knocked down in specific subsets of T4/T5s: T4a-d, T4/T5ab and T5cd, showing autonomous defects in each subtype. These guidance defects are shown to be dependent on the regulation of the adhesion molecule, Connectin, by the Sox family TFS in two

distinct mechanisms: Firstly, SoxN is required for Sox102F expression which suppresses Connectin expression. Secondly, SoxN is required for Connectin expression in a Sox102F independent manner (Schilling et al. 2019). Lastly, the combined action of Ato and Dac in late IPC progenitors ensures the downstream expression of SoxN/Sox102F and in turn correct target selection by Connectin expression level. Taken together, the results of these studies suggest hierarchical regulation of terminal neuronal features by temporal patterning events in their respective progenitors. In the case of T4/T5 neurons, dIPC NBs enter a late temporal window triggered by Tll-mediated silencing of the D window, and activation of Dac and Ato in the NB. The coordinate action of Dac and Ato activates the downstream TF effectors SoxN and Sox102F, which in turn regulate levels of the cell-surface protein Connectin, and ensure proper axon and dendrite connectivity in each T4/T5 subtype. Although this is one example of a linear pathway, it is likely that the TTFs at the top of the regulatory hierarchy regulate suites of intermediate identity TFs that coordinately regulate the expression of combinatorial codes of CSMs/cytoskeletal machinery/neurotransmitter machinery to ensure proper connectivity as has been suggested by mechanistic studies in *C. elegans* (Hobert 2011, Hobert, 2016). Interestingly, previous work identified a role of another Sox family TF, SoxD, in the neurite targeting of T4/T5 neurons (Contreras et al. 2018), suggesting that multiple Sox family proteins might coordinate in a molecular code to ensure proper wiring.

Transcriptomics provide insight into mechanisms of temporal patterning:

In order to further understand the hierarchical regulation of complex morphological features of visual system neurons, a comprehensive understanding of how

TTFs regulate downstream suites of TFs and effector genes is required. The advent of single-cell sequencing has allowed for an unprecedented ability to profile gene expression in developing celltypes. Application of this approach to understand how the 8 T4/T5 neuron subtypes are transcriptionally established over time supports a model in which key identity TFs specify a combinatorial code of downstream effectors in each celltype. Single-cell sequencing of T4/T5 neurons reveals that separate transcriptional programs correspond to specific features of the wiring process. Common T4/T5 features are established by a combination of TF expressed in all 8 subtypes (Lim1, Drgx, acj6), manipulation of these factors results in gross defects to all T4/T5 dendrite and axon morphologies (Kurmangaliyev et al. 2019). This overall genetic program is diversified by feature-specific transcriptional programs, with separate pathways regulating axon and dendrite specification: Expression of *Bi* sets up LoP targeting domains, while *grn* levels specify different LoP layers. Perturbations of each TF only affect these respective processes and not gross morphology. In a parallel mechanism, dendritic targeting is determined by binary expression of *TfAP-2*. Each of these programs is characterized by a specific code of TFs as well as cell-surface proteins, including Ig superfamily proteins (Kurmangaliyev et al. 2019). These modular programs support a model in which TTFs sit at the top of the hierarchy, activating separate combinatorial codes of iTFs in their progeny to regulate separate aspects of morphology and connectivity. Although these features are specified at the level of TTf window and lineage, single-cell sequencing has also revealed the ability of NotchON/OFF decisions to set up higher-order neuronal decisions through hemilineage-specific transcriptional programs. Sequencing of OPC derived optic lobe lineages reveals that *ap* is expressed in NotchON neurons (*Lim3* and *tj*

in Notch OFF neurons) in four of the five OPC TTF windows (Konstantinides et al. 2018), demonstrating combinatorial codes for hemilineage identity. Additionally, transient expression of TTFs in NB is encoded by downstream effectors TFs whose expression persists into the post-mitotic stage (Konstantinides et al. 2018). When transcriptional changes is Ol neurons were tracked across development into the pupea, differences between closely related celltypes were found to be much less distinguishable at earlier developmental stages and to increase in complexity with maturity: for example at earlier stages Tm1,Tm2 and Tm4 neurons were not distinguishable and clustered together Interestingly, single-cell approaches are able to resolve heterogeneity within 20orphologically identical subsets of neurons such as Dm8, which comprised two transcriptionally-distinct subtypes with different synaptic specificities despite a common morphology (Kurmangaliyev et al. 2019). Closely related cell-types are seen to express similar combinations of intermediate TFs, however it is more difficult to interpret the combinatorial codes of cell-adhesion molecules (**CAMs**) used by neurons for circuit wiring. Many CAMs were seen to be expressed transiently during development, showing differences in expression in the same celltype at different developmental timepoints: for example, Tm1 neurons were found to express dpr17 at similar levels to C3 cells, but with a different temporal pattern, while Tm2 and Mi4 neurons expressed dpr17 at lower levels, but with a similar temporal pattern (Kurmangaliyev et al. 2019). In depth single-cell analysis of temporal patterning in OL neurons reveals TTFs play important roles in the specification of identity, independent of neuron maturation, where neuronal differentiation is specified by a different genetic network, while the action of TTF in regulating downstream TFs (such as Bsh, Dfr, Toy, Traffic-jam, Otd) generates identity

(Konstantinides et al. 2021). Recent scRNAseq approaches demonstrate the power of the technique to further uncover the nuances of how temporal patterning generates staggering neuronal diversity during development. Konstantinides et al. performed single-cell sequencing of OL neurons to determine the TTF cascade in these lineages with higher resolution. Single-cell analysis confirms that TTFs are expressed in overlapping windows to create combinatorial codes which specify neuronal fate, uncovering 12 putative TTF windows that when combined with five spatial patterning domains and further Notch-dependent hemilineage diversification sufficiently explain the generation of the roughly 120 cell types in the medulla. Interestingly, they also find that not all TTFs use the same mechanism to contribute to the cascade: some TTFs directly control the activation of the next step in the cascade by activating the next TF and repressing the previous one, while others play more complex roles as "integrators" of temporal information by consolidating activating and inhibitory signals from several other TTFs. While scRNAseq approaches offer large advantages in depth of information, these data paint a picture of the dynamic nature of gene expression in mature neurons. For example, the eight subtypes of T4/T5 neurons are easily distinguishable at the P50 pupal stage, however they are not distinguishable in the adult, as many of the subtype specific markers are turned on in these post-mitotic stages in the adult (Ozel et al. 2020). These insights will help to shape the way scRNAseq data is analyzed and interpreted, and challenge the concept that each neuron has a "hardwired" identity that persists throughout the entire post-mitotic life of thes neuron. Instead, the data paints a picture of an explosive period of fate determination during early development, in which TTFs specify neuronal subtypes through the hierarchical regulation of intermediate levels of TFs controlling different cellular

processes. Following this period of growth and circuit assembly, the transcriptome of mature neurons is more highly correlated with activity and circuit function than developmental origin.

Bridge:

In this chapter, I describe the role of temporal patterning in generating diversity in the developing *Drosophila* nervous system. I describe the initial findings from the VNC that demonstrated how each NB changes gene expression over time to sequentially generate distinct neuronal progeny. I consider how TTF expression in neurons relates to higher-order neuronal features, such as hemilineage determination of sensory circuit involvement in the VNC. I also describe in detail how temporal patterning functions in the *Drosophila* visual system in a parallel mechanism to that seen in the VNC, where data supports the role of TTFs in the determination of neuronal identity and connective preferences.

In the next chapter, we test the role of the TTF Hb in specifying morphology and targeting in the well-characterized NB7-1 lineage. We ask whether it is (1) the time a neuron is born and enters the environment (birth-time) that determines its morphology and synaptic partner choice, or (2) it is intrinsic TTF function inherited from the progenitor which acts to pre-determine these mature neuronal features.

CHAPTER II

THE HUNCHBACK TEMPORAL TRANSCRIPTION FACTOR DETERMINES MOTOR NEURON AXON AND DENDRITE TARGETING IN DROSOPHILA

Introduction :

Axon and dendrite targeting is an essential step in neural circuit formation, and may even be sufficient for proper connectivity in some cases, as postulated in Peters' rule (Peters and Feldman, 1976; Rees et al., 2017; Stepanyants and Chklovskii, 2005). In both *Drosophila* and mammals, individual progenitors generate a series of neurons that differ in axon and dendrite targeting (Doe, 2017; Kohwi and Doe, 2013; Li et al., 2013a; Pearson and Doe, 2004; Rossi et al., 2016). In these examples, neurons born at different times have intrinsic molecular differences due to temporal transcription factors (TTFs) present at their time of birth (reviewed by Kohwi and Doe, 2013), which could specify neuronal morphology. Conversely, there are likely to be changing extrinsic cues present at the time of neuronal differentiation that could also influence neuronal morphology, such as modulation of global pathfinding cues or addition of axon and dendrite processes throughout neurogenesis. Teasing out the relative contributions of intrinsic or extrinsic factors requires heterochronic experiments where either intrinsic or

extrinsic cues are altered to create a mismatch, and the effects on axon and dendrite targeting are assessed.

Several experiments highlight the importance of extrinsic cues present at the time of neuronal differentiation in establishing axon or dendrite targeting. For example, transplantation of rat fetal occipital cortical tissue into the rostral cortex of a more developmentally mature newborn host results in axonal projections characteristic of the host site (O'Leary and Stanfield, 1989; Schlaggar and O'Leary, 1991; Stanfield and O'Leary, 1985). Similarly, transplantation of embryonic day 15 fetal occipital tissue into newborn occipital cortex reveals that the transplanted tissue receives thalamic projections typical of the host site and developmental stage (Chang et al., 1986). More recent work in zebrafish shows that vagus motor neurons extend axons sequentially to form a topographic map, and that the time of axon outgrowth directs axon target selection (Barsh et al., 2017). Similarly, recent work in *Drosophila* has shown that sequential axon outgrowth of R7/R8 photoreceptor neurons, coupled with a temporal gradient in the levels of the transcription factor Sequoia, is essential for axon spacing during retinotopic map formation within the medulla neuropil (Kulkarni et al., 2016). In all of these systems, the relative importance of neuron intrinsic factors and changing environmental cues remain unknown.

In contrast, heterochronic experiments where donor neurons maintain donor identity are more consistent with intrinsic temporal identity specifying neuronal axon and dendrite targeting. For example, heterochronic experiments in ferrets show that late cortical progenitors transplanted into younger hosts generate neurons with late-born deep layer position and subcortical axonal projections (McConnell, 1988). Transplantation of

older post-natal cerebellum into embryonic host mice results in the neurons maintaining donor 'late-born' identity based on molecular markers and neuronal morphology (Jankovski et al., 1996). Similarly, experiments carried out in grasshopper embryos show that delaying the birth of the first-born aCC motor neuron in the NB1-1 lineage leads to defects in the initial axon trajectory (extending anterior instead of posterior) but the temporally delayed aCC invariably finds and exits through the proper nerve root in the adjacent anterior segment (Doe et al., 1986). In all of these heterochronic experiments, it is likely that intrinsic temporal identity is unaltered and helps maintain donor neuron identity despite their altered time of differentiation. However, none of these experiments shows that intrinsic temporal identity is unchanged in the transplanted neurons, and none of these experiments manipulates intrinsic temporal identity to directly assess its role in establishing proper axon or dendrite targeting.

We sought to test the relative contribution of neuronal time of differentiation versus neuronal intrinsic temporal identity in establishing motor neuron axon and dendrite targeting. Our model system is the NB7-1 lineage in the *Drosophila* ventral nerve cord (VNC), a segmentally repeated structure analogous to the mammalian spinal cord. The VNC offers several benefits for the study of neurogenesis due to its individually identifiable neuroblasts (NBs), which produce a stereotyped sequence of distinct neuronal cell types whose identities are determined by a well-characterized temporal transcription factor (TTF) cascade (reviewed by Doe, 2017; Kao and Lee, 2010; Kohwi and Doe, 2013; Rossi et al., 2016; Skeath and Thor, 2003) (Fig. 1; Fig. S1). For example, NB7-1 sequentially expresses the four TTFs: Hunchback (Hb), Kruppel, Pdm and Castor. During each NB TTF expression window, a different motor neuron is

born: U1 and U2 during the Hb window; U3, U4 and U5 during the later three TTF windows (Isshiki et al., 2001; Kanai et al., 2005; Kohwi et al., 2013; Pearson and Doe, 2003). Importantly, the two Hb^+ U1-U2 motor neurons have a morphology, neuropil targeting and connectivity that is clearly different from the later-born U3-U5 motor neurons (Fig. 1; Fig. S1). The ability to individually identify the U1-U5 neurons, and to cleanly change their intrinsic temporal identity in an otherwise normal CNS, make the NB7-1 lineage an ideal system to study the relative contribution of time of differentiation and intrinsic temporal identity in establishing neuron morphology, targeting and connectivity.

Fig. 2.1 Models: intrinsic temporal identity or time of differentiation determines U1-U5 motor neuron morphology (Next page). (A) NB7-1 (top) sequentially expresses the temporal transcription factors Hb, Kr, Pdm and Cas. The U1-U2 neurons (bottom) born during the Hb window have an 'early-born' identity (green) characterized by contralateral dendrites, an axon projection to dorsal body wall muscles DO1 and DO2, and little or no nuclear Zfh2. The U3-U5 neurons born after the Hb window have a 'late-born' identity (red) characterized by ipsilateral dendrites, an axon projection to more ventral muscles DA3/LL1 and high nuclear Zfh2. All U1-U5 neurons have nuclear Eve. (B) Models for specification of U1-U5 axon and dendrite targeting. (i) Intrinsic temporal identity could determine axon and dendrite targeting. (ii) Neuronal time of differentiation could determine axon and dendrite targeting. (iii) Misexpression of Hb can generate late-differentiating neurons with an early intrinsic temporal identity; this mismatch reveals which mechanism is more important for axon and dendrite targeting.

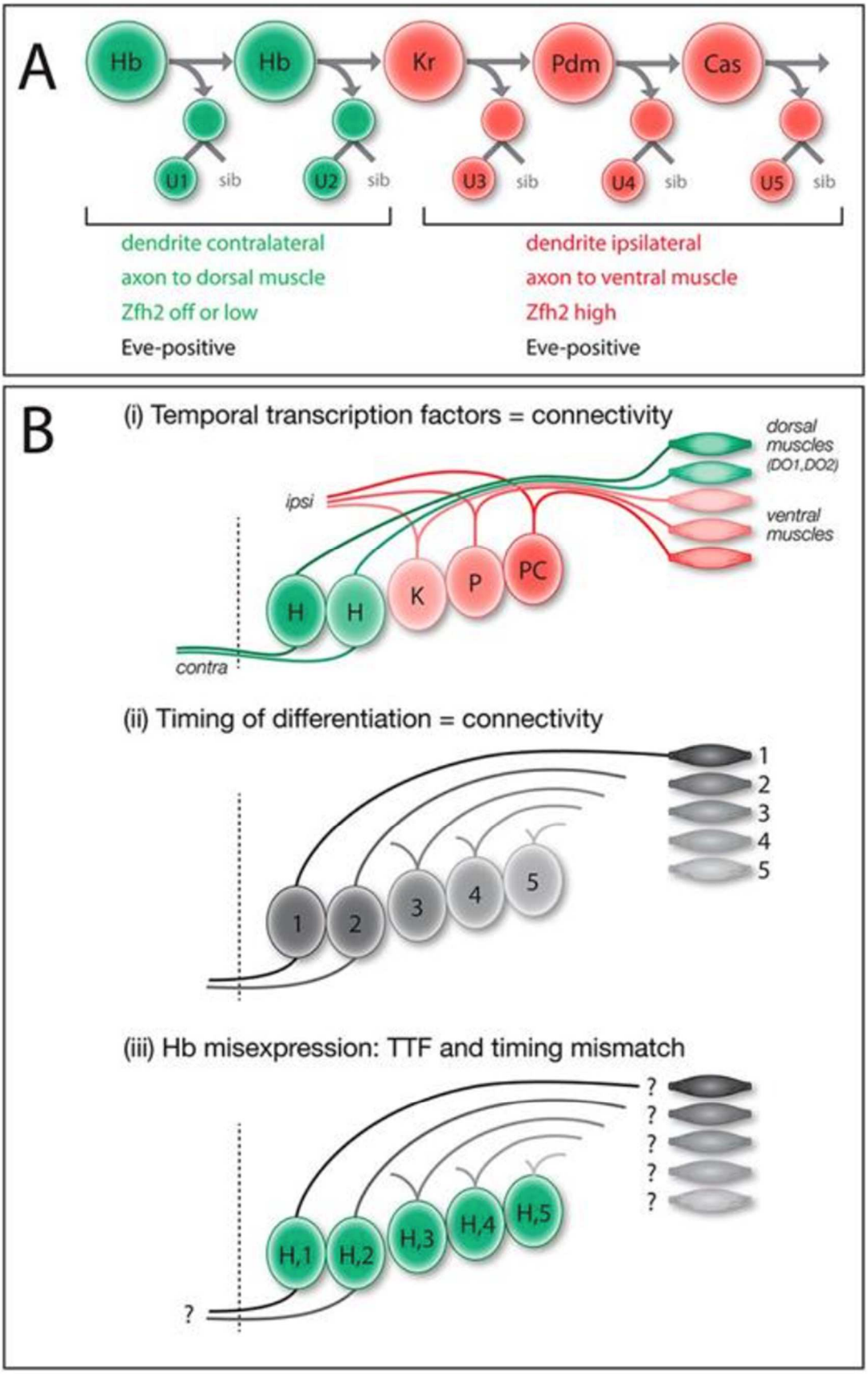
A
Hb
Hb
Kr
Pdm
Cas
U1
sib
U2
sib
U3
sib
U4
sib
U5
sib
dendrite contralateral
axon to dorsal muscle
Zfh2 off or low
Eve-positive
dendrite ipsilateral
axon to ventral muscle
Zfh2 high
Eve-positive
B
(i) Temporal transcription factors = connectivity
dorsal muscles (DO1,DO2)
ventral muscles
ipsi
contra
H
H
K
P
PC
(ii) Timing of differentiation = connectivity
1
2
3
4
5
(iii) Hb misexpression: TTF and timing mismatch
H,1
H,2
H,3
H,4
H,5
?

Previously, we have shown that misexpression of Hb throughout the NB7-1 lineage results in an extended series of 'ectopic U1' motor neurons based on molecular markers and axon projections to dorsal body wall muscles (Isshiki et al., 2001; Pearson and Doe, 2003); however, the ectopic U1 motor neurons were not assayed for their specific muscle targets, nor was dendrite morphology and targeting assessed, nor was it known whether U1-U5 motor neurons extended axons or dendrites synchronously or sequentially. Here, we focus on the difference between early-born Hb^+ U1-U2 neurons and later-born U3-U5 neurons. U1-U2 are bipolar, have contralateral dendrites and innervate dorsal body wall muscles; in contrast, U3-U5 neurons are monopolar, have ipsilateral dendrites and innervate more ventral body wall muscles. Although there are molecular differences between U1-U2 and between U3-U5 (Isshiki et al., 2001), in this article we focus on the major morphological differences between these two groups of neurons. We show for the first time that the U1-U5 neurons extend axons sequentially, and subsequently extend dendrites sequentially. We test whether U1-U5 motor neurons project to their normal CNS and muscle targets due to their intrinsic temporal identity (Fig. 1Bi) or due to their time of differentiation (Fig. 1Bii) – two mechanisms that are normally tightly correlated. To break this correlation, we misexpress the early TTF Hb specifically in the NB7-1 lineage to create 'ectopic U1' motor neurons with an early intrinsic temporal identity but late time of differentiation (Fig. 1Biii). Moreover, we show that the heterochronic placement of an 'ectopic U1' into the later developmental environment does not affect the ability of the 'ectopic U1' to project dendrites to the proper neuropil domain or axons to the proper body wall muscle. Our results show that

intrinsic temporal identity is an important determinant of neuronal morphology, and axon and dendrite targeting.

Results:

U1-U5 motor neurons extend axons and dendrites sequentially

To determine whether U1-U5 motor neuron axon target selection is correlated with intrinsic temporal identity or time of differentiation, we first needed to investigate the timing of U1-U5 motor neuron axon outgrowth. If the U1-U5 motor neurons have synchronous axon outgrowth, despite being born sequentially, we can rule out time of axon outgrowth as a mechanism for specifying their differential axon target selection. Conversely, if the U1-U5 motor neurons extend their axons sequentially, then both models remain possible.

To determine the time of U1-U5 axon outgrowth, we used MultiColorFlpOut (MCFO) (Nern et al., 2015) which produces randomized multi-color labeling of neurons within the expression domain of any Gal4 line. We restricted labeling to the NB7-1 lineage using a new split-gal4 killer zipper line (NB7-1-Gal4^{KZ}). This new line is based on our published NB7-1-Gal4 line (*ac-VP16 gsb-DBD*) (Kohwi and Doe, 2013) but also includes an R25A05-KillerZipper construct to block expression in NB6-1, which was commonly observed in the previously described NB7-1 split Gal4 line (Kohwi and Doe, 2013; see Materials and Methods for quantification). This new NB7-1-Gal4^{KZ} line was used for all MCFO or Hb misexpression experiments. Within the NB7-1 lineage, early-born neurons are located close to the midline and later-born neurons are located more

laterally (Pearson and Doe, 2003) (Fig. S1A). As expected, MCFO labeling of the entire wild-type NB7-1 lineage shows neurons spread from medial to lateral within the CNS, with ipsilateral motor projections and contralateral dendrite projections (Fig. 2A); we call these dendrites because they have a large number of post-synaptic densities but no pre-synaptic sites when analyzed by electron microscopy (Fig. S2). We analyzed embryos where MCFO differentially labeled early-born and late-born neurons in the NB7-1 lineage at embryonic stages 12-15 (staging according to Hartenstein, 1993). In all cases, the medial early-born neurons invariably extended axons further than the lateral later-born neurons (Fig. 2A,B; n=10, P<0.0001, two-tailed unpaired t-test). This observation remained consistent at all tested embryonic stages and independent of the position at which the lineage was subdivided along the medial-lateral axis. In all cases, the U neurons showed axon projections that are staggered until they reach their muscle targets; they never stall and become synchronized prior to innervating their target muscle. Furthermore, in every case where MCFO differentially labeled only a pair of neurons, we always found the medial (early-born) neuron had a longer axon projection than the lateral (later-born) neuron (Fig. 2E,F, n=8, P<0.0001, two-tailed paired t-test). We conclude that during wild-type embryonic development, the U1-U5 motor neurons project axons sequentially out the nerve root.

Fig. 2.2 The U1-U5 motor neurons extend axons and dendrites sequentially (Next page).

(A-H) Axon outgrowth timing in early- and late-born neurons of the NB7-1 lineage in stage 13-15 embryos. (A-B) Wild-type multicellular MCFO labeling (*NB7-1-Gal4^{KZ} UAS-MCFO*). Analysis was restricted to lineages in which early-born medially located neurons were stochastically labeled in one MCFO color, and in which the later-born laterally located neurons were stochastically labeled in a different MCFO color. (A) All labeled cells. (A′-A‴) Early-born medial neurons (green) project out of the CNS ahead of later-born lateral neurons (magenta). (B) Quantification of axon length as a representation of timing of axon outgrowth; early-born neurons project further (earlier) than late-born neurons (***P<0.001). (C-D) Hb misexpression (*NB7-1-Gal4^{KZ} UAS-hb UAS-MCFO*) multicellular MCFO labeling. (C) All labeled cells. (C′-C‴) Early-born medial neurons (green) project out of the CNS ahead of later-born lateral neurons (magenta). (D) Quantification of axon length as a representation of timing of axon outgrowth; early-born neurons project further (earlier) than late-born neurons (***P<0.001). (E-F) Wild-type single-neuron MCFO labeling (*NB7-1-Gal4^{KZ} UAS-MCFO)*. I A single early-born medial neuron (green) always projects out of the CNS ahead of a single later-born lateral neuron (magenta). (F) Quantification of axon length as a representation of timing of axon outgrowth; early-born neurons project further (earlier) than late-born neurons (***P<0.001). (G-H) Hb misexpression (*NB7-1-Gal4^{KZ} UAS-hb UAS-MCFO*) single-neuron MCFO. (G-G″) A single early-born medial neuron (green)

always projects out of the CNS ahead of a single later-born lateral neuron (magenta). Quantification of axon length as a representation of timing of axon outgrowth; early-born neurons project further (earlier) than late-born neurons (***P<0.001). (I-L) Dendrite outgrowth timing in early- and late-born neurons of the NB7-1 lineage in stage 13-15 embryos. (I-I″) Wild-type single-neuron MCFO labeling (*NB7-1-Gal4^{KZ} UAS-MCFO*). A single early-born medial neuron (green) extends a dendrite before a single later-born lateral neuron (magenta). (J) Quantification of axon length as a representation of the timing of axon outgrowth; early-born neurons project further (earlier) than late-born neurons (***P<0.001). (K-K″) Hb misexpression (*NB7-1-Gal4^{KZ} UAS-hb UAS-MCFO*) single neuron MCFO labeling. A single early-born medial neuron (green) extends a dendrite before a single later-born lateral neuron (magenta). (L) Quantification of axon length as a representation of timing of axon outgrowth; early-born neurons project further (earlier) than late-born neurons (P<0.001). Arrowheads indicate the early-born axon (green) and late-born axon (magenta); dashed line indicates the midline. Scale bars: 5 μm.

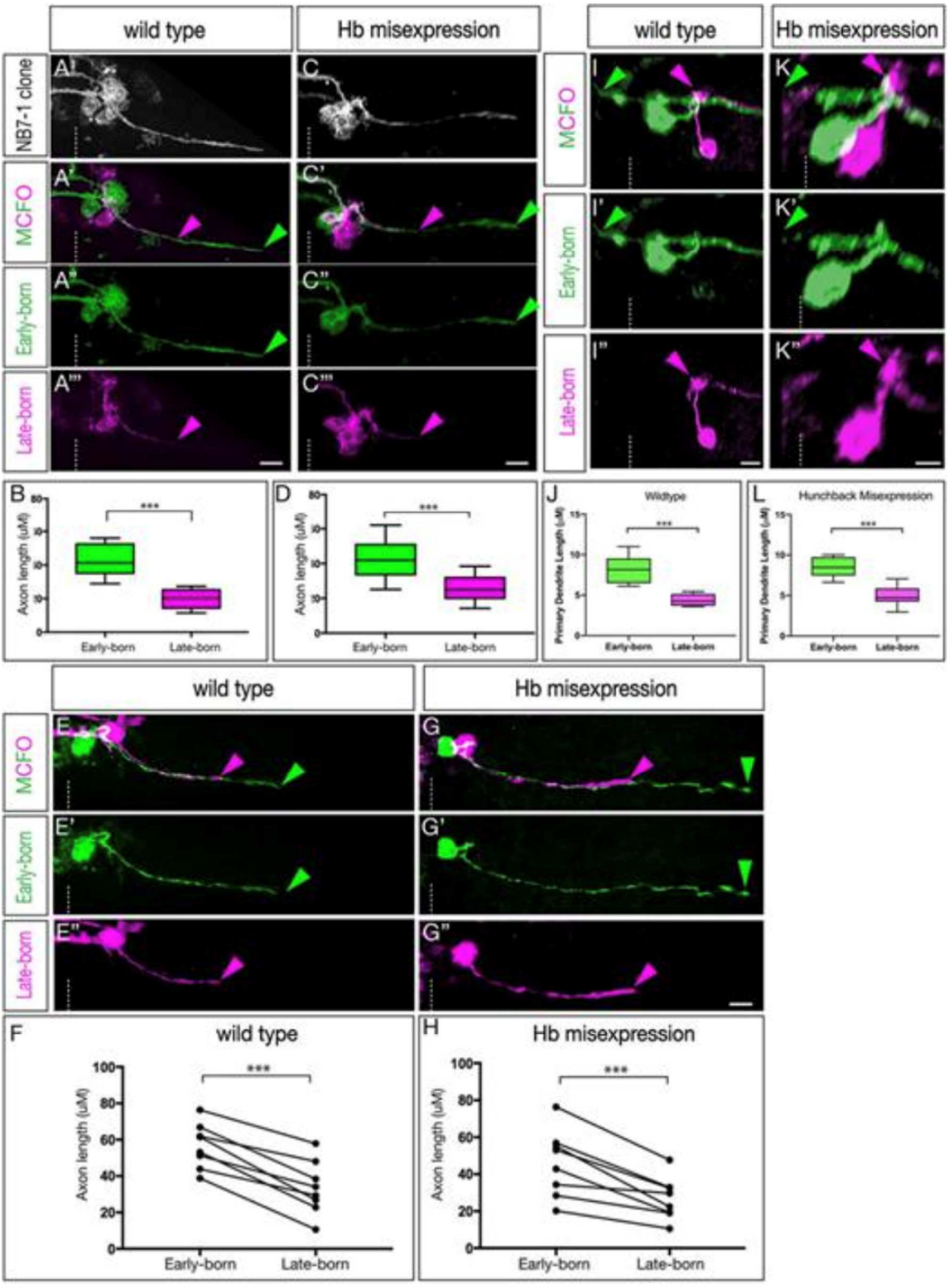
wild type
Hb misexpression
wild type
Hb misexpression
NB7-1 clone
MCFO
Early-born
Late-born
A'
C
I
K
A'
C'
I'
K'
A''
C''
I''
K''
A'''
C'''
B
D
J
L
Axon length (uM)
Primary Dendrite Length (uM)
Early-born
Late-born
Wildtype
Hunchback Misexpression
***
wild type
Hb misexpression
E
G
E'
G'
E''
G''
F
H
wild type
Hb misexpression
Axon length (uM)
Early-born
Late-born
***

We next wanted to determine whether misexpression of Hb throughout the NB7-1 lineage, known to produce many ectopic U1 motor neurons (Isshiki et al., 2001; Kohwi and Doe, 2013; Pearson and Doe, 2003), would alter the timing of motor axon outgrowth. We misexpressed Hb in the NB7-1 lineage, and used MCFO to differentially label early-born and late-born neurons. MCFO marking the entire NB7-1 lineage did not change the gross distribution of neurons (Fig. 2C). Importantly, in every case where MCFO differentially labeled early-born and late-born neurons, we found that early-born neurons projected axons out of the CNS before later-born neurons (Fig. 2C-D; n=10, P<0.0001, two-tailed unpaired t-test). As in the wild type, in every case where MCFO differentially labeled just a pair of neurons, we always found the more medial (early-born) neuron had a longer axon projection than the lateral (later-born) neuron (Fig. 2G-H, n=8, P<0.001, two-tailed paired t-test). Moreover, the axon length differential between early-born and late-born neurons was indistinguishable in wild-type and Hb-misexpression lineages (n=17, P=0.41, two-tailed unpaired t-test, data not shown).

We next examined the time course of dendrite extension. In wild type, we observed that earlier-born cells elaborated their dendritic processes before their later-born counterparts (Fig. 2I,J; n=7, P<0.003, two-tailed unpaired t-test); the same was observed in Hb misexpression animals (Fig. 2K,L; n=7, P<0.001, two-tailed unpaired t-test). We conclude that sequentially born motor neurons project axons and dendrites sequentially, in both wild type and following Hb misexpression. This raises the question: is intrinsic temporal identity or time of differentiation more important for U1-U5 axon or dendrite target selection?

Late-born neurons with early intrinsic temporal identity have 'early' contralateral dendrite targeting

To determine whether neuronal morphology was correlated with intrinsic temporal identity or time of differentiation, we first needed to define the morphology of the U1-U5 motor neurons. Previous work has mapped generic U neuron axonal projections (Landgraf et al., 1997), but did not identify muscle targets for specific U1-U5 motor neurons. To precisely define U1-U5 motor neuron identity, we used the serial section transmission electron microscopy (EM) (Ohyama et al., 2015) to reconstruct U1-U5 morphology (Fig. 3A-E; Fig. S2). We detected two striking differences in morphology between early-born U1-U2 neurons and later-born U3-U5 neurons: U1-U2 have bipolar projections, whereas U3-U5 have monopolar projections; and U1-U2 have contralateral dendrites, whereas U3-U5 have ipsilateral dendrites (Fig. 3A-E).

Fig. 2.3 Late-born neurons with early intrinsic temporal identity have 'early' dendrite morphology. (Next page) (A-E) U1-U5 neuronal morphology determined by EM reconstruction in the first instar larval CNS. Early-born U1-U2 neurons (green) have a bipolar morphology with a contralateral dendrite arbor (left of dashed midline), whereas later-born U3-U5 neurons (red) have a monopolar morphology and ipsilateral dendritic arbors. Neuronal birth-order is determined by mediolateral position (U1 most medial/earliest, U5 most lateral/latest). (F-J) Wild-type U1-U5 single neuronal morphology by MCFO in L1 larvae (*NB7-1-Gal4^{KZ} UAS-MCFO*). Neurons are shown from left to right based on birth-order, determined by their position within the five Eve^{+} neurons (inset). Scale bar: 5 μm. (K-O) Hb misexpression U1-U5 single neuronal

morphology by MCFO in L1 larvae (*NB7-1-Gal4^{KZ} UAS-MCFO*). Neurons are shown from left to right based on birth-order, determined by their position within the Eve^{+} neurons (inset). The later-born neurons ('ectopic U1') have acquired a contralateral dendrite, more consistent with their early intrinsic temporal identity than their late time of differentiation. Scale bar: 5 μm. (P,Q) Quantification. In wild type, early-born U1-U2 neurons have low/no nuclear Zfh2, a marker for their early intrinsic temporal identity, and contralateral dendrites; later-born neurons have high Zfh2 and no contralateral projection. In Hb misexpression embryos, all neurons with low/no Zfh2 have a contralateral dendrite, even when they have a late-born time of differentiation (>3 Eve^{+} nuclei from the midline). The number of neurons scored is shown within each bar.

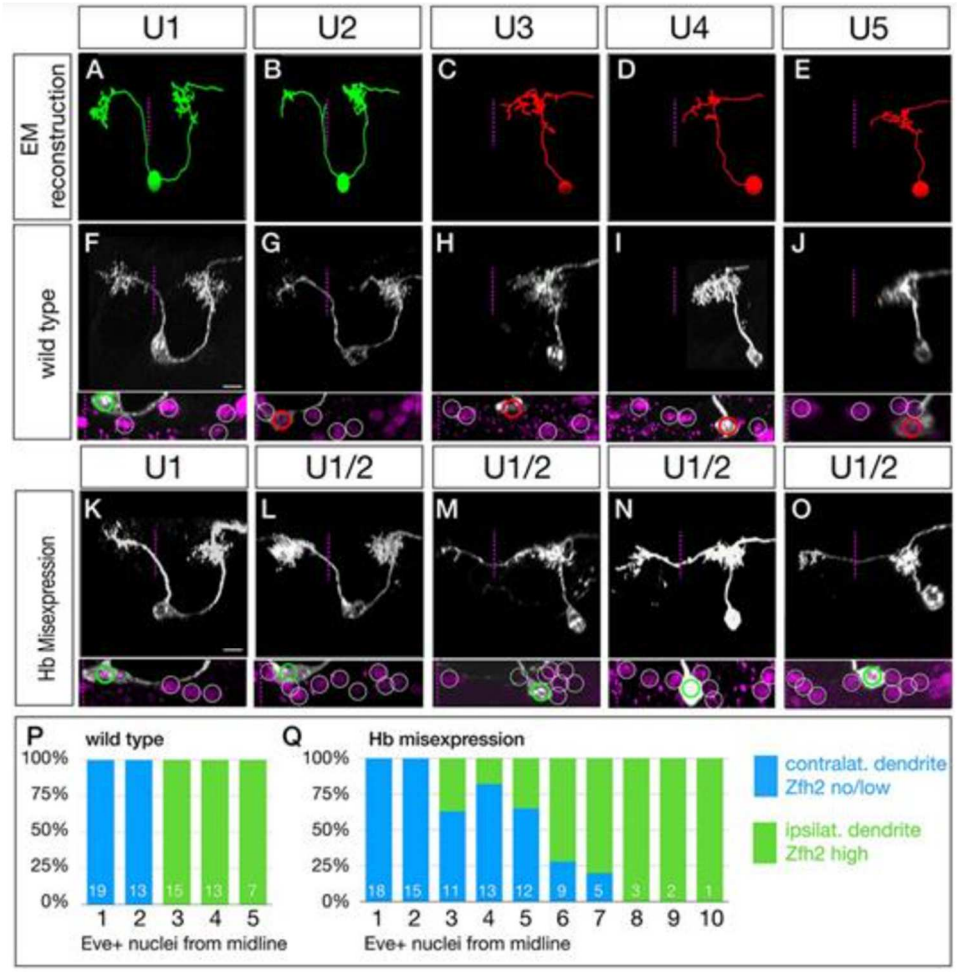

To determine whether the U1-U5 morphology seen in the larval EM reconstruction are reproducible and present in the larval VNC, we generated MCFO labeling of single U1-U5 motor neurons in early L1 larvae (Fig. 3F-J). Previous work showed that U1-U5 are positive for the Even-skipped (Eve) transcription factor, and are arranged from medial (U1) to lateral (U5) (Isshiki et al., 2001; Kohwi and Doe, 2013; Pearson and Doe, 2003), which we confirm here (Fig. 3F-J, bottom panels, and quantified in Fig. 3P). We observed that the larval U1-U5 motor neurons had a morphology closely matching the larval U1-U5 motor neurons in the EM reconstruction (compare Fig. 3A-E with F-J). We conclude that the early-born U1-U2 neurons and the late-born U3-U5 neurons have distinctive, stereotyped neuronal morphologies.

In wild type, intrinsic temporal identity and time of axon outgrowth are tightly linked; neurons with early intrinsic temporal identity extend axons first, neurons with late intrinsic temporal identity extend axons later. We sought to break this correlation by misexpressing Hb in the NB7-1 lineage so that both early-differentiating and late-differentiating neurons have an early U1 intrinsic temporal identity (Isshiki et al., 2001; Kohwi and Doe, 2013; Pearson and Doe, 2003). To perform this experiment, we needed to monitor neuronal birth order (a proxy for time of differentiation), intrinsic temporal identity and neuronal morphology. Birth order was determined by the neuron position in the medio-lateral series of Eve^+ nuclei (medial, early-differentiating; lateral, late-differentiating); intrinsic temporal identity was determined by molecular markers (U1 is Eve^+ $Zfh2^-$, whereas neurons with later temporal identities are Eve^+ $Zfh2^+$; and neuronal morphology was determined by MCFO (Fig. 3K-O). As expected, misexpression of Hb had no effect on the morphology of the endogenous Hb^+ U1 or U2

neurons (Fig. 3K,L; U1 *n*=13). In contrast, all late-differentiating neurons with an ectopic U1 intrinsic temporal identity (Eve^+ $Zfh2^-$) had a morphology similar the endogenous U1 neurons: both producing a dorsal contralateral dendritic arbor (Fig. 3M-O, arrowheads). The penetrance of the transformation declined in neurons with progressively later birthdates (quantified in Fig. 3Q). The failure to project a contralateral dendrite was perfectly correlated with the failure to repress Zfh2 (Fig. 3Q; Fig. S3), leading us to conclude that these $Zfh2^+$ late-born neurons are simply not being transformed to a U1 identity, and thus fail to project contralaterally. Interestingly, even the transformed ectopic U1 neurons (Eve^+ $Zfh2^-$) had their contralateral process emerging from a dorsal location, rather than from the cell body, as observed for endogenous U1 neurons, indicating that the morphological transformation was not complete (Fig. 3M-O, Movies 1 and 2). Nevertheless, the ectopic U1 neurons are more similar to the endogenous early-born U1-U2 neurons than to the later-born U3-U5 neurons. We conclude that neuronal morphology is more tightly linked to intrinsic temporal identity than to neuronal birth order.

Late-born neurons with early intrinsic temporal identity target their dendrites to the early-born U1 dendritic domain

The experiments described above show that late-differentiating neurons with early intrinsic temporal identity have gross morphological features matching their intrinsic temporal identity, rather than their time of differentiation. In this section and the next, we investigate whether these ectopic U1 neurons target their axons to the normal U1 muscle target (the dorsal DO1 and DO2 muscles) and target their dendrites to the normal U1

neuropil target (a contralateral, dorsal volume of neuropil). In this section we assay dendritic projections; in the following section we assay axonal projections.

In wild type, the endogenous U1 neurons have ipsilateral and contralateral dendrites that are colocalized in the same region of dorsal neuropil, as seen by EM reconstruction (Fig. 4A) or dual color MCFO labeling (Fig. 4B). To map dendrite targeting of 'heterochronic' ectopic U1 motor neurons, we misexpressed Hb in the NB7-1 lineage and then screened for MCFO labeling in which one hemisegment had the endogenous U1 motor neuron labeled (identified by its medial position and 'U' shaped neuronal morphology), and the opposite hemisegment had an ectopic U1 neuron labeled (identified by its lateral cell body position and dorsal contralateral dendrite process). In every case, we found the 'heterochronic' ectopic U1 neuron dendrite precisely targeted to the normal dorsal neuropil target of the U1 neuron, with both ectopic and endogenous U1 dendritic arbors tightly intermingled (Fig. 4B,B‴; n=10). For each dendrite assessed, correct neuropil localization was confirmed through quantification of the distance of the dendrite from the midline, the anteroposterior distance of the dendrite from the directly anterior hemisegment in relation to the labelled cell, and the position of the dendrite in the dorsoventral axis (Fig. 4C). We observed no significant differences between the dendritic localization of the wild-type U1 neurons and our ectopic early-born cells across any of our positional metrics (Fig. 4C, two-way ANOVA, P=0.71). We conclude that intrinsic temporal identity, not time of dendrite outgrowth, generates precise dendrite targeting to the appropriate region of the neuropil.

Fig. 2.4 Ectopic U1 dendrites target the normal U1 neuropil domain. (Next page) (A-A‴) Wild-type bilateral U1 neurons (green, magenta) assayed in the EM reconstruction of the L1 larval CNS. A U1 neuron (magenta) targets its contralateral dendrite to the same neuropil volume as the ipsilateral dendrite of the contralateral U1 neuron (green; boxed region in A,A′, shown enlarged in A″). (B-B‴) Hb misexpression (*NB7-1-Gal4^{KZ} UAS-hb UAS-MCFO*) assayed by MCFO labeling in L1 larvae, showing an endogenous U1 (magenta; defined by its medial cell body position, bipolar morphology and contralateral projection) and an ectopic U1 neuron (green; defined by its lateral cell body position, monopolar morphology and contralateral projection). The endogenous and ectopic U1 neurons target the same dorsal neuropil domain (boxed in B,B′ shown enlarged in B″). Dashed line indicates the midline; all views are cross-sections; dorsal is upwards except A″ and B″ (dorsal views, anterior upwards). Scale bars: 5 μm. I Quantification. Endogenous and ectopic U1 dendrites are the same distance from the midline, anterior-posterior (AP) border and ventral edge of the CNS. *N*=10 for U1 and ectopic U1. Images were analyzed using IMARIS, and viewed in 3D. Channels were balanced in IMARIS, and the slice tool was used to clear features which obscure the view of the neurons of interest. The EM reconstruction was accessed remotely through a custom software, and neuron skeletons and synapses were also rendered using this strategy.

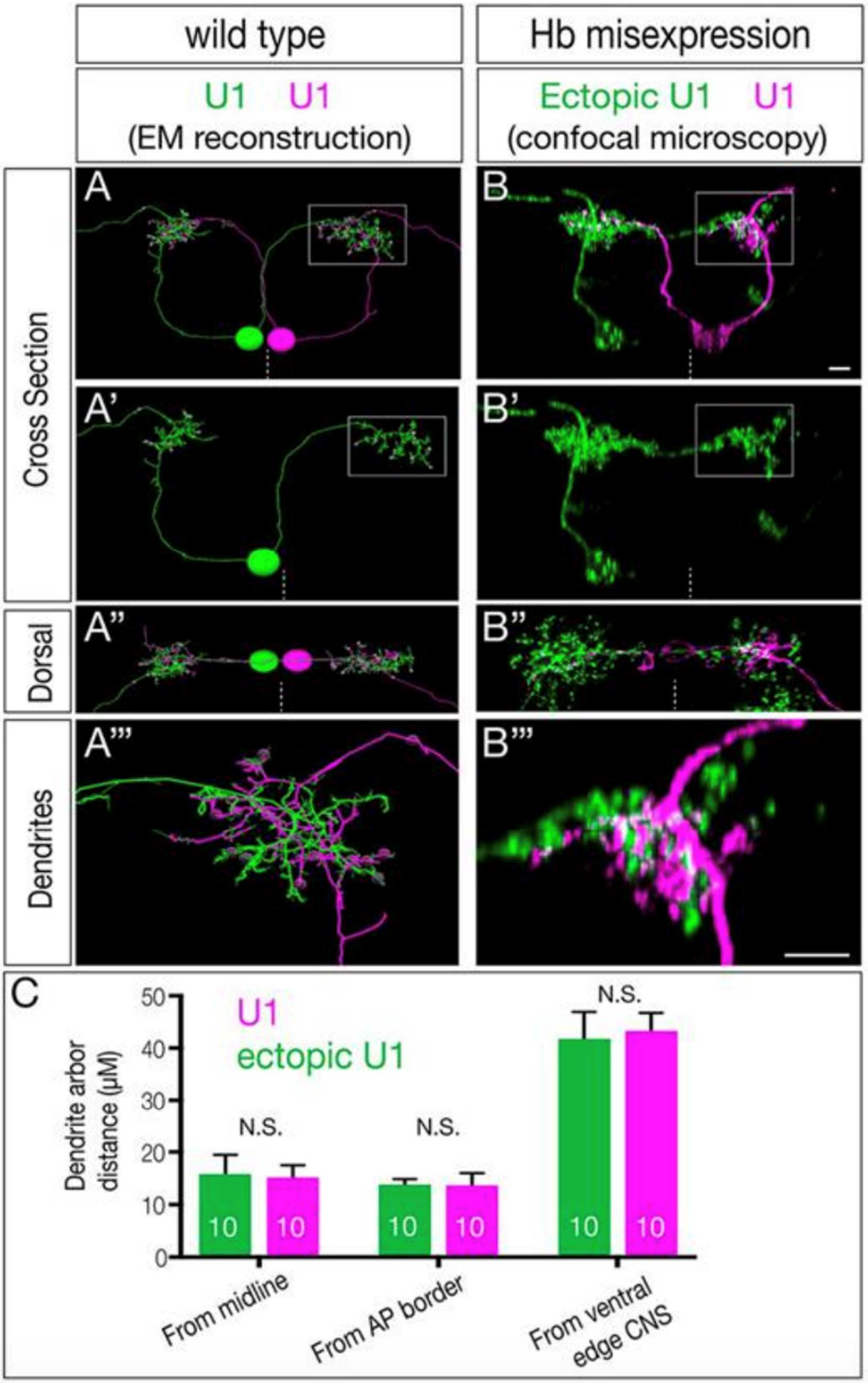
wild type
Hb misexpression
U1 U1
(EM reconstruction)
Ectopic U1 U1
(confocal microscopy)
Cross Section
Dorsal
Dendrites
A
B
A'
B'
A''
B''
A'''
B'''
C
U1
ectopic U1
Dendrite arbor distance (μM)
50
40
30
20
10
0
N.S.
N.S.
N.S.
10
10
10
10
10
10
From midline
From AP border
From ventral edge CNS

Ectopic U1 axons project to dorsal body wall muscles and lack ventral muscle targets

Here, we determine whether late-born neurons with early intrinsic temporal identity project their axons to dorsal muscles normally targeted by neurons with early temporal identity or to more ventral muscles normally targeted by late-born neurons. We focus our analysis on L1 larvae, where neuromuscular junctions have formed and are functional for locomotion. In wild type, we find that the U1-U2 motor neurons innervate the dorsal-most oblique muscles DO1and DO2, and the U3-U5 motor neurons innervate more ventral muscles in the area of DA3 and DO4 (Fig. 5A-A‴; quantified in Fig. 5A‴). All motor neurons make varicosities, indicating presynaptic differentiation at their muscle targets, but here we do not assay functional synaptic connectivity, simply axon targeting. In contrast, Hb misexpression results in a complete loss of the more ventral axon varicosities, while still exhibiting varicosities at the site of the DO1 and DO2 dorsal muscles (Fig. 5B-B‴; quantified in Fig. 5A‴). These results suggest that later-born motor neurons in the lineage have been transformed into an early intrinsic temporal identity and thereby target the normal early U1-U2 muscle targets. For these reasons, it is possible to conclude that TTF identity, and not the time a neuron is born, is a greater determinant of overall neuronal morphology and connectivity. This provides insight into how circuitry is specified during development, and how we might decode these genetic processes to ultimately create therapeutic strategies for rewiring neuronal circuits.

Fig. 2.5 Ectopic U1 axons project to dorsal muscles and lack ventral muscle targets. **(Next page)** (A-B‴) Wild-type (*NB7-1-Gal4^{KZ} UAS-GFP*) and Hb-misexpression (*NB7-1-Gal4^{KZ} UAS-hb UAS-GFP*) L1 larvae stained for U motor neurons (green) and muscles (magenta). (A-A‴) Wild type: U motor neurons project axons to dorsal muscles (DO1/DO3) and more ventral muscles in the LL1/DA3 region. (B-B‴) Hb misexpression: U motor neurons project only to dorsal muscle targets (magenta, shown in B′) consistent with ectopic U1-U2 identity at the expense of U3-U5 neuronal identity. Arrowheads indicate U1-U2 muscle targets (green) and U3-U5 muscle targets (red). (A‴′) Quantification. (C-C″,D-D″,E-E″) Hb misexpression L1 larvae (*NB7-1-Gal4^{KZ} UAS-hb UAS-MCFO*) showing MCFO-labeled single neurons. (C-C″) The endogenous U1 motor neuron (green; closest to midline). I Dorsal view showing medial cell body position, contralateral dendrites and ipsilateral axon (Zfh2 negative; not shown). (C′) Cross-sectional view of the same U1 neuron. (C″) Dorsal view of the body wall showing the U1 axon (green arrowhead) projecting to the most dorsal extent of the FasII^{+} motor neurons (magenta arrowhead). (C‴) Quantification. (D-D″) An ectopic U1 motor neuron (green). (D) Dorsal view showing lateral cell body position, contralateral dendrites and ipsilateral axon (Zfh2 negative; not shown). (D′) Cross-sectional view of the same neuron; the contralateral dendrite has a dorsal origin and there is a lack of bipolar morphology. (D″) Dorsal view of body wall showing the ectopic U1 axon (green arrowhead) projecting to the most dorsal extent of the FasII^{+} motor neurons (magenta arrowhead). (D‴) Quantification. (E-E″) A late-born laterally positioned U3, U4 or U5 motor neuron that was not transformed (based on being Zfh2^{+}; not shown). I Dorsal view showing far

lateral cell body position, ipsilateral dendrites and ipsilateral axon. (E′) Cross-sectional view of the same neuron. (E″) Dorsal view of the body wall showing the U3-U5 axon (green arrowhead) projecting to a more ventral region along the FasII^{+} motor neurons (magenta arrowhead). (E‴) Quantification.

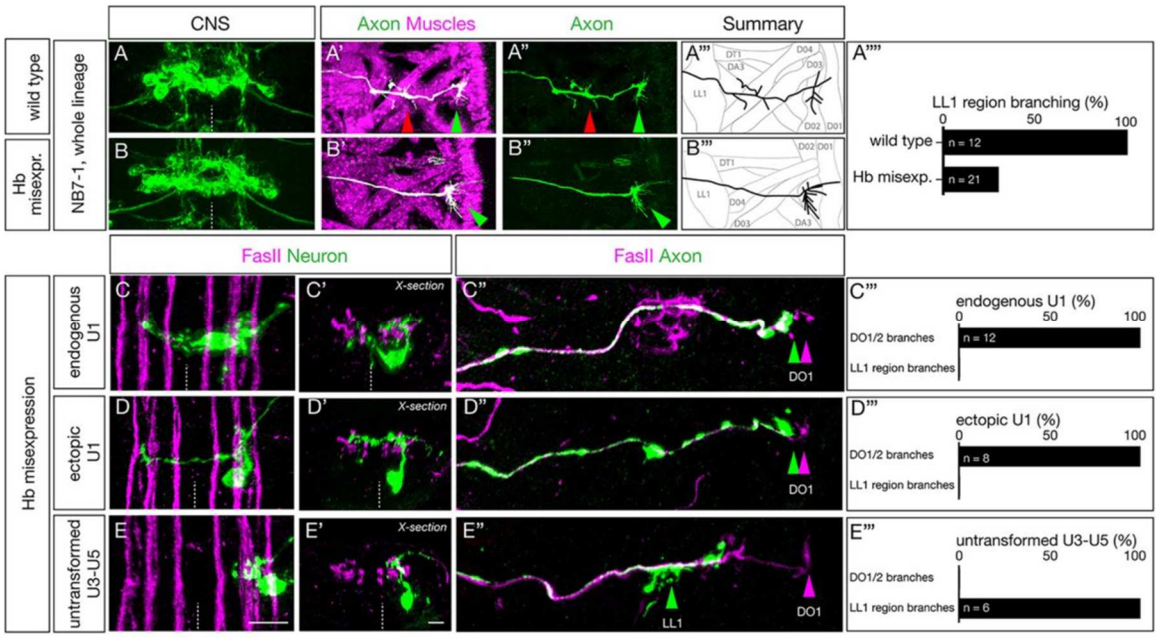

To examine individual motor neurons, we used MCFO following Hb misexpression throughout the NB7-1 lineage. We observed endogenous early-born U1 motor neurons, identified by their medial position and bipolar morphology (Fig. 5C-C′), that project to DO1/DO2 dorsal muscles (Fig. 5C″; quantified in Fig. 5C‴). We also observed 'ectopic U1' motor neurons identified by their displacement from the midline, their monopolar morphology and their dorsal originating contralateral dendrite projection (Fig. 5D,D′); these neurons project to the same DO1/DO2 dorsal muscles as the endogenous U1 motor neuron (Fig. 5D″; quantified in Fig. 5D‴). These heterochronic 'ectopic U1' motor neurons are clearly different from the normal late-born U3-U5 motor

neurons, identified by their lateral position and lack of contralateral dendrites (Fig. 5E,E′), that project to the region of the more ventral muscle LL1 (Fig. 5E″; quantified in Fig. 5E‴). We conclude that intrinsic temporal identity, not time of axon outgrowth, generates precise axon targeting to the appropriate body wall muscles.

To examine the ability of these 'ectopic U1' motor neurons to create putative synaptic inputs onto the DO1/DO2 dorsal muscles, we quantified the numbers of pre-synaptic Bruchpilot (Brp) puncta formed by U neurons on their dorsal longitudinal muscle targets. Brp is an active zone marker that is a good measure of pre-synapse location. In wild type, U1-U2 neurons form Brp^{+} synapses on the most dorsal longitudinal muscles DO1/DO2, and the later-born U3-U5 neurons form synapses with the slightly more ventral muscles in the LL1 region (Fig. 6A-D; quantified in Fig. 6I-K). In contrast, the 'ectopic U1' motor neurons have a significant shift towards more dorsal muscle targets (Fig. 6E-H). There is a significant loss of pre-synaptic Brp^{+} puncta in the LL1 region (Fig. 6F, quantified in Fig. 6I), while simultaneously increasing their amount of synaptic input onto the dorsal muscle DO2 (Fig. 6G,H, quantified in Fig. 6J). We saw an insignificant difference in synaptic input onto DO1 between wild-type and Hb-misexpression samples (Fig. 6H quantified in Fig. 6K). We conclude that intrinsic temporal identity, not time of axon outgrowth, determines the position of Brp^{+} presynaptic puncta on the dorsal longitudinal muscle targets.

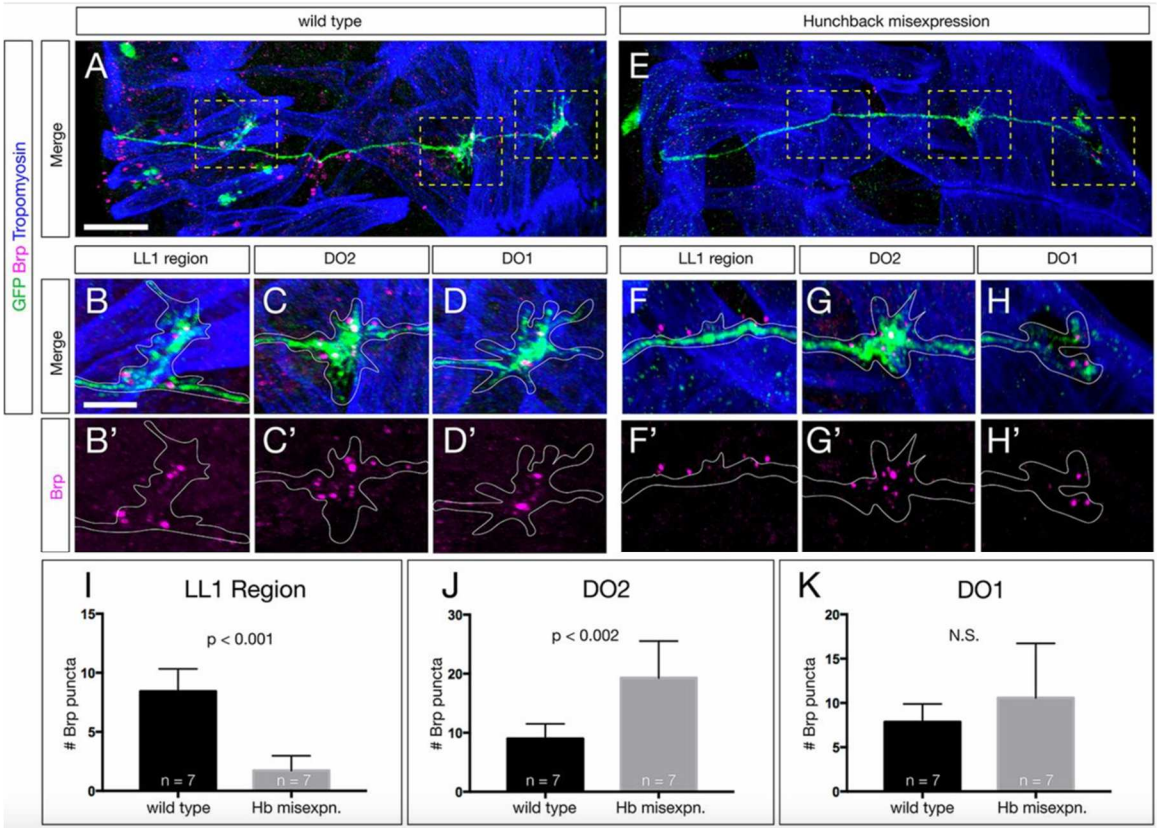

Fig. 2.6 Ectopic U1 axons shift synaptic input from ventral to dorsal muscle targets. (A-D′) Wild-type L1 larva stained for all U motor neurons in the NB7-1 lineage (GFP, green), Brp^{+} puncta (magenta) and body wall muscles (Tropomyosin, blue). The U motor neurons have Brp^{+} puncta contacting muscles around LL1 (B,B′), the DO2 muscle (C,C′) and the DO1 muscle (D,D′). (E-H′) Hb-misexpression L1 larva (*NB7-1-Gal4^{KZ} UAS-hb*) stained for all U motor neurons in the NB7-1 lineage (GFP, green), Brp^{+} puncta (magenta) and body wall muscles (Tropomyosin, blue). There are reduced Brp^{+} puncta around LL1 (F,F′), increased Brp^{+} puncta on the DO2 muscle (G,G′) and a similar number of Brp^{+} puncta on the DO1 muscle (H,H′). Areas outlined in A and E are shown at higher magnification in B-D′ and F-H′, respectively. (I-K) Quantification. Scale bars: 15 μm in A,E; 5 μm in B-H′.

Discussion:

During neurogenesis, intrinsic temporal identity and time of differentiation are typically tightly correlated. For example, the *Drosophila* NB7-1 sequentially generates the U1-U5 motor neurons, which have distinct intrinsic temporal identities and distinct times of differentiation. Our work shows that intrinsic temporal identity is more important than the time of neuronal differentiation for establishing proper axon and dendrite targeting. We generated ectopic motor neurons with an early-born U1 intrinsic temporal identity in a later extracellular environment, breaking the correlation between intrinsic temporal identity and time of differentiation. These late-born ectopic U1 neurons sent their axons to the DO1/2 muscles (together with endogenous U1 neurons), and their dendrites to a dorsal contralateral neuropil domain (together with endogenous U1-U2 neurons). Furthermore, ectopic U1 neurons are also born in a much more lateral location in the CNS, and yet are able to find their correct axon and dendrite targets. Overexpression of Hunchback in other neuroblast lineages generates early-born neuronal identity based on molecular marker expression (Isshiki et al., 2001; Moris-Sanz et al., 2015; Novotny et al., 2002; Tran and Doe, 2008), but here we characterize the pre- and post-synaptic targeting of these 'heterochronic' neurons. Our data show that intrinsic temporal identity is an important determinant of neuronal axon and dendrite targeting.

Temporal transcription factors (TTFs) are known to regulate neuronal cell fate in multiple neuroblast lineages in *Drosophila* (Doe, 2017). In mushroom body neuroblasts, TTFs are known to specify the molecular and morphological features of the Kenyon cells (Kao and Lee, 2010; Liu et al., 2015; Zhu et al., 2006). Similarly, in type II neuroblast intermediate neural progenitor (INP) lineages, recent work has shown that the late TTF

Eyeless specifies the molecular identity and axon/dendrite targeting of several classes of central complex neurons (Sullivan et al., 2019). In contrast, the INP parental type II neuroblasts express a different set of TTFs (Syed et al., 2017), but nothing is yet known about their role in axon/dendrite targeting (Ren et al., 2017; Syed et al., 2017). Recent work has shown that optic lobe neuroblasts express TTFs that specify the molecular identity and axon targeting of visual system neuronal subtypes, but it is unknown whether sequentially born neurons project axons sequentially or synchronously (Bertet et al., 2014; Erclik et al., 2017; Li et al., 2013b). The antero-dorsal larval brain neuroblast expresses TTFs that govern the identity of olfactory projection neurons, as well as regulating the dendritic targeting to specific antennal lobe glomeruli, but it is unknown whether the projection neuron dendrites project sequentially or synchronously (Jefferis et al., 2001; Liu et al., 2015). Taken together, abundant data suggest that TTFs control neuronal molecular identity, with a growing number of studies showing that TTFs also regulate axon/dendrite targeting to specific neuropil domains or muscles.

Previous work has demonstrated that motor neurons in different lineages project axons at different times, e.g. aCC prior to RP2 (Sanchez-Soriano and Prokop, 2005). Similarly, we have found that the U1-U5 motor neurons extend axons sequentially, and independently of their intrinsic temporal identity. This suggests that the initial timing of axon extension is regulated by an internal clock mechanism in each cell, likely beginning upon its terminal cell division. In *C. elegans*, the HSN motor neurons require expression of *lin-18* mRNA to initiate axon extension (Olsson-Carter and Slack, 2010); whether a similar mechanism is used by U1-U5 motor neurons is unknown. We also show that dendrite elaboration occurs much later than axon extension in the U motor neurons. The

observation that axon outgrowth precedes dendrite outgrowth has been widely reported (Gerhard et al., 2017; Mason, 1983; Mumm et al., 2006; Ramon y Cajal, 1909), although the mechanism that sets the time of axon or dendrite outgrowth is poorly understood. Hb misexpression robustly transformed later-born U motor neurons into ectopic U1 neurons, yet there were two limitations. First, ectopic U1 neurons do not have a bipolar cell body: they branch off dendrites from the dorsal axon, rather than from the cell body. Nevertheless, despite their novel dorsal outgrowth, ectopic U1 dendrites targeted a contralateral neuropil volume indistinguishable from the endogenous U1 neurons. The failure of the ectopic U1 neurons to generate a bipolar somata may be due to: (1) incomplete transformation of neuronal identity; (2) an abnormal lateral cell body position; (3) changing extrinsic cues; or (4) intrinsic changes in the neuronal cytoskeletal that are not under Hb regulation. A second limitation is the decline in Hb potency as the NB7-1 lineage progresses. We find that, following Hb misexpression, there are always some laterally positioned Eve^{+} motor neurons that fail to repress Zfh2 and fail to extend contralateral dendrites (Fig. S3); we conclude these neurons are simply untransformed. The inability of Hb to fully transform late-born neurons has been well documented (Kohwi et al., 2013; Pearson and Doe, 2003). The striking correlation between Zfh2 expression and ipsilateral dendrite projection raises the possibility that Zhf2 levels regulate dendrite midline crossing. For example, Zfh2 might activate Robo expression in late-born neurons to keep them ipsilateral, whereas early-born neurons lacking Zfh2 would lack Robo expression, allowing midline crossing. Testing this hypothesis would require generating *UAS-zfh2* transgenics for NB7-1-specific overexpression, and an FRT *zfh2* mutant fourth chromosome to make *zfh2* mutant clones in NB7-1.

The NB7-1 cell cycle is ~50 min (Hartenstein et al., 1987), which means that ectopic U1 motor neurons can be born up to six divisions or 300 min later than normal and yet still find their normal axon and dendrite targets. This suggests that the guidance cues used for endogenous U1 pathfinding are still present many hours later. Consistent with this, the major pathfinding ligands regulating sensory axon targeting and motor dendrite targeting in the CNS – NetrinA/B, Slit, Semaphorin1/2 and Wnt5 (Mauss et al., 2009; Wu et al., 2011; Yoshikawa et al., 2016; Zlatic et al., 2003, 2009) – all maintain their graded expression patterns during this window of neurogenesis (Fradkin et al., 2004; Harris et al., 1996; Mitchell et al., 1996; Rothberg et al., 1988; Yoshikawa et al., 2003; Zlatic et al., 2009). Although we cannot exclude the possibility of the endogenous and ectopic U1 neurons using different cues to find their proper targets, e.g. later-born neurons may project along 'pioneer neuron' processes formed earlier in neurogenesis, it is more likely that both early-born endogenous U1 neurons and later-born ectopic U1 neurons use the same guidance cues for axon and dendrite targeting.

In the future, it will be important to understand the mechanism by which the Hb transcription factor confers U1 neuron axon and dendrite targeting. As mentioned above, it is likely that the endogenous and ectopic U1 motor dendrites target the proper neuropil domain by responding to the known Netrin, Slit, Semaphorin and Wnt5 ligand gradients (Mauss et al., 2009; Wu et al., 2011; Yoshikawa et al., 2016; Zlatic et al., 2003, 2009). Thus, we hypothesize that Hb induces expression of distinct receptor combinations that allow the endogenous and ectopic U1 axon and dendrite to respond to these persistent pathfinding ligand gradients. Hb may directly regulate receptor gene expression, or it may act via an intermediate tier of transcription factors, similar to the 'morphology

transcription factors' that act downstream of temporal transcription factors in establishing adult leg motor neuron axon and dendrite targeting (Enriquez et al., 2015). Understanding how Hb directs axon and dendrite targeting will require characterization of receptor expression in endogenous and ectopic U1 neurons, and/or single cell RNA-seq to characterize the endogenous and ectopic U1 neuron transcriptomes.

Methods:

Fly stocks

Male and female *Drosophila melanogaster* were used. The chromosomes and insertion sites of transgenes (if known) are shown in parentheses next to genotypes. Previously published Gal4 lines, mutants and reporters used were: *hs-FLPG5;;MCFO* (I and III; FBst0064086), *UAS-hunchback*/*CyO* (II) (Isshiki et al., 2001) and *10XUAS-IVS-mCD8::GFP* (III, FBst0032185).

New NB7-1-Gal4^{KZ} line

We generated a new NB7-1-Gal4^{KZ} line that uses an enhancer killer zipper construct to eliminate the NB6-1 off-target expression seen in the published NB7-1 split-Gal4 line (Kohwi et al., 2013). The previous NB7-1-Gal4 line showed NB6-1 expression in 65% of hemisegments (n=20); the NB7-1-Gal4^{KZ} line shows NB6-1 expression in just 25% of hemisegments (n=20). The new split gal4 genotype is *ac-VP16 gsb-DBD, R25A05-KillerZipper/CyO* (II; attP40), where R25A05 is an enhancer expressed in NB6-1. The full stock was created as follows. The Syn21-Kzip(+)-P10 fragment was PCR amplified

from CCAP-IVS-Syn21-Kzip(+)-P10 (Dolan et al., 2017) (a gift from Benjamin White, National Institutes of Health) and fused via Gibson assembly with NheI/HindIII-digested pBPGal80Uw-6 (Pfeiffer et al., 2008) to create pBP-Syn21-Kzip. The Janelia Research Campus enhancer R25A05 (FBst0000162964) was introduced into pBP-Syn21-Kzip by gateway cloning (Pfeiffer et al., 2008) to generate *R25A05-Kzip*, which was then integrated into attP40 site by standard injection (Bestgene).

Immunofluorescence staining

Primary antibodies were: rabbit anti-Hunchback #5-25 (1:200) (Tran and Doe, 2008), rabbit anti-Eve #2472 (1:100, Doe Lab), chicken anti-GFP (1:1000, Abcam, 13970), rat anti-Zfh2 (1:250) (Tran et al., 2010), mouse anti-HA-Alexa Fluor 488 conjugate (1:200, Cell Signaling, 2350S), rat anti-HA (1:100, Sigma, 11867423001), chicken anti-V5 (1:1000, Bethyl, A190-218A), rat anti-FLAG (1:400, Novus, NBP1-06712) and mouse anti-FasII (1:60, DSHB, 1D4). Secondary antibodies were from Jackson ImmunoResearch and were used at 1:350: anti-Rb 405 (Dylight 405, 711-475-152), anti-Rat 647 (AlexaFluor 647, 712-605-153), anti-Ck 488 (AlexaFluor 488, 703-545-155), anti-Mouse 647 (AlexaFluor 647, 715-605-151).

Embryos were blocked overnight in 0.3% PBST (1X PBS with 0.3% Triton X-100) with 5% normal goat serum and 5% donkey serum (PDGS), followed by incubation in primary antibody overnight at 4°C. Next, embryos underwent three 30 min washes in PBST, followed by an overnight secondary antibody incubation at 4°C. Embryos were then dehydrated in a glycerol series (10%, 50%, 90%) for 20 min each followed by 90% glycerol with 4% n-propyl Gallate overnight before imaging.

Whole L1 larvae were washed for 2 h in methanol, blocked overnight in 0.3% PBST (1×PBS with 0.3% Triton X-100) with 5% normal goat serum and 5% donkey serum (PDGS), followed by incubation in primary antibody for 2 nights at 4°C. Next, larvae were washed overnight in PBST, followed by secondary antibody incubation for 2 nights at 4°C. Embryos were dehydrated in a glycerol series (10%, 50% and 90%) for 20 min each followed by 90% glycerol with 4% n-propyl Gallate overnight before imaging. Larval brains were dissected in 0.3% PBST, fixed in 4% paraformaldehyde in PBST, rinsed and blocked in PDGS with 0.3% Triton X-100. Staining was carried out as above for embryos, but after the secondary antibody incubation brains were mounted in Vectashield (Vector Laboratories).

MCFO labeling

MCFO labeling in wild type used *ac-gsb-Gal4, R25A05-KillerZipper* (II) *x hsFLPG5;;UAS-MCFO* (I and III) and in Hb misexpression used *ac-gsb-Gal4, R25A05-KillerZipper* (II) *x hsFLPG5;UAS-Hunchback;UAS-MCFO* (I, II and III). Embryos were collected for 2 h at 25°C, aged for 4 h and heat shocked at 37°C (15-20 min for dense labeling, 8-10 min for sparse labelling), then left to develop until desired stages.

Imaging

Images were captured with a Zeiss LSM 710 or Zeiss LSM 800 confocal microscope with a *z*-resolution of 0.35 μm. Images were processed using the open-source software FIJI (https://fiji.sc) and Photoshop (Adobe). Figures were assembled in Illustrator CS5 (Adobe). Three-dimensional reconstructions, morphometrics and level adjustments were generated using Imaris (Bitplane). Any level adjustment was applied to the entire image.

Statistical analysis

Statistical significance is indicated by asterisks: ****P<0.0001; ***P<0.001; **P<0.01; *P<0.05; n.s., not significant. The following statistical tests were performed: two-tailed unpaired *t*-test (Fig. 2B,D,J,I,H,I,J); two-tailed paired *t*-test (Fig. 2F,H); and two-way ANOVA (Fig. 4). All analyses were performed using Prism8 (GraphPad). The results are stated as mean±s.d., unless otherwise noted.

Serial section electron microscopy

We accessed a previously published serial section transmission electron microscopic volume of the newly hatched larval CNS using CATMAID software (Ohyama et al., 2015) to describe the U1-U5 motor neurons in the first abdominal segment. U1-U5 motor neurons were identified based on their published unique dendritic morphology (Landgraf et al., 1997).

Author Contributions

Conceptualization: C.Q.D., A.Q.S.; Methodology: A.Q.S.; Formal analysis: A.Q.S.; Investigation: C.Q.D., A.Q.S.; Data curation: A.Q.S.; Writing – original draft: C.Q.D., A.Q.S.; Writing – review & editing: C.Q.D., A.Q.S.; Visualization: A.Q.S.; Supervision: C.Q.D.; Project administration: C.Q.D.; Funding acquisition: C.Q.D.

Bridge:

In this chapter, we demonstrate that the intrinsic TTF identity of a neuron is a major determinant of its higher-order features, such as axonal and dendritic morphology and synaptic partner choice. Extending the early Hb TTF window selectively in the NB7-1 lineage results in the generation of ectopic early-born U1 motoneurons fates, which extend axonal and dendritic projections to appropriate early-born targets despite abnormal time of birth and spatial location. In the next chapter, we identify a previously unknown Kr^+/Pdm^+ temporal identity window in the NB7-1 lineage. We demonstrate that the combined expression of Kr and Pdm is sufficient to generate the $Nkx6^+$ VO motorneuron fate, and that the ventral targeting of this neuron is dependent on Nkx6 expression. These results suggest that the ability of TTFs to specify complex connective features is generalizable, and is not a specialized feature of Hb.

CHAPTER III

A NOVEL TEMPORAL IDENTITY WINDOW GENERATES ALTERNATING EVE^{+}/NKX6^{+} MOTOR NEURON SUBTYPES IN A SINGLE PROGENITOR LINEAGE

Introduction:

Neural diversity from flies to mice arises from two major developmental mechanisms. First, neural progenitors acquire a unique and heritable spatial identity based on their position along the rostrocaudal or dorsoventral body axes (Kohwi and Doe, 2013; Sagner and Briscoe, 2019). Second, temporal patterning based on neuronal birth-order results in individual progenitors producing a diverse array of neurons and glia (Holguera and Desplan, 2018; Kohwi and Doe, 2013; Miyares and Lee, 2019). Temporal patterning is best characterized in *Drosophila*; neural progenitors (neuroblasts) located in the ventral nerve cord, central brain, and optic lobes all undergo temporal patterning, in which the neuroblast sequentially expresses a cascade of TTFs that specify distinct neuronal identities (Allan and Thor, 2015; Doe, 2017; Holguera and Desplan, 2018; Miyares and Lee, 2019). Although all neuroblasts undergo temporal patterning, the TTFs are different in each region of the brain (Allan and Thor, 2015; Doe, 2017; Holguera and Desplan, 2018; Miyares and Lee, 2019). Similar mechanisms are used in the mammalian cortex, retina, and spinal cord, although many TTFs remain to be identified (Alsiö et al.,

2013; Delile et al., 2019; Elliott et al., 2008; Mattar et al., 2015; Sockanathan and Jessell, 1998; Stam et al., 2011).

A major open question is how transient expression of TTFs like Kr and Pdm lead to long-lasting specification of molecular and morphological neuronal diversity. Good candidates for integrating spatial and temporal cues to consolidate motor neuron identity are homeodomain transcription factors expressed in post-mitotic motor neurons (Hobert, 2016). In vertebrates, dorsoventral domains of the spinal cord are partitioned into 12 distinct cardinal classes of neurons – each characterized by development from a common progenitor domain, expression of unique homeodomain transcription factors with cross-repressive interactions to stabilize boundaries, and generating neurons with common morphology (Sagner and Briscoe, 2019). We adapt this nomenclature to define Eve^{+} and $Nkx6^{+}$ (Flybase: HGTX) motor neurons as two "cardinal classes" of motor neurons: each class expresses a homeodomain transcription factor (Eve or Nkx6) with cross-repressive interactions, and each class consists of motor neurons with related neuronal morphology (Eve^{+} motor neurons project to dorsal and lateral longitudinal muscles; $Nkx6^{+}$ motor neurons project to ventral muscle groups) (Broihier et al., 2004).

The *Drosophila* neuroblast 7–1 (NB7–1) is arguably the best characterized system for understanding TTF expression and function. Similar to most other ventral nerve cord neuroblasts, NB7–1 expresses the canonical TTF cascade Hb-Kr-Pdm-Cas with each TTF inherited by the GMCs born during an expression window, and transiently maintained in the two post-mitotic neurons produced by each GMC. The TTF cascade generates diversity among the five Eve^{+} U1-U5 motor neuron progeny of NB7–1: Hb specifies U1 and U2, Kr specifies U3, Pdm specifies U4, and Pdm/Cas together specify U5 (Cleary

and Doe, 2006; Grosskortenhaus et al., 2006; Isshiki et al., 2001; Pearson and Doe, 2003). Identifying TTF target genes, including transcription factors and cell surface molecules, will provide a comprehensive view of how developmental determinants direct neuronal morphology and synaptic partner choices.

It has long been thought that the cardinal classes of motor neurons derive from distinct progenitors; Eve^+ motor neurons derive from NB7–1, NB1–1, and NB4–2 whereas $Hb9^+$ or $Nkx6^+$ motor neurons derive from NB3–1 and others. However, DiI labeling of NB7–1 identified a potentially unknown motor neuron innervating ventral muscles, which is distinct from dorsal and lateral longitudinal muscles targeted by the Eve^+ motor neurons (Schmid et al., 1999). The observed ventral projection in this lineage could reflect transient exuberant outgrowths that are lost during larval life, or they could be due to an uncharacterized motor neuron that forms stable synapses with ventral muscles.

Here, we show that a newly discovered Kr/Pdm TTF window generates an $Nkx6^+$ Eve^- motor neuron, born between U3 and U4 in the NB7–1 lineage, that projects to ventral oblique (VO) muscles. We also show that overexpression of Kr/Pdm together, or Nkx6 alone, generates ectopic VO motor neurons based on molecular marker expression. Finally, we demonstrate that Nkx6 is required for proper motor neuron axon targeting to ventral oblique muscles. Our results establish a genetic pathway from TTFs (Kr/Pdm), to a cardinal motor neuron transcription factor (Nkx6) to motor axonal targeting. We also make the unexpected discovery that a single progenitor can alternate production of different cardinal motor neuron classes.

Results:

The NB7–1 lineage has a Kr^+ Pdm^+ temporal identity window that generates a $Nkx6^+$ motor neuron

The existence of a Kr^+ Pdm^+ temporal identity window had been predicted by computational methods (Averbukh et al., 2018), so we sought to confirm this in vivo using a previously-characterized highly-specific NB7–1 split gal4 line (*NB7–1-gal4* [21]) to express *UAS-myr:GFP* in NB7–1 and its progeny (Fig. S1, Fig. 1a-d). This driver line is expressed during the early part of the lineage, including the time U1-U5 neurons are born, but fades out before the end of the lineage (Seroka and Doe, 2019). We observed that NB7–1 expresses Kr alone in the early-stage 11 embryo, followed by Kr/Pdm co-expression mid-stage 11, and switches to the sole expression of Pdm by late-stage 11 (Fig. S1). To determine the identity of the neurons originating from the Kr^+ Pdm^+ temporal identity window, we used Eve to identify the U1-U5 motor neurons within the lineage, and Zfh1 to label all motor neurons (Layden et al., 2006). We identified a single Eve^- $Zfh1^+$ motor neuron in the lineage (Fig. 1a-d). For reasons described below, we call this the VO neuron. This Eve^- $Zfh1^+$ VO motor neuron was Kr^+ Pdm^+ (Fig. 1a, b), consistent with originating from the previously defined Kr^+ Pdm^+ GMC within the NB7–1 lineage (Averbukh et al., 2018).

Fig. 3.1 NB7–1 generates an Eve$^-$ Nkx6$^+$ motor neuron. (Next page) a-d The NB7–1 lineage is labeled with GFP (green). One hemisegment of a stage 16 embryo is shown (except where noted); ventral midline, dashed line. Eve$^+$ Zfh1$^+$ U1-U5 motor neurons, white circles; Eve$^-$ Zfh1$^+$ motor neuron, yellow circle. Neurons are montaged from different z-axis positions with their X-Y position preserved (see Methods). Left column: Eve marks U1-U5 motor neurons. Middle column: Zfh1 marks all motor neurons, although in U2 motor neurons, Zfh1 staining is fainter. Additional Zfh1$^+$ motor neurons can be seen outside the GFP$^+$ lineage. Right column: Kr is expressed in U1-U3 and the Eve$^-$ Zfh1$^+$ presumptive VO neuron. Pdm is expressed in the Eve$^-$ Zfh1$^+$ presumptive VO motor neuron and the Eve$^+$ U4-U5 motor neurons. Note that Pdm is shown at stage 13 before it fades. Hey is expressed in U1-U5 and the presumptive VO motor neuron, indicating they are all Notch-ON progeny from different GMCs. Note that Hey expression declines after GMC division, resulting in higher Hey levels in the latest born motor neurons (U4/U5). Nkx6 is expressed in the Eve$^-$ Zfh1$^+$ presumptive VO motor neuron (yellow circle) and other neurons outside the lineage. Scale bar: 10 μm. Far right column: summary. **E** Proposed NB7–1 lineage

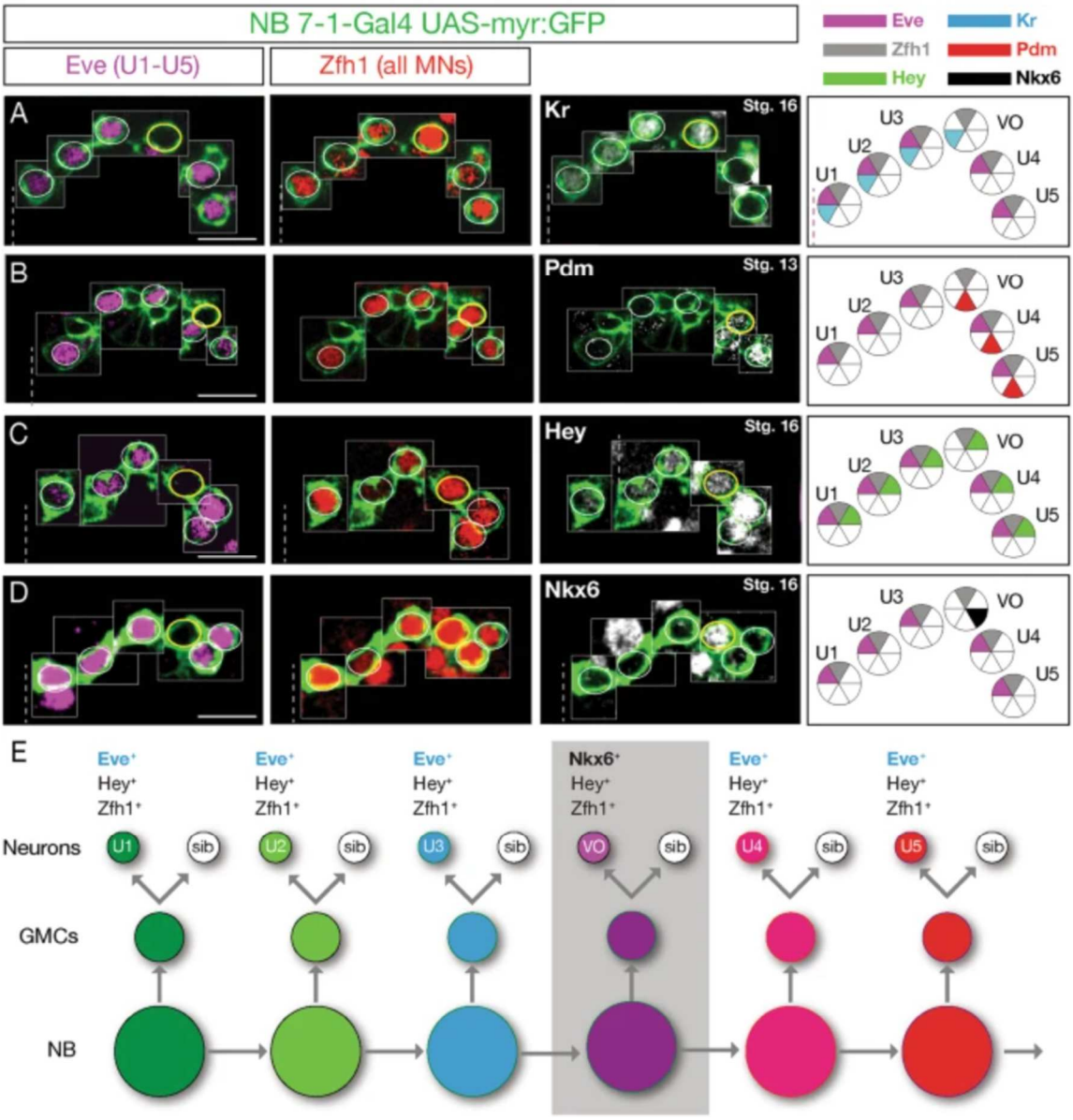

The U1-U5 motor neurons arise from neurons that have active Notch signaling at their terminal division; their sibling neurons lack active Notch signaling (Skeath and Doe, 1998). To determine whether the Kr^{+} Pdm^{+} motor neuron is a U1-U5 sibling, we stained for the Notch reporter gene Hey (Monastirioti et al. 2010, Ulvklo et al. 2012). As expected, all U1-U5 motor neurons transiently expressed the Notch reporter Hey, leading

to strong expression in the latest-born neurons (U4/U5) and weaker expression in the earlier-born neurons (U1-U3). Importantly, Kr^+ Pdm^+ motor neuron also expressed Hey (Fig. 1c), and thus the Kr^+ Pdm^+ motor neuron is not a U sibling neuron. This further supports our conclusion that it originates from the fourth-born Kr^+ Pdm^+ GMC in the NB7–1 lineage (Averbukh et al., 2018).

The transcription factors Eve and Nkx6 have cross-repressive interactions (Broihier et al., 2004), raising the possibility that the Kr^+ Pdm^+ motor neuron might be $Nkx6^+$. Indeed, we confirmed that the Kr^+ Pdm^+ motor neuron was $Nkx6^+$ (Fig. 1d). Interestingly, this $Nkx6^+$ motor neuron was negative for other ventral neuron markers, including Hb9, Islet and Lim3 (data not shown). We conclude that the NB7–1 lineage produces two cardinal classes of motor neurons: Eve^+ motor neurons and an $Nkx6^+$ motor neuron; unexpectedly, these cardinal classes are produced in an alternating mode from a single progenitor lineage: 3 Eve motor neurons > 1 Nkx6 motor neuron > 2 Eve motor neurons (Fig. 1e). This is surprising, and one of the few examples of a progenitor alternating cell types within its lineage (see Discussion).

The $Nkx6^+$ motor neuron projects to ventral oblique muscles

All of the $Nkx6^+$ motor neurons that have been characterized to date project to ventral body wall muscles (Broihier et al., 2004). To identify the muscle target of the Kr^+ Pdm^+ $Nkx6^+$ motor neuron in the NB7–1 lineage, we first examined single neuroblast DiI clones (Schmid et al. 1999) and looked for muscles with innervation distinct from the known U1-U5 dorsal muscle targets. DiI labeling of NB7–1 marked all clonal progeny at embryonic stage 17, and showed innervation of all known U1-U5 dorsal and lateral

longitudinal muscle targets, plus innervation of the ventral oblique muscles 15, 16, and 17 via the intersegmental nerve d branch (ISNd) (Fig. 2A). We independently confirmed these results using *NB7–1-gal4* to drive GFP expression, which labeled all U1-U5 dorsal and lateral longitudinal muscle targets plus ventral oblique muscles in a majority of hemisegments (Fig. 2B-C; 54/93 hemisegments). These data are consistent with the $Nkx6^{+}$ Eve^{-} motor neuron in the NB7–1 lineage projecting to ventral oblique muscles, but without single neuron labeling we can't make a conclusive match.

Fig. 3.2 NB7–1 generates a motor neuron that innervates ventral oblique muscles. **(Next page)** (A) NB7–1 DiI clone (red) generated as described in Schmid et al. (1999). Green bracket, U1-U5 motor neurons innervating dorsal and lateral longitudinal muscles; magenta bracket, unknown neuron(s) innervating more ventral muscles. Scale bar: 7 μm. (B-B″) NB7–1 lineage marked by GFP (green) stained for the motor axon marker FasII (blue). Stage 17; one hemisegment shown; ventral midline, dashed at left; dorsal to the right. The NB7–1 lineage produces motor neurons branching out to innervate dorsal and lateral longitudinal muscles (green bracket) and ventral muscles (magenta bracket), similar to the DiI clone in panel A. Scale bar: 10 μm. (C) Schematic of muscle groups, including the ventral oblique muscles (magenta) and the dorsal and lateral longitudinal muscles (green). The U1-U5 motor neurons of the NB7–1 lineage project to dorsal and lateral longitudinal muscle targets through the ISN (black line), while an unidentified subset of NB7–1 progeny project to ventral oblique muscle targets through ISNd.

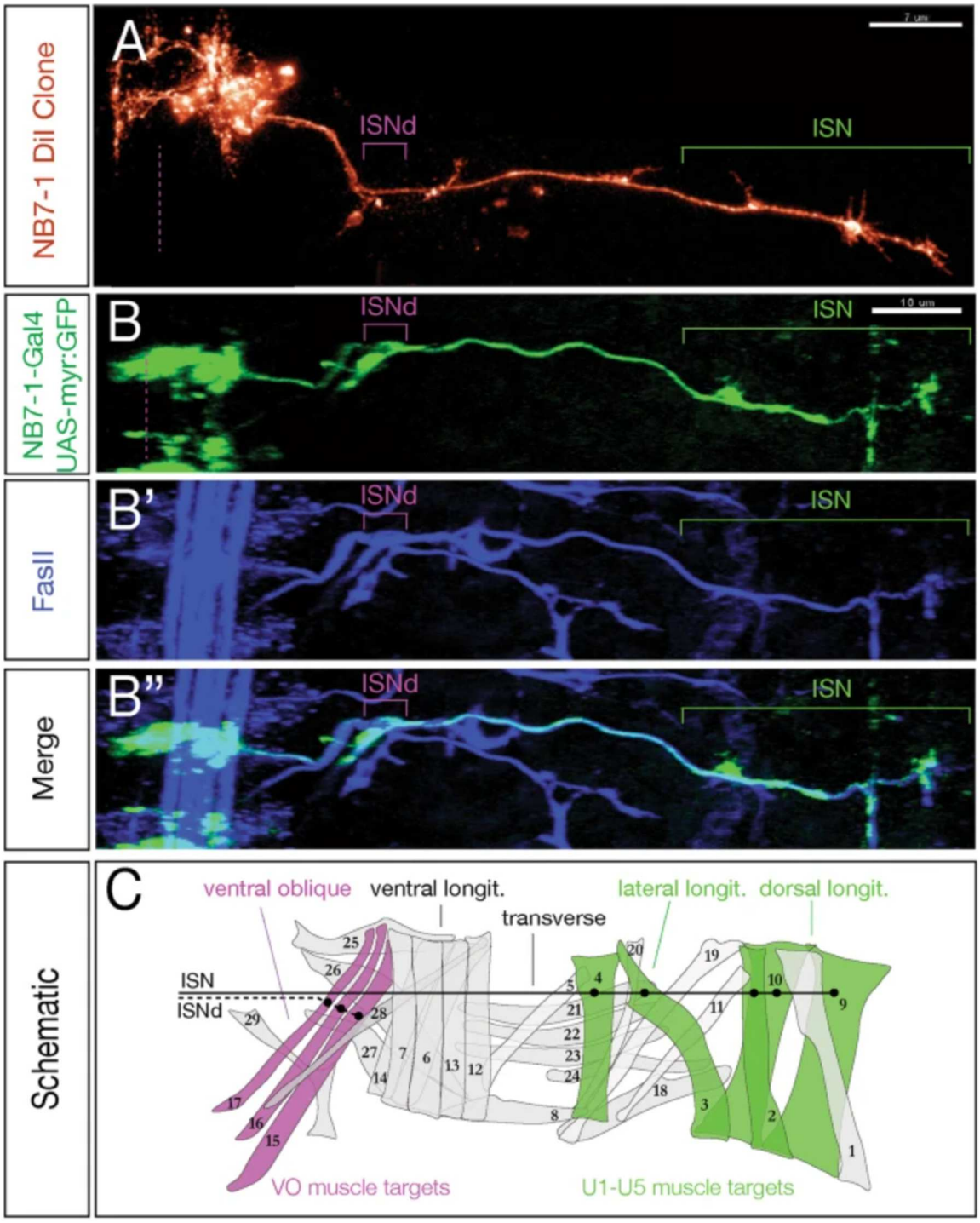
NB7-1 DiI Clone
A
ISNd
ISN
NB7-1-Gal4
UAS-myr:GFP
B
ISNd
ISN
FasII
B'
ISNd
ISN
Merge
B''
ISNd
ISN
Schematic
C
ventral oblique
ventral longit.
transverse
lateral longit.
dorsal longit.
ISN
ISNd
VO muscle targets
U1-U5 muscle targets

To visualize the morphology of individual motor neurons in the NB7–1 lineage, we generated single cell flip out clones (see methods for genotype) to stochastically label single neurons with HA (Fig. 3A‘). In addition, we used GFP to label all neurons in the lineage and FasII to detect all motor axons and their muscle targets (Fig. 3A-A”’). As expected, full lineage labeling revealed innervation of ventral oblique muscles via ISNd. In addition, HA labeling identified an individual motor neuron that specifically targeted the ventral oblique muscles via ISNd (Fig. 3A’-A”’; Supp. Movie 1). This motor neuron had an ipsilateral dendritic process that approached the midline (Fig. 3A’, yellow arrow), indistinguishable from the previously identified MN17 that innervates the ventral oblique muscles (Landgraf et al., 2003). For this reason, we call the Kr^{+} Pdm^{+} $Nkx6^{+}$ motor neuron in the NB7–1 lineage the VO motor neuron.

Fig. 3.3 NB7–1 derived $Nkx6^{+}$ motor neuron projects axon to ventral oblique muscles and dendrites to the dorsal neuropil. (Next page) (A-A”‘) Single cell flip out labels a single VO motor neuron with HA (red) within the NB7–1 lineage (green). Note the single VO neuron has an axon projection to the ISNd nerve branch known to innervate the ventral oblique muscle group, and a dendritic projection to the midline (yellow arrowhead). FasII staining shows the ISN and ISNd nerves (blue). Stage 16 embryo; ventral midline, dashed line. Scale bar: 7 μm. (B-B″) Single cell flip out labels a single Eve^{-} VO motor neuron (green) with an axon projection exiting the CNS and its dendrites projecting to the dorsal-most region of the neuropil. Eve^{+} U3/U4 motor neurons, magenta; white arrows in B. Newly hatched larva; posterior (cross-section) view; dorsal up, ventral midline, dashed line; neuropil boundary, dashed circle. VO motor neuron cell body lies between the U3 and U4 neuron cell bodies (white arrows), similar to its position

in the late embryo (see Fig. 1). Scale bar: 10 μm. (C,C′) The VO motor neuron (green) is identifiable in a TEM reconstruction of the newly hatched larval CNS, previously named MN15/16/17 [26]. Note that the VO has similar morphology in both light and TEM volumes (compare panels B and C), and that the VO has a similar cell body position between U3/U4 (compare panels B′ and C′). Posterior (cross-section) view; dorsal up, ventral midline, dashed line; approximate neuropil boundary, translucent shading; only neurons in A1R are shown. Dashed box, region enlarged in D,D'. (D,D') VO and U3/U4 form postsynapses in different regions of the neuropil. Dorsal up, midline, white dashed line; only neurons in A1R are shown

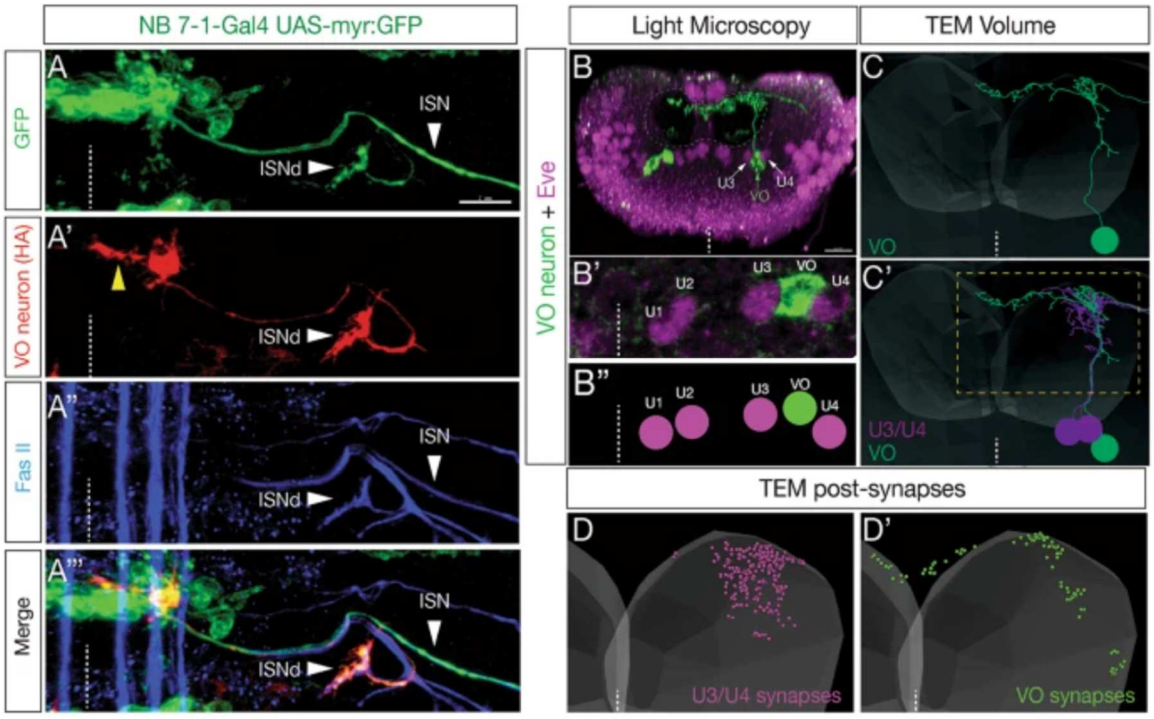

We next wanted to determine whether the Nkx6^{+} VO motor neuron and the Eve^{+} U1-U5 motor neurons have distinctive dendritic morphology or premotor innervation, as expected based on their distinctive axon targeting to different muscle groups. We repeated the sparse-HA labeling experiment in newly hatched larvae (Fig. 3B-B") so we could identify VO motor neuron morphology, and identify it in a TEM atlas of all abdominal motor neurons in newly hatched larvae (Zarin et al., 2019). We identified the NB7-1 VO motor neuron in the TEM volume based on its characteristic central nervous system (CNS) projections and cell body position between U3 and U4 (compare Fig. 3B and C). Interestingly, VO and U3/U4 motor neurons had different dendrite projections (Fig. 3C'), as well as different postsynapse locations within the neuropil (Fig. 3D,D'). Furthermore, they had distinctive premotor inputs: top inputs to VO are A06c and A18b2 interneurons, whereas top inputs to U3/U4 are A31k and A18a interneurons (Zarin et al., 2019). We conclude that the NB7-1 lineage produces two cardinal classes of motor neurons: dorsal projecting Eve^{+} motor neurons and a ventral projecting Nkx6^{+} VO motor neuron, each with distinct morphology and connectivity.

Overexpression of Kr/Pdm generates ectopic Nkx6^{+} VO motor neurons

Hb, Kr, Pdm, and Pdm/Cas each specify a distinct temporal identity within multiple neuroblast lineages (Doe, 2017). In contrast, the newly discovered Kr/Pdm temporal identity window (Averbukh et al., 2018) has not yet been tested for a role in specifying neuronal identity. Here we ask whether co-expression of Kr and Pdm can induce ectopic VO neurons. To test this hypothesis, we overexpressed Kr and Pdm together specifically in the NB7–1 lineage (*NB7–1-gal4 UAS-Kr UAS-Pdm UAS-*

myr:GFP). Controls always had an Eve^- $Nkx6^+$ $Zfh1^+$ VO motor neuron located between the Eve^+ U3 and U4 (Fig. 4a; quantified in 4c). In contrast, Kr/Pdm co-expression resulted in 2–3 additional $Nkx6^+$ $Zfh1^+$ VO motor neurons (Fig. 4b; quantified in 4c). We note that Kr/Pdm overexpression was not able to alter earlier temporal identities (Hb^+ U1/U2 and Kr^+ U3 neurons), similar to the well-characterized inability of later TTFs to alter earlier TTF cell fates (Cleary and Doe, 2006; Grosskortenhaus et al., 2006; Isshiki et al., 2001; Pearson and Doe, 2003; Tran and Doe, 2008). We conclude that Kr/Pdm TTFs can induce $Nkx6^+$ VO motor neuron identity beginning with the fourth division of the NB7–1 lineage. It is unknown if Kr/Pdm acts directly or indirectly to promote *nkx6* expression (see Discussion).

Fig. 3.4 Kr/Pdm co-expression induces ectopic $Nkx6^+$ VO motor neuron molecular identity (Next page). **A-c** Kr/Pdm overexpression (OE) induces ectopic $Nkx6^+$ VO motor neurons. (A) Control lineages (*NB7–1-Gal4 UAS-myr:GFP*) have one $Nkx6^+$ Eve^- VO motor neuron (yellow arrow). **B** Kr/Pdm overexpression (*NB7–1-Gal4 UAS-myr:GFP UAS-Kr UAS-Pdm*) increases the number of $Nkx6^+$ Eve^- VO motor neurons. **C** Quantification. Asterisk, GFP-negative EL neurons from NB3–3. Scale bar: 10 μm. **D-f** Kr/Pdm overexpression (OE) reduces Eve^+ motor neurons. **D** Control lineages (*NB7–1-Gal4 UAS-myr:GFP*) have five Eve^+ motor neurons including Hb^+ U1/U2 and $Runt^+$ U4/U5. **E** Kr/Pdm overexpression (*NB7–1-Gal4 UAS-myr:GFP UAS-Kr UAS-Pdm*) reduces the number of Eve^+ U4/U5 motor neurons. **F** Quantification. Scale bar: 10 μm. **G** Summary

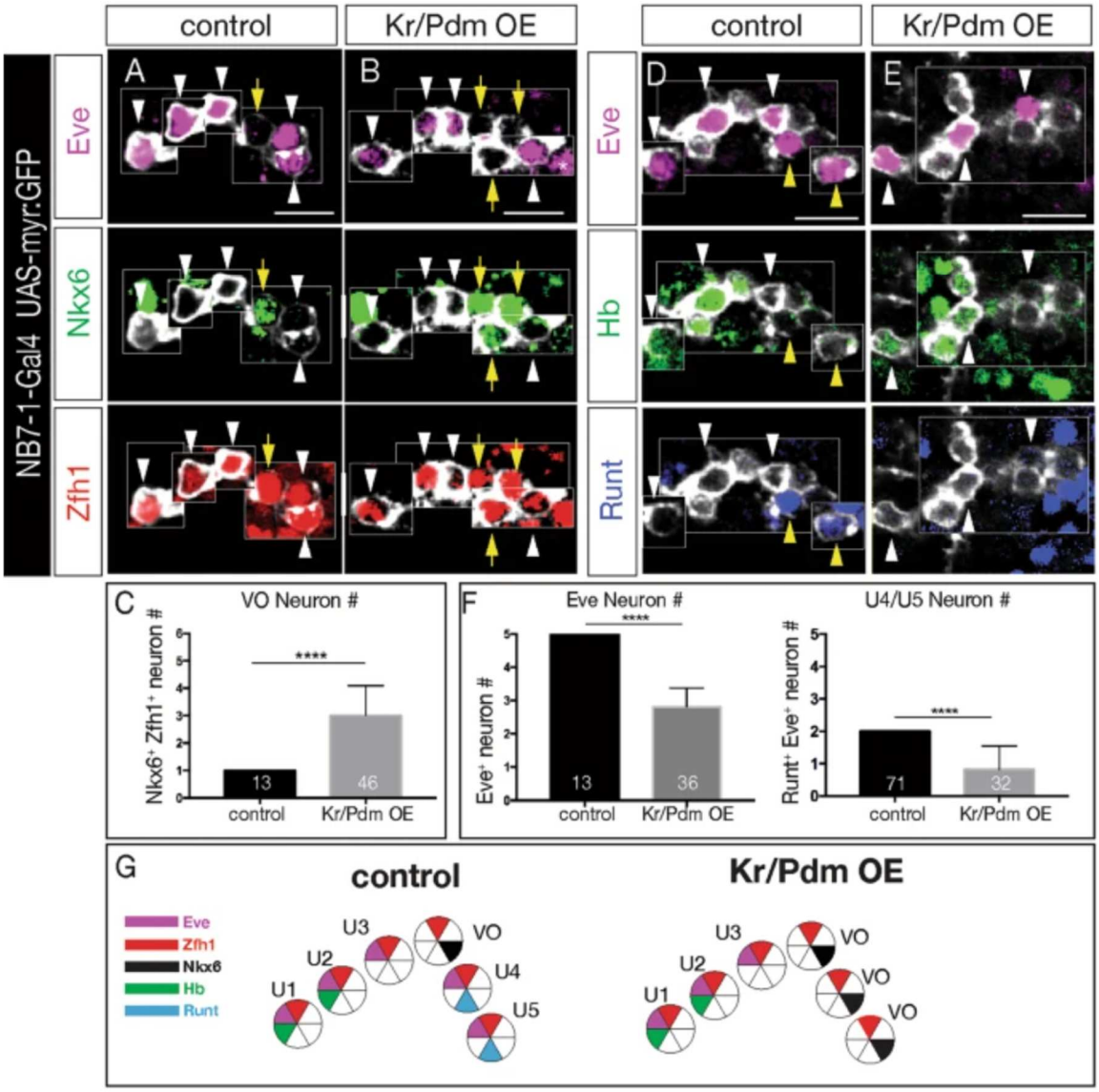
control
Kr/Pdm OE
control
Kr/Pdm OE
NB7-1-Gal4 UAS-myr:GFP
Eve
Nkx6
Zfh1
Eve
Hb
Runt
A
B
D
E
C
VO Neuron #
Nkx6⁺ Zfh1⁺ neuron #
****
13
46
control
Kr/Pdm OE
F
Eve Neuron #
Eve⁺ neuron #
****
13
36
control
Kr/Pdm OE
U4/U5 Neuron #
Runt⁺ Eve⁺ neuron #
****
71
32
control
Kr/Pdm OE
G
control
Kr/Pdm OE
Eve
Zfh1
Nkx6
Hb
Runt
U1
U2
U3
U4
U5
VO
VO
VO
VO

We next asked whether Kr/Pdm co-expression delays production of the later-born Eve$^+$ U4-U5 motor neurons until after birth of the ectopic VO motor neurons (lineage extension model), or replaces the Eve$^+$ U4-U5 motor neurons with ectopic VO motor neurons (conversion model). Both outcomes have been observed following misexpression of other temporal transcription factors (Kohwi et al., 2013; Meng et al., 2019; Pearson and Doe, 2003; Seroka and Doe, 2019). We overexpressed Kr/Pdm in the NB7–1 lineage (*NB7–1-gal4 UAS-Kr UAS-Pdm UAS-myr:GFP*), and assayed the fate of the Eve$^+$ U1-U5 motor neurons. In controls, we always observed five Eve$^+$ U1-U5 motor neurons, including two Runt$^+$ U4/U5 motor neurons (Fig. 4d; quantified in 4f). In contrast, Kr/Pdm overexpression led to a loss of the Runt$^+$ U4/U5 motor neurons (Fig. 4e; quantified in 4f). We conclude that overexpression of Kr/Pdm in the NB7–1 lineage generates ectopic Nkx6$^+$ VO motor neurons at the expense of the later-born U4/U5 motor neurons, supporting the conversion model (summarized in Fig. 4g).

Overexpression of Kr/Pdm generates ectopic Nkx6$^+$ motor neurons that project correctly to ventral oblique muscles

In the section above, we show Kr/Pdm overexpression can induce ectopic VO motor neurons based on molecular markers. Here we determine whether Kr/Pdm overexpression can generate ectopic VO motor neurons that project correctly to ventral oblique muscles. We used *NB7–1-gal4* to drive prolonged co-expression of Kr/Pdm, membrane targeted GFP to visualize axon projections, and FasII to identify the ISNd branch to the ventral oblique muscles. In controls, NB7–1 progeny projected in the ISNd to innervate ventral oblique muscles (Fig. 5A, S2, S3; axon volume in ISNd quantified in

Fig. 5C; Fig. S2). Following Kr/Pdm overexpression specifically in the NB7–1 lineage, we detected increased axon volume at the ISNd (Fig. 5B, S2, S3; quantified in Fig. 5C), consistent with ectopic VO motor neurons taking the normal VO pathway via ISNd to the ventral oblique muscles. To conclusively show that multiple ectopic VO motor neurons target the ISNd, we used multi-color flip out (MCFO) (Nern et al., 2015) to express HA and V5 on different neurons within the NB7–1 lineage. Following Kr/Pdm overexpression specifically in the NB7–1 lineage, we identified NB7–1 lineages with distinct HA^+ and $V5^+$ motor neurons that projected via ISNd to the ventral oblique muscles (Fig. 5D). We conclude that prolonged Kr/Pdm co-expression is sufficient to generate VO motor neurons that correctly project out of the ISNd nerve root to innervate ventral oblique muscles. Thus, Kr/Pdm induces both molecularly and morphologically normal VO motor neurons.

Fig. 3.5 Kr/Pdm induces ectopic motor neurons targeting ventral oblique muscles.

(Next page) (A-C) Kr/Pdm overexpression results in ectopic motor neuron projections to the ventral oblique muscles (arrowhead). (A) Controls (*NB7–1-gal4 UAS-myr:GFP*) show NB7–1 progeny innervating the ventral oblique muscle (ISNd). (A') Enlargement of boxed region in A. (A") GFP marking NB7–1 progeny; (A"') FasII marking all motor axons. (B) Kr/Pdm overexpression (*NB7–1-gal4 UAS-myr:GFP UAS-Kr UAS-Pdm)* induces ectopic VO motor neuron projections to the ventral oblique muscles (arrow). Scale bar: 10 μm. (C) Quantification. See Fig. S2 for methods. (D) Kr/Pdm overexpression analyzed by single neuron MCFO showing two motor neurons projecting to the ventral oblique muscles. (D') Enlargement of boxed region in D. (D", D"')

Individual motor neurons labeled with V5 or HA projecting to ventral oblique muscles.

Scale bar: 10 μm

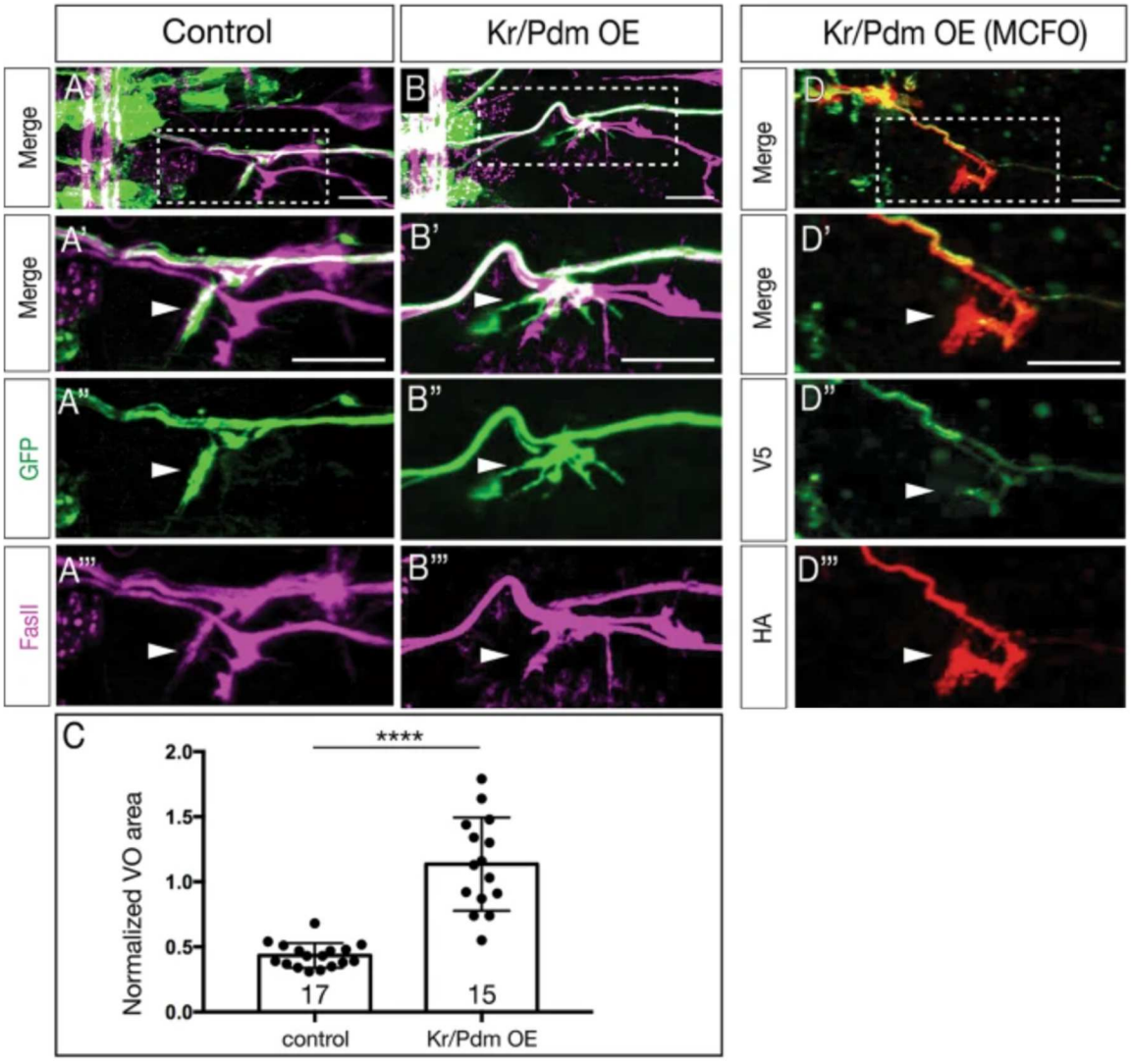

Nkx6 is necessary and sufficient to generate VO motor neurons in the NB7–1 lineage

We have shown above that the TTF combination of Kr/Pdm can induce Nkx6$^+$ motor neurons that project to the ventral oblique muscles. This raises the question of whether there is a linear genetic pathway from Kr/Pdm to Nkx6 to VO motor neuron identity, or whether Kr/Pdm drives expression of multiple genes required for VO motor neuron identity. Thus, we asked if Nkx6 alone was sufficient to specify VO motor neuron identity. In controls (*NB7–1-gal4 UAS-myr:GFP*), we always detected the U1-U5 Eve$^+$ Zfh1$^+$ motor neurons and a single Nkx6$^+$ Zfh1$^+$ VO motor neuron (Fig. 6A). In contrast, overexpression of Nkx6 (*NB7–1-gal4 UAS-myr:GFP UAS-Nkx6*), produced loss of U3-U5 Eve$^+$ motor neurons and ectopic VO motor neurons (Fig. 6B; quantified in 6E). The opposite phenotype was observed when we reduced Nkx6 levels by RNAi (*NB7–1-gal4 UAS-myr:GFP UAS-Nkx6-RNAi*): loss of the Nkx6$^+$ Zfh1$^+$ VO motor neuron and the production of a single ectopic Eve$^+$ Zfh1$^+$ motor neuron (Fig. 6C; quantified in 6E). We conclude (1) that Nkx6 is necessary to consolidate a VO motor neuron fate from the fourth GMC in the lineage, because without Nkx6 this GMC generates a sixth Eve$^+$ neuron; and (2) that Nkx6 is sufficient to specify VO motor neuron identity following production of the fourth GMC in the NB7–1 lineage.

Fig. 3.6 Nkx6 is necessary and sufficient to specify VO motor neuron molecular identity. (A) Controls (*NB7–1-gal4 UAS-myr:GFP*) have one Nkx6^{+} Eve^{-} VO motor neuron. (B) Nkx6 overexpression (*NB7–1-gal4 UAS-myr:GFP UAS-Nkx6*) results in ectopic VO motor neurons at the expense of Eve^{+} U3-U5 motor neurons. (C) Nkx6 RNAi (*NB7–1-gal4 UAS-myr:GFP UAS-Nkx6-RNAi*) lack the VO motor neuron and possess an ectopic Eve^{+} "U?" motor neuron at that location (cyan arrowhead). (D, D') Quantification. I Summary. Scale bars, 5 μm

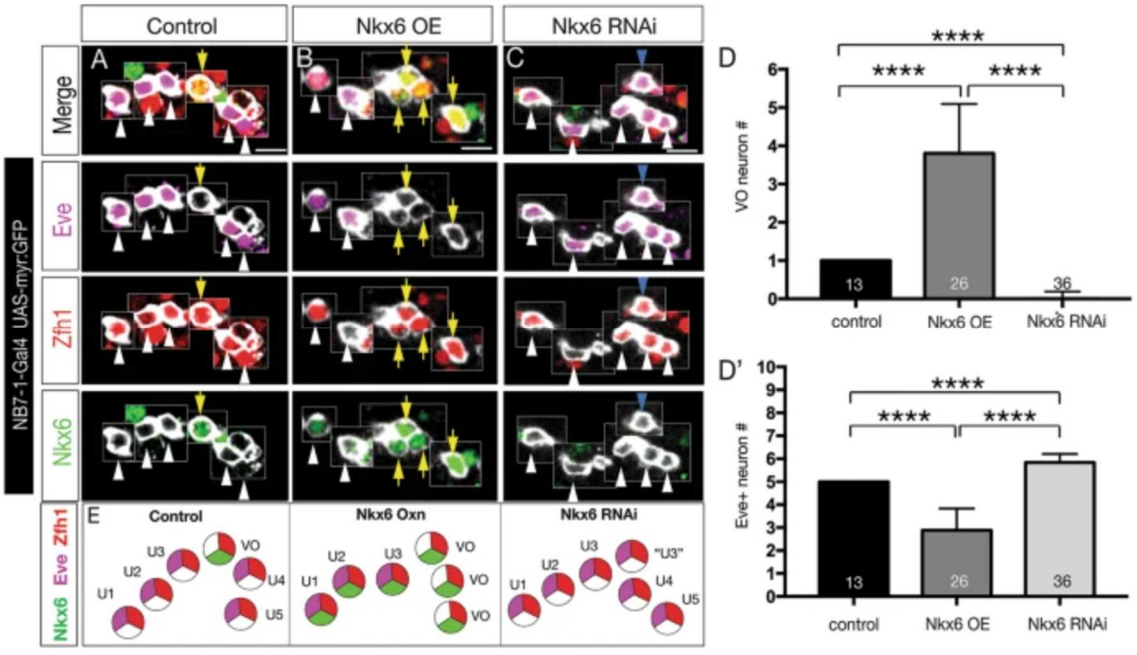

We next asked whether Nkx6 was sufficient to generate VO motor neurons that correctly target the ventral oblique muscles. In wild type, NB7–1 always generated a

motor neuron that exits the ISNd and targets ventral oblique muscles (Fig. 7a; volume of ISNd projections quantified in 7d). Overexpression of Nkx6 in the NB7–1 lineage generated additional innervation of the ISNd and ventral oblique muscles (Fig. 7b; quantified in Fig. 7d, S3). Importantly, the same phenotype was observed when individual neurons within the NB7–1 lineage are labeled by MCFO, showing that two distinct neurons in the lineage innervate ISNd (Fig. 7c), showing that at least one ectopic VO neuron can accurately project out the ISNd. These results are summarized in Fig. 7e. Conversely, when we reduced Nkx6 levels by RNAi (*NB7–1-gal4 UAS-myr:GFP UAS-Nkx6-RNAi*), we detected a loss of ISNd projections (Fig. 7f; compare to Fig. 7a). We conclude that Nkx6 is necessary and sufficient to generate VO motor neurons that project via ISNd to the ventral oblique muscles. Moreover, our data support a linear pathway in which the Kr/Pdm TTFs induce Nkx6 expression which specifies the molecular and morphological features of the VO motor neuron (see Discussion).

Fig. 3.7 Nkx6 is necessary and sufficient to specify VO motor neuron axon targeting to ventral oblique muscles. (Next page) a In controls (*NB7–1-gal4 UAS-myr:GFP*), NB7–1 progeny project to the ventral oblique muscles. **B** Nkx6 overexpression (*NB7–1-gal4 UAS-myr:GFP UAS-Nkx6*) leads to ectopic projections to ventral oblique muscles. Scale bar: 10 μm. **C** MCFO labeling of single motor neurons in the NB7–1 lineage shows two different HA^+ and $V5^+$ motor neurons projecting via the ISNd to the ventral oblique muscles. Scale bar: 7 μm. **D** Quantification. **E** Summary. **F** Reducing Nkx6 levels (*NB7–1-gal4 UAS-myr:GFP UAS-Nkx6-RNAi*) decreases projections out the ISNd to the ventral oblique muscles.

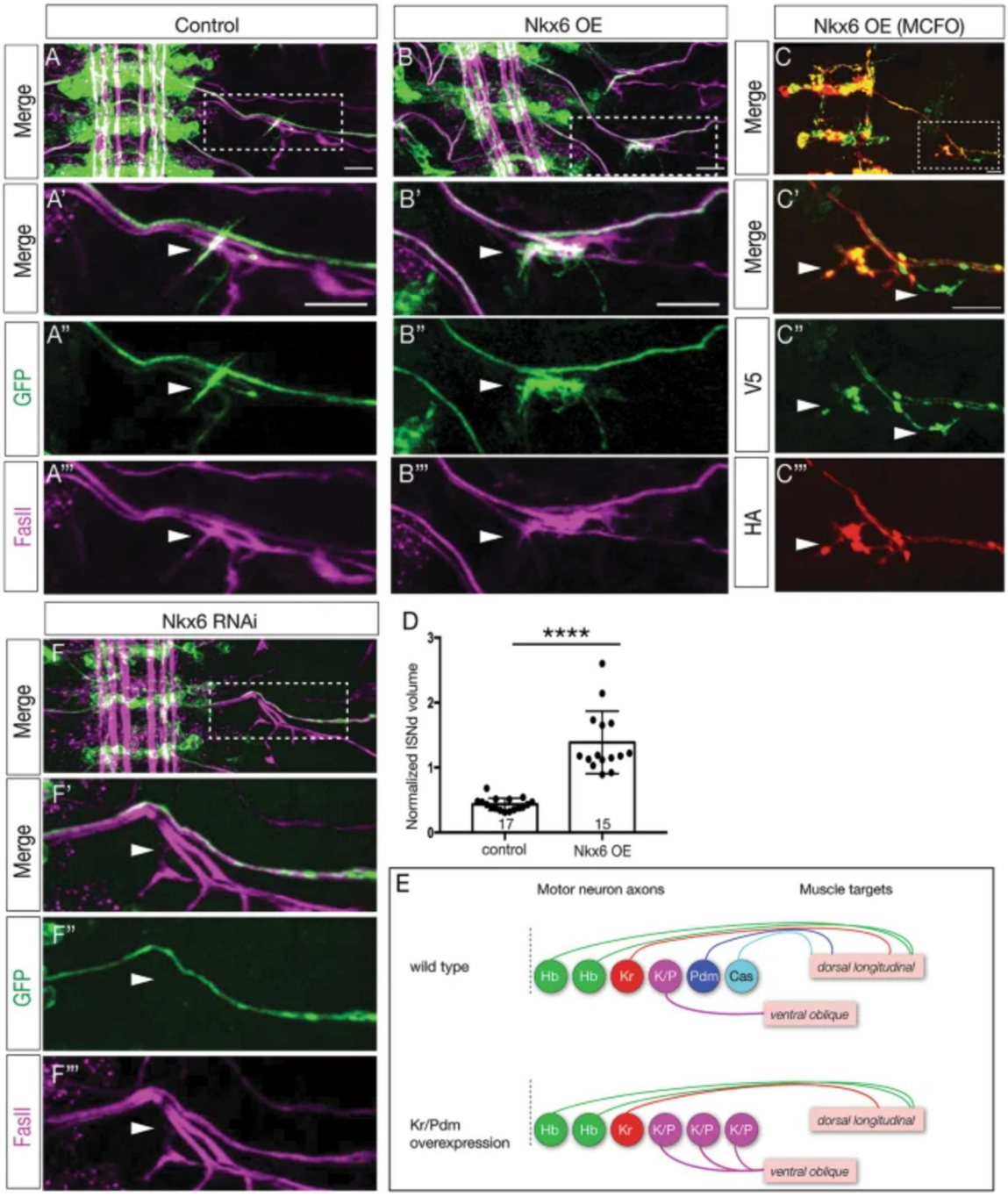
Control
Nkx6 OE
Nkx6 OE (MCFO)
Merge
GFP
FasII
V5
HA
A
A'
A''
A'''
B
B'
B''
B'''
C
C'
C''
C'''
Nkx6 RNAi
F
F'
F''
F'''
D
****
Normalized lSNd volume
17
15
control
Nkx6 OE
E
Motor neuron axons
Muscle targets
wild type
Hb
Hb
Kr
K/P
Pdm
Cas
dorsal longitudinal
ventral oblique
Kr/Pdm
overexpression
K/P
K/P

Discussion:

Kr/Pdm co-expression has been detected in several neuroblast lineages (Doe, 2017; Isshiki et al., 2001), but until now there has not been evidence that this TTF combination could specify neuronal identity. We previously showed that the Kr/Pdm window generates a Kr/Pdm GMC (Averbukh et al., 2018) (Fig. S1), and here we show that this GMC generates an $Nkx6^+$ ventral-projecting motor neuron. It is unknown whether Kr/Pdm directly or indirectly activate *nkx6* expression. The *nkx6* gene lies in a 45 kb region devoid of genes, and there are only a few, sparse predicted Kr or Pdm binding sites in this genomic expanse. How do Kr and Pdm together specify one fate ($Nkx6^+$ VO motor neuron) whereas Kr or Pdm alone specify completely different fates (Eve^+ dorsal motor neurons)? It is likely that Kr/Pdm together activate a different suite of target genes than either alone. For example, Kr/Pdm together may directly activate nkx6 expression, whereas neither alone has that potential. The emergence of single cell transcriptome and ChIP studies (Stuart and Satija, 2019) will help to reveal how the combination of Kr/Pdm TTFs generates different cell fate output compared to Kr or Pdm alone.

The production of an $Nkx6^+$ VO motor neuron in Kr/Pdm window interrupts the sequential production of Eve^+ dorsal motor neurons in the NB7–1 lineage, resulting in an Eve>Nkx6 > Eve alternation of cardinal motor neuron production within the lineage. This is unusual, as in most cases neurons with similar morphology or function are produced together in a lineage. In mammals, progenitors generate neurons first, followed by glia (Kohwi and Doe, 2013), we know of no examples of neuron>glia>neuron production from a single lineage. Similarly, *Drosophila* central brain neuroblast lineages produce the

mushroom body γ neurons, then α'/ β' neurons, and lastly α/β neurons, with no evidence for alternating or interspersed fates (Lee et al., 1999). In the abdominal NB3–3 lineage, the early-born cells are in a mechanosensitive circuit, whereas the late-born cells are in a proprioceptive circuit (Wreden et al., 2017). To our knowledge, the only possible example of interleaved production of two morphological classes of neurons is in the *Drosophila* lateral antennal lobe neuroblast lineage, which alternate between uniglomerular and multiglomerular (AMMC) projection neurons (Lin et al., 2012). The use of clonal and temporal labeling tools will be needed to examine additional lineages to determine the prevalence of lineages producing temporally interleaved neuronal subtypes as in the NB7–1 lineage.

Overexpression of Kr/Pdm or Nkx6 can induce only 2–3 ectopic VO motor neurons within the NB7–1 lineage. Clearly not all neurons in the lineage are competent to respond to these transcription factors. Early-born temporal identities specified by Hb and Kr (U1-U3) are unaffected by Kr/Pdm or Nkx6 overexpression, which is similar to previous data showing that early temporal fates are not affected by overexpression of later TTFs in multiple lineages (Cheesman et al., 2004; Grosskortenhaus et al., 2006; Tran and Doe, 2008). It remains a puzzle why the Kr^+ U3 neuron does not switch to a VO fate upon overexpression of Kr/Pdm. There may need to be an equal level of Kr and Pdm to specify VO fate, although this would not explain why Kr/Pdm overexpression converts the Pdm^+ U4 motor neuron to a VO fate. Alternatively, there may be an early chromatin landscape that blocks access to relevant Pdm target loci.

We note that our assay of VO neuronal identity was done in newly-hatched larvae. Although motor circuits are functional at this time, larvae grow for five more days. We

have no data on whether the ectopic VO motor neurons are functional or are maintained through the life of the larvae. This would be an important question for the future.

Nkx6 and Eve have cross-repressive interactions (Broihier et al., 2004), but with some limitations: early-born Eve^+ motor neurons are not affected by Nkx6 overexpression (our work and Broihier et al., 2004; Cheesman et al., 2004). Wild type animals even show sporadic expression of Nkx6 in the Eve^+ U2 motor neuron (data not shown), but in these neurons it has no effect on Eve expression, nor does it promote targeting to ventral oblique muscles. There appears to be a mechanism to block endogenous or overexpressed Nkx6 function in the early lineage of neuroblasts producing Eve^+ motor neurons. The mechanism "protecting" early-born Eve^+ neurons from Nkx6 repression of Eve is unknown. Early lineages may lack an Nkx6 cofactor; Nkx6 could act indirectly via an intermediate transcription factor missing in early lineages; the early TTFs Hb or Kr may block Nkx6 function; or the *eve* locus could be in a subnuclear domain inaccessible to Nkx6.

Nkx6 promotes motor neuron specification in both *Drosophila* and vertebrates (Broihier et al., 2004; Cheesman et al., 2004; Sander et al., 2000). In Drosophila, loss of Nkx6 reduces ventral projecting motor neuron numbers and increases the number of Eve^+ neurons, while overexpression increases ventral projecting motor neuron numbers at the expense of Eve^+ neurons (our work and Broihier et al., 2004). In vertebrates the Nkx6 family members Nkx6.1/Nkx6.2 appear to play a broader role in motor neuron specification. Nkx6.1/Nkx6.2 show early expression throughout the pMN domain; mice mutant for both Nkx6 family members lack most somatic motor neurons; and Nkx6.1 overexpression in chick or zebrafish can induce ectopic motor neurons (Briscoe et al.,

2000; Cheesman et al., 2004; Sander et al., 2000). It would be interesting to investigate whether vertebrate Nkx6.1/Nkx6.2 are required to suppress a specific motor neuron identity, similar to the antagonistic relationship between Nkx6 and Eve in *Drosophila*.

Neuroblasts in all regions of the *Drosophila* CNS (brain, ventral nerve cord, optic lobe) use TTF cascades to generate neuronal diversity (Allan and Thor, 2015; Doe, 2017; Holguera and Desplan, 2018; Miyares and Lee, 2019) yet less is known about TTF target genes. It is likely that TTFs induce expression of suites of transcription factors that persist in neurons and confer their identity. Examples may include the "morphology transcription factors" that specify adult leg motor neuron dendrite projections (Enriquez et al., 2015) but in this case it remains unknown whether these transcription factors control all other aspects of adult motor neuron identity. It is possible that "morphology transcription factors" are one module downstream of a broader regulatory tier similar to the terminal selector genes in *C.* elegans (Hobert, 2016).

We identified a linear pathway from Kr/Pdm to Nkx6 which specifies VO motor neuron identity. TTFs could act by two non-mutually exclusive mechanisms: inducing a stable combinatorial codes of transcription factors that consolidate neuronal identity, or by altering the chromatin landscape to have a heritable, long lasting effect on motor neuron gene expression. Our observation that Nkx6 is maintained in the VO neuron after fading of Kr/Pdm expression (data not shown) supports the former mechanism. Identification of Kr/Pdm or Nkx6 target genes would give a more comprehensive understanding of TTF specification of neuronal identity.

The results presented in this work lead to several interesting directions. Other embryonic VNC lineages exhibit a Kr/Pdm window; does this window generate neurons

in these lineages? Are there common features to neurons born in the Kr/Pdm window? Furthermore, do ectopic VO neurons make functional presynapses with the ventral oblique muscles, and do they have the normal inputs to their dendritic postsynapses? In only a few cases has it been shown the TTF-induced neurons are functionally integrated into the appropriate circuits (Meng et al., 2019). Kr and Pdm orthologs have been identified in vertebrates. Looking for dual expression of Kr and Pdm orthologs in vertebrates may reveal a role in specifying temporal identity, similar to evidence for Hb and Cas TTFs having vertebrate orthologs that specify temporal identity (Alsiö et al., 2013; Elliott et al., 2008; Mattar et al., 2015; Mattar et al., 2020).

Methods:

Fly stocks

Male and female *Drosophila melanogaster* were used. The chromosomes and insertion sites of transgenes (if known) are shown next to genotypes. Previously published gal4 lines, mutants and reporters used were: *NB7–1-gal4*^{KZ} (II) [21], called *NB7–1-gal4* here; *10XUAS-IVS-myr::sfGFP-THS-10xUAS(FRT.stop)myr::smGdP-HA* (RRID:BDSC_62127); *UAS-nkx6* (RRID:BDSC_9932); *UAS-nkx6*^{RNAi} (RRID:BDSC_61188); *UAS-Kr* (II and III) [15, 17]; *UAS-Pdm2* (II and III) [16, 28]; *hs-FLPG5.PEST.Opt* (RRID:BDSC_77140); *hs-FLPG5.PEST, 10xUAS(FRT.stop)myr::smGdP-OLLAS 10xUAS(FRT.stop)myr::smGdP-HA 10xUAS(FRT.stop)myr::smGdP-V5-THS-10xUAS(FRT.stop)myr::smGdP-FLAG* (RRID:BDSC_64086).

Immunostaining and imaging

Primary antibodies were: mouse anti-Eve (5 μg/mL, DSHB, 2B8), rabbit anti-Eve #2472 (1:100, Doe lab), mouse anti-FasII (1:50, DSHB, 1D4), chicken anti-GFP (1:1000, RRID:AB_2307313, Aves Labs, Davis, CA), rabbit anti-HA epitope tag, DyLight™ 549 conjugated (1:100, Rockland, 600–442-384, Limerick, PA), rat anti-HA (1:100, MilliporeSigma, 11,867,423,001, St. Louis, MO), guinea pig anti-Hey (1:1000, gift from S. Bray, University of Cambridge), guinea pig anti-Kr (1:500, Doe lab), rat anti-Nkx6 (1:500, gift from J. Skeath, Washington University in St. Louis), rat anti-Pdm2 (abcam, ab201325, Cambridge, MA), guinea pig anti-Runt (1:1000, gift from C. Desplan, New York University), chicken anti-V5 (Bethyl Laboratories, Inc. A190-118A, Centennial, CO), rabbit anti-Zfh1 (1:1000, gift from R. Lehman, New York University), guinea pig anti-Zfh1 (1:1000, gift from J. Skeath, Washington University in St. Louis), and. Fluorophores-conjugated secondary antibodies were from Jackson ImmunoResearch (West Grove, PA) and were used at 1:200.

Embryos and the whole newly hatched larvae were fixed and stained as previously described [21]. In some cases, larval brains were dissected in PBS, fixed in 4% paraformaldehyde, and then stained by following protocols as described [21]. The samples were mounted either in Vectashield (Vector Laboratories, Burlingame, CA) or DPX [41].

Images were captured with a Zeiss LSM 710 or Zeiss LSM 800 confocal microscope with a *z*-resolution of 0.35 μm. Due to the complex 3-dimensional pattern of each marker assayed, we could not show NB7–1 progeny marker expression in a maximum intensity projection, because irrelevant neurons in the z-axis obscured the

neurons of interest; thus, NB7–1 progeny were montaged from their unique z-axis position while preserving their X-Y position. This was done in Figs. 1, 4, and 6. Images were processed using the open-source software FIJI (https://fiji.sc). Figures were assembled in Adobe Illustrator (Adobe, San Jose, CA). Three dimensional reconstructions, and level adjustments were generated using Imaris (Bitplane, Zurich, Switzerland). Any level adjustment was applied to the entire image.

Quantification of normalized ISNd volume

In order to generate a reliable volume metric for determining changes to the size of the ISNd nerve, FasII staining was used to identify SNc in a 3D IMARIS volume of the confocal image stack in order to normalize for variance in embryonic age and development. SNc was chosen to normalize against as we observed it to be unaffected by our genetic manipulations. Default parameters were used to generate a surface over the FasII channel labeling SNc and ISNd respectively, generating precise volume measurements. We then used these volume measurements to generate a ISNd/SNc ratio which was used for statistical analysis (see Fig. S1). This metric exhibited low variance across the wildtype controls, allowing for accurate comparison to genetically manipulated embryos.

Statistics

Statistical significance is denoted by asterisks: ****$p < 0.0001$; ***$p < 0.001$; **$p < 0.01$; *$p < 0.05$; n.s., not significant. The following statistical tests were performed: Mann-Whitney U Test (non-normal distribution, non-parametric) (two-tailed p value)

(Figs. 4c, f, i, j, 6D); Welch's t-test (normal distribution, non-parametric) (two-tailed *p* value) (Figs. 5C, 7d). All analyses were performed using Prism8 (GraphPad). The results are stated as mean ± s.d., unless otherwise noted.

Contributions

A.Q.S., S.-L.L and C.Q.D. conceptualized the work. A.Q.S., R.M.Y. and S.-L.L. performed experiments and analyzed results. All authors contributed to writing the manuscript. The author(s) read and approved the final manuscript.

CHAPTER IV

CONCLUDING SUMMARY

Constructing the nervous system requires the complex coordination of spatial and temporal gene expression. First, early patterning genes segment the developing embryo into regions. One of these regions adopts a neuroectodermal fate, and is further segmented into a grid along the AP-DV axes by spatial patterning. Each of the segments of the grid generates a neuroblast, which delaminates from the neuroectoderm to begin generating their respective neuronal lineages. As each NB undergoes a series of asymmetric divisions they undergo temporal patterning, diversifying each lineage. The temporal identity of each neuron sets up hierarchical regulation of downstream TFs which coordinately regulate higher-order identity features such as axonal and dendritic targeting, molecular identity, neurotransmitter fate and electrophysiological properties. This robust developmental process generates the appropriate neurons in the correct spatial location and time during development, ensuring the wiring of circuits crucial for animal behavior and survival.

While this model explains many features of early neurogenesis, there are many remaining questions concerning the relationship of these developmental determinants to terminal circuit wiring and function in the adult animal. The development of newer, high-throughput techniques to understand gene regulation in neural progenitors and their progeny is essential to a full understanding of circuit function. Recent work has demonstrated the power of transcriptomics to uncover new information about neurogenesis. Targeted DamID was recently used to profile the genomic binding sites of Hunchback in VNC NB lineages 5-6 and 7-4, which generate unqiue and identifiable

progeny (Sen et al. 2019). These experiments revealed that Hunchback binds different genomic targets in each lineage, and that each neuroblast exhibits different heterochromatin structure. Interestingly, the open chromatin states of NB5-6 and 7-4 correlate with the binding sites of the early spatial factors that establish neuroblast identity in early development. Together, these experiments describe a model in which early spatial factors establish neuroblast-specific open chromatin domains, which are acted upon differentially by temporal patterning, allowing the same temporal transcription factor to give rise to completely different progeny in different neuroblast lineages.

Another recent study used single-cell RNA sequencing in the larval optic lobe to reveal a surprising level of complexity in the temporal cascade and identify new temporal transcription factors. In this work, Konstantinides et al. (2021) identify 12 distinct temporal windows in optic lobe neuroblasts, that along with 5 spatial patterning domains and $Notch^{ON/OFF}$ hemilineage determination comprehensively explains the generation of roughly 120 distinct neuronal celltypes in the optic lobe. This work also demonstrates that not all temporal transcription factors have equivalent function: some TTFs directly control temporal progression by activating the next TTF in the cascade and repressing the previous one, while other perform a more complex function of integrating activating and inhibitory singlas from several other TTFs (Konstantinides et al. 2021). Use of this new methodology revealed that temporal patterning is more complex than previously thought, and many open questions remain to be addressed.

While recent advances have elucidated the mechanisms that shape neuronal identity in the *Drosophila* embryo, the relatively little is known about the relationship

between vertebrate lineage and neuronal identity. It is likely that similar mechanisms specify neuronal identity in higher organisms, such as mammals, and applying similar technological advances to these systems will likely yield advances in the field of stem cell therapeutics. Recent advances have been made in the application of single-cell transcriptomics to understanding human brain development, and highlight differences in neurogenesis between mice and humans. In mouse, excitatory cortical neurons are derived from cortical progenitors, while inhibitory interneurons are derived from progenitors located in the ganglionic eminence (Anderson et al, 2001). Recent work from the Nowakowski lab led to the development of a barcoding strategy to enable clonal lineage tracing of more than 1,900 human cortical progenitors and demonstrates that human cortical progenitors can generate both excitatory and inhibitory neuronal progeny, in stark contrast to cortical neurogenesis in the mouse (Delgado et al. 2021). Without the application of cutting-edge genomic strategies, it would have been difficult to elucidate these subtle differences between human and mouse neurogenesis.

Ultimately, addressing the genetic control of neurogenesis in flies, zebrafish, mouse and human tissue is necessary to paint a complete picture of how diverse populations of neurons arise in the embryo. This work will drive progress in the field of human stem cell therapeutics, with the goal of comprehensively understanding the regulation of gene networks that give rise to particular neuronal fates. Using insights from model organisms the field will be able to move towards customized therapeutic approaches for human patients, such as inducing patient-derived fibroblasts into a pluripotent state, and using combinations of transcription factors to reliably patterns these induced progenitors into the correct types of neurons for transplantation back into the

patient. These approaches will revolutionize regenerative therapies, and provides hope for patients dealing with neurological disorders such as ALS, or spinal cord injury.

APPENDIX A

SUPPLEMENT TO CHAPTER II

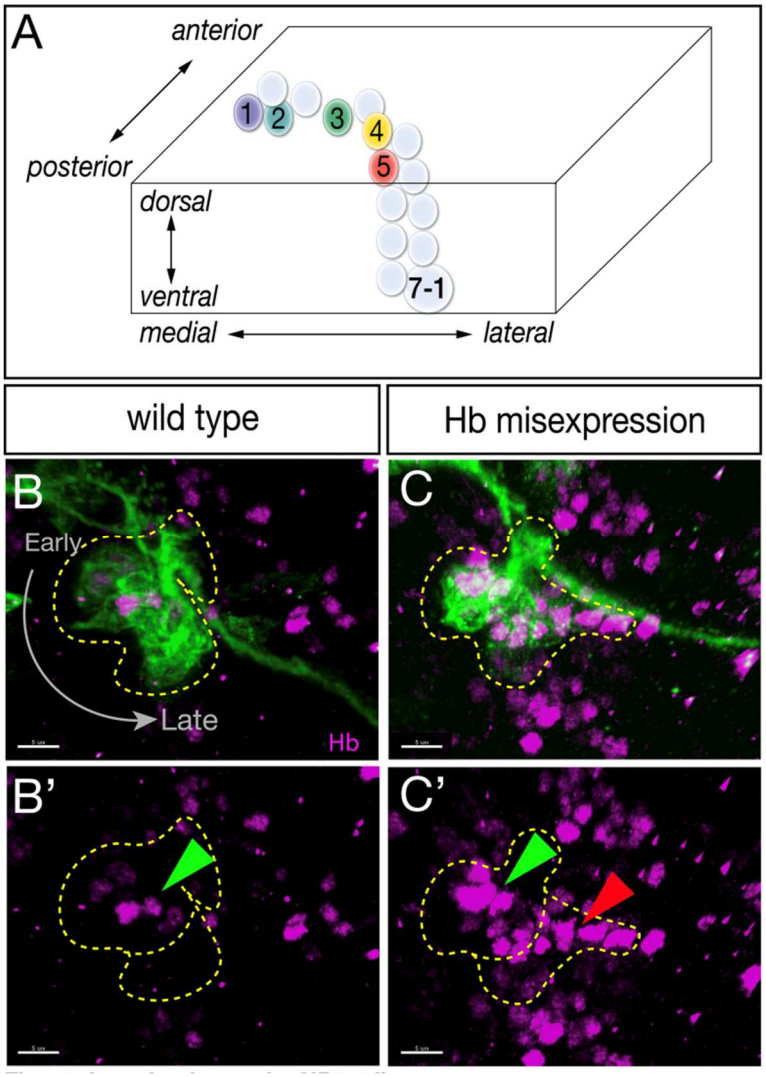

Fig. S1: Introduction to the NB7-1 lineage
(A) NB7-1 moves laterally as it divides, resulting in early-born neurons (U1-U2) having a medial position and later-born neurons (U3-U5) having a more lateral position (Pearson et al., 2003). **(B)** In wild type, NB7-1-Gal4 used for dense MCFO shows most or all progeny (green), but only medial cells in the lineage are Hb+ (magenta, green arrowhead); lineage outlined in dashed lines. **(C)** Hb misexpression (magenta) throughout the NB7-1 lineage results in Hb+ early-born neurons (green arrowhead) and Hb+ late-born neurons (red arrowhead); most of these late-born neurons have an early temporal identity (Kohwi et al., 2013).

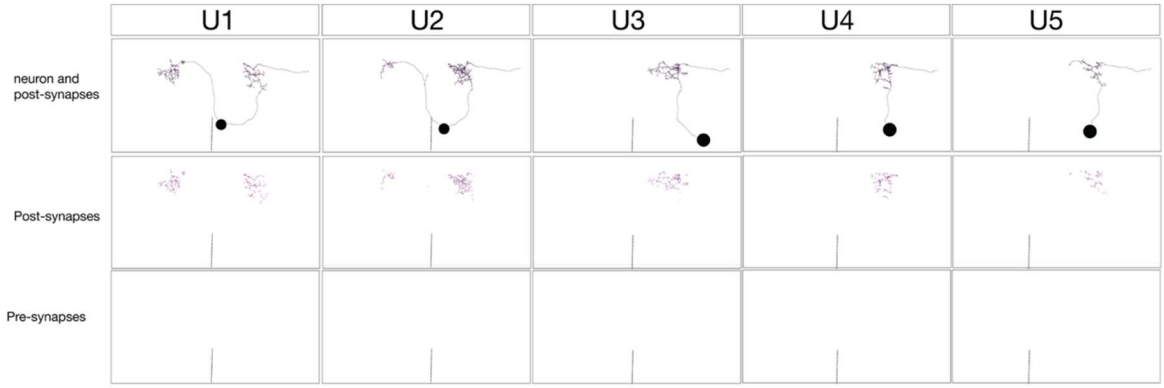

Fig. S2: U1-U5 motor neurons have dendrites within the neuropil that have abundant post-synaptic input but no pre-synaptic output.
Serial section transmission electron microscopy volume of the entire newly hatched larval CNS contains U1-U5 motor neurons in segment A1 left (black tracing, top row). U1-U5 were identified by their unique neuronal morphology and dendritic arbor location in the neuropil (see Methods). Top row: U1-U5 neurons with post-synapses shown (blue dots). Middle row: the post-synapses are shown (blue dots). Bottom row: the pre-synapses are shown; there are no pre-synapses, and thus we call the CNS arbors "dendritic." Midline, dashed line.

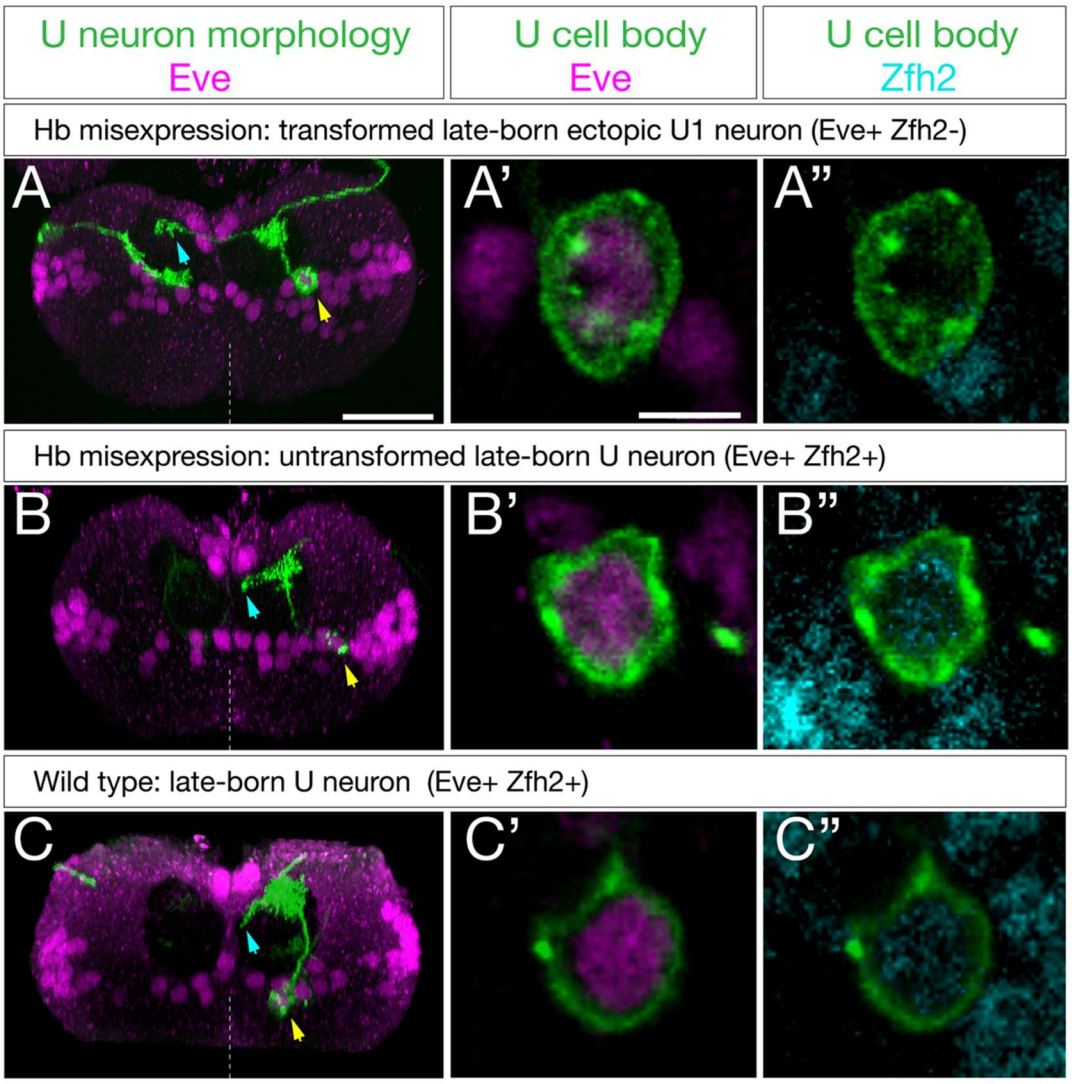

Fig. S3: U neurons that fail to repress Zfh2 fail to project contralaterally.
(A) Representative example of Hb misexpression in the NB7-1 lineage transforming later-born, laterally-positioned U neurons into an ectopic U1 identity based on Zfh2 repression and contralateral dendrite projections. (A', A'') Enlargement of somata shown in (A). (B) Representative example of Hb misexpression in the NB7-1 lineage failing to transform a later-born, laterally-positioned U neuron-based failure to repress Zfh2 and failure to extend a contralateral dendrite projection. (B', B'') Enlargement of somata shown in (B). (C) Representative example of a wild type later-born, laterally-positioned U3-U5 neuron based Zfh2 expression and failure to extend a contralateral dendrite projection. (C', C'') Enlargement of somata shown in (C). Posterior view, dorsal up, midline dashed. Scale bars, 15μm (A,B,C), 5 μm (other panels).

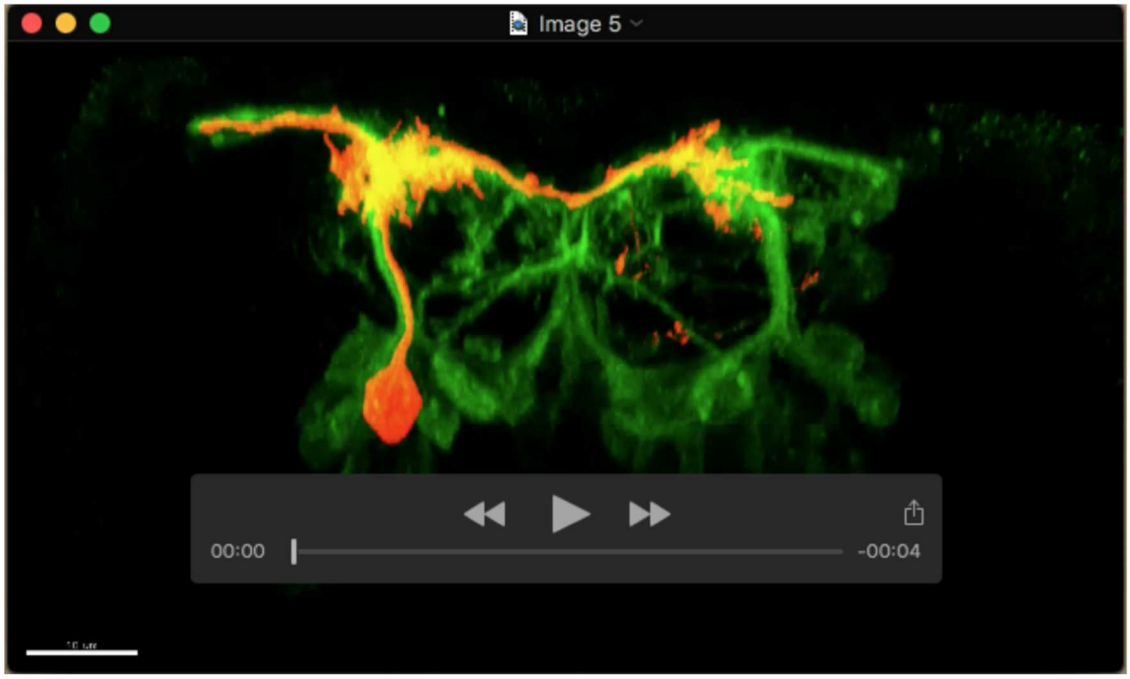

Movie S4: 3D morphology of an ectopic U1 motor neuron within a NB 7-1 clone.
Hb misexpression (NB7-1-Gal4 KZ UAS-hb UAS-MCFO) assayed by MCFO labeling in L1 larvae, showing an ectopic U1 neuron (red; defined by its lateral cell body position, monopolar morphology, and contralateral projection) in the context of rest of the NB 7-1 clone (green).

URL: https://movie.biologists.com/video/10.1242/dev.175570/video-1

Movie S5: 3D morphology of an ectopic U1 motor neuron within a NB 7-1 clone.
Hb misexpression (NB7-1-Gal4^{KZ} UAS-hb UAS-MCFO) assayed by MCFO labeling in L1 larvae, showing an ectopic U1 neuron (red; defined by its lateral cell body position, monopolar morphology, and contralateral projection) alone.

URL: https://movie.biologists.com/video/10.1242/dev.175570/video-2

APPENDIX B

SUPPLEMENT TO CHAPTER III

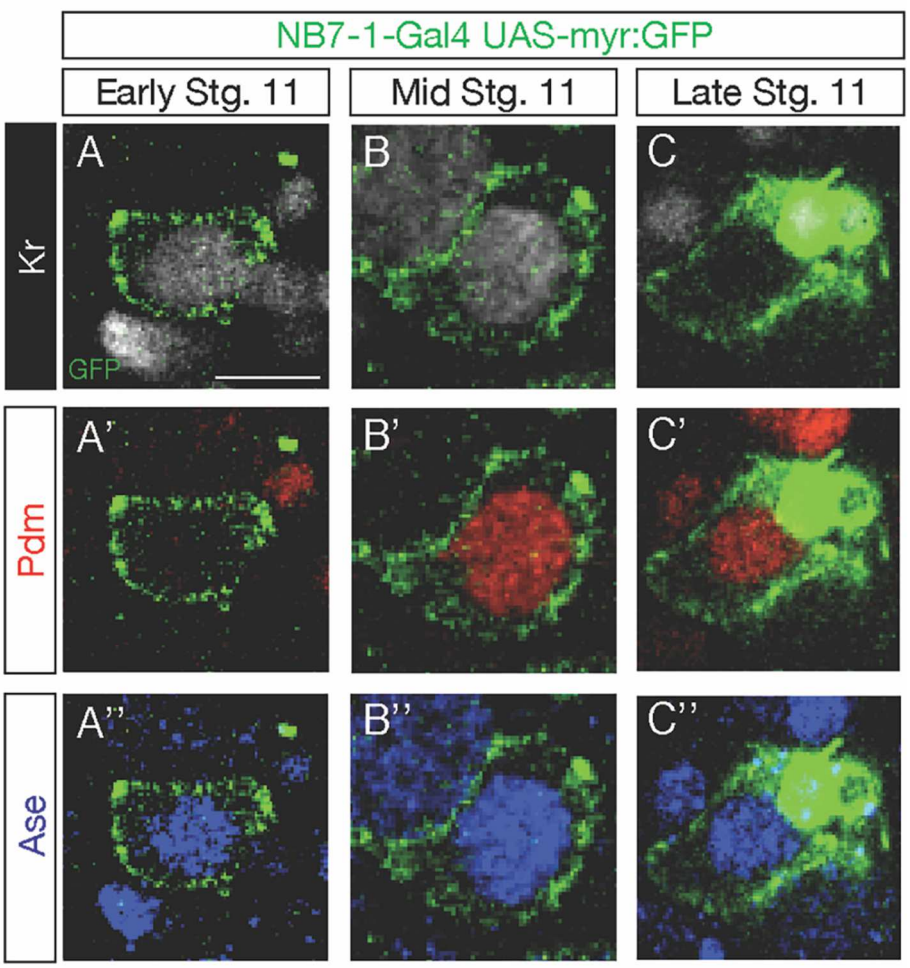

Fig. S6: NB7–1 sequentially expresses Kr, Kr/Pdm, and Pdm.
NB7–1 is identified by expression of NB7–1-Gal4 UAS-myr:GFP (green) and Asense (Ase; blue). (A) At early stage 11, NB7–1 is Kr^{+} Pdm^{-}. (B) At mid stage 11, NB7–1 is Kr^{+} Pdm^{+}. (C) At late stage 11, NB7–1 is Kr^{-} Pdm^{+}. Scale bar: 5 μm.

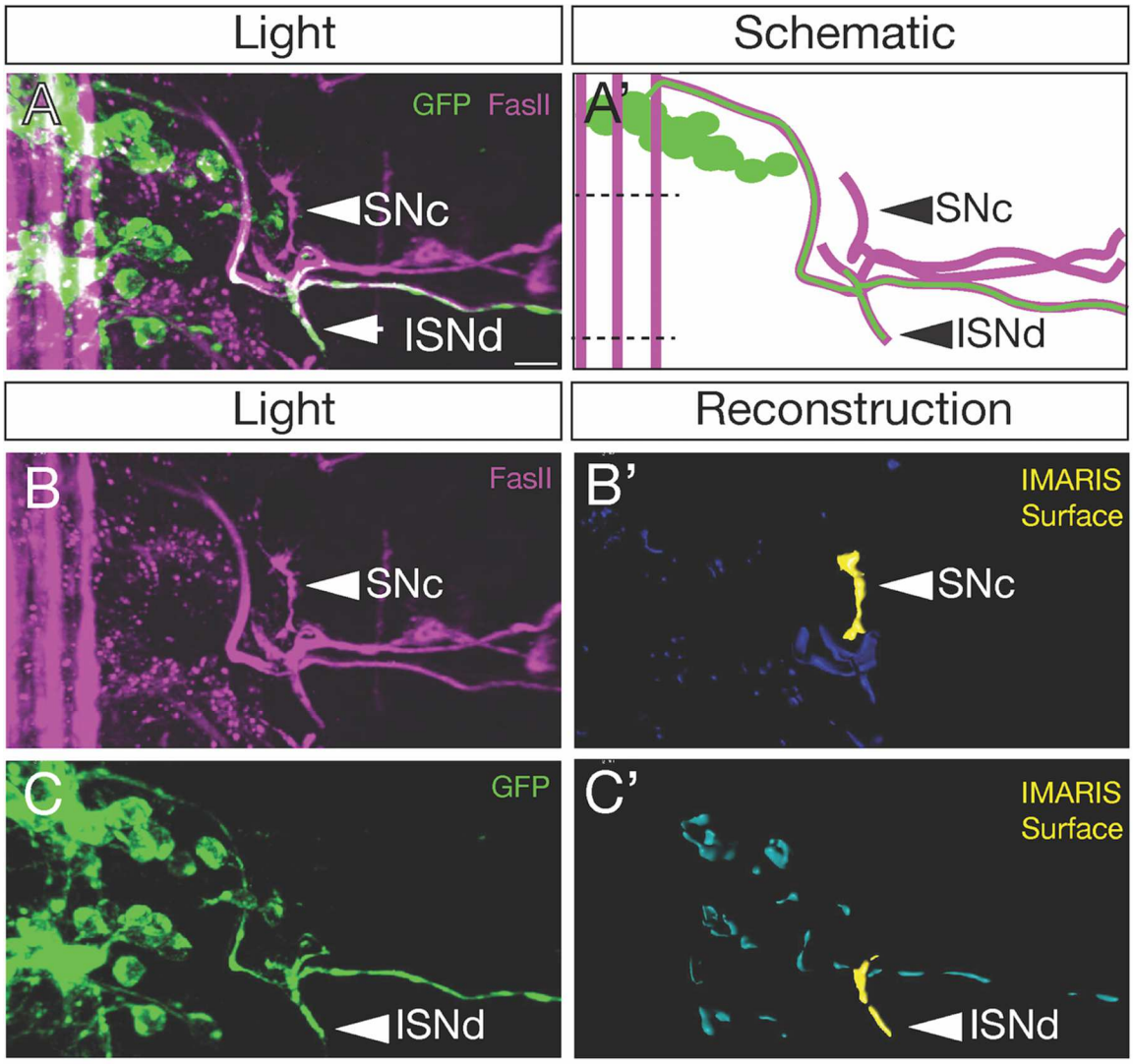

Fig. S7: Methodology for quantifying ISNd and SNc motor neuron localization.
(A,A') The volume of the ISNd was normalized to that of SNc to account for slight differences in embryo staging. ISNd and SNc were identified by the pan-motor axon marker FasII (magenta) in embryos expressing GFP (green) in the NB7–1 lineage (NB7–1-gal4 UAS-GFP). (B,B′) FasII (magenta) was used to identify SNc in a maximum intensity projection, and the volume quantified using the Imaris Surface function. (C,C′) FasII (magenta) was used to identify ISNd in a maximum intensity projection, and the volume quantified using the Imaris Surface function.

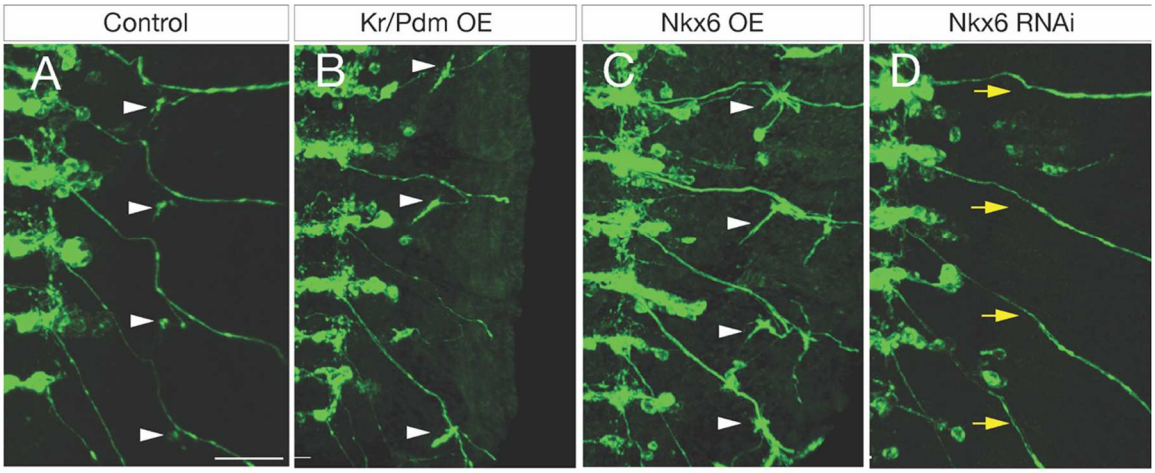

Fig. S8: Nkx6 induces ectopic VO motor neurons targeting ventral oblique muscles.
(A) Control (NB7–1-gal4 UAS-GFP) shows innervation of the ISNd and ventral oblique muscles (arrowhead). (B) Overexpression of Kr and Pdm (NB7–1-gal4 UAS-myr:GFP UAS-Kr UAS-Pdm) lead to increased ISNd innervation (arrowhead). (C) Overexpression of Nkx6 (NB7–1-gal4 UAS-myr:GFP UAS-Nkx6) leads to excessive, broad, and disorganized innervation of ventral oblique muscles (arrowhead). (D) Nkx6 RNAi (NB7–1-gal4 UAS-myr:GFP UAS-Nkx6-RNAi) results in loss of ventral motor projections to ISNd (yellow arrow). Scale bar: 15 μm for all panels.

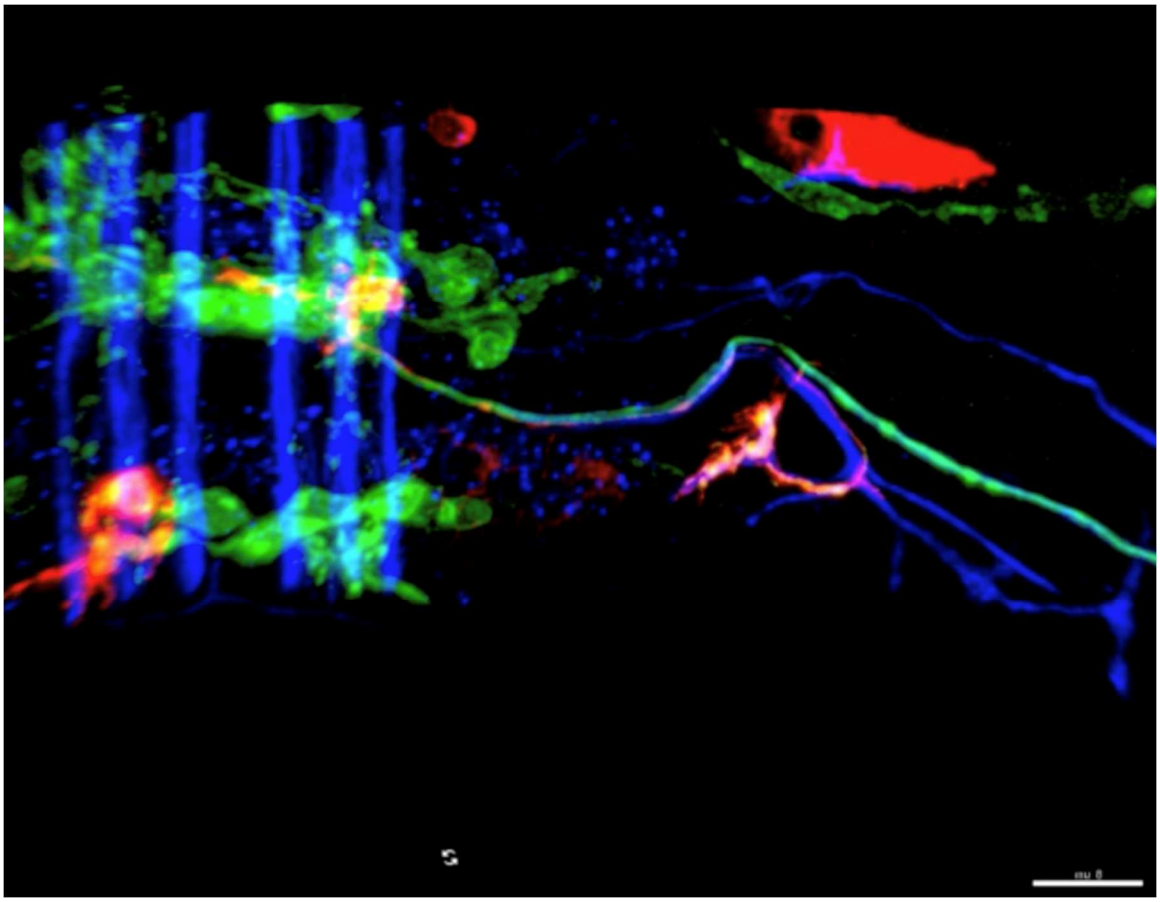

Fig. S9: MCFO labels a single VO motor neuron within the NB7–1 lineage.
(0:00–0:09) One hemisegment of a stage 16 embryo is shown in which the entire NB7–1 lineage is labelled (NB7–1-gal4 UAS-GFP, green), and a single neuron from the lineage is sparsely labelled with an HA tag (red). Viewed together with FasII (blue) labelling nerve bundles, the axon of this morphologically-distinct motor neuron travels through the ISNd nerve route and terminates in a unique NMJ in the region of the ventral oblique muscles. Scale bar: 8 μm. (0:09–0:18) The VO motor neuron (HA, red), shown in relation to FasII (blue) possess a uniquely identifiable dendritic and axonal morphology.

URL: https://static-content.springer.com/esm/art%3A10.1186%2Fs13064-020-00146-6/MediaObjects/13064_2020_146_MOESM4_ESM.mov

REFERENCES CITED

Allan DW, Thor S. Transcriptional selectors, masters, and combinatorial codes: regulatory principles of neural subtype specification. WIREs Dev Biol. 2015;4:505–28.

Allen, Aaron M., Megan C. Neville, Sebastian Birtles, Vincent Croset, Christoph Daniel Treiber, Scott Waddell, and Stephen F. Goodwin. "A Single-Cell Transcriptomic Atlas of the Adult Drosophila Ventral Nerve Cord." *ELife* 9 (April 21, 2020). https://doi.org/10.7554/eLife.54074.

Alsiö JM, Tarchini B, Cayouette M, Livesey FJ. Ikaros promotes early-born neuronal fates in the cerebral cortex. Proc Natl Acad Sci. 2013;110:E716–25.

Anderson SA, Marín O, Horn C, Jennings K, Rubenstein JL. Distinct cortical migrations from the medial and lateral ganglionic eminences. Development. 2001 Feb;128(3):353-63. PMID: 11152634.

Apitz, Holger, and Iris Salecker. "A Region-Specific Neurogenesis Mode Requires Migratory Progenitors in the Drosophila Visual System." *Nature Neuroscience* 18, no. 1 (January 1, 2015): 46–55. https://doi.org/10.1038/NN.3896.

Apitz, Holger, and Iris Salecker. "Spatio-Temporal Relays Control Layer Identity of Direction-Selective Neuron Subtypes in Drosophila." *Nature Communications 2018 9:1* 9, no. 1 (June 12, 2018): 1–16. https://doi.org/10.1038/s41467-018-04592-z.

Averbukh I, Lai S-L, Doe CQ, Barkai N. A repressor-decay timer for robust temporal patterning in embryonic Drosophila neuroblast lineages. eLife. 2018;7:168.

Barsh, G.R., A.J. Isabella, and C.B. Moens. 2017. Vagus Motor Neuron Topographic Map Determined by Parallel Mechanisms of hox5 Expression and Time of Axon Initiation. Current biology : CB. 27:3812-3825.e3813.

Bertet, C., X. Li, T. Erclik, M. Cavey, B. Wells, and C. Desplan. 2014. Temporal patterning of neuroblasts controls Notch-mediated cell survival through regulation of Hid or Reaper. Cell. 158:1173-1186.

B, Egger, Gold KS, and Brand AH. "Notch Regulates the Switch from Symmetric to Asymmetric Neural Stem Cell Division in the Drosophila Optic Lobe." *Development (Cambridge, England)* 137, no. 18 (September 15, 2010): 2981–87. https://doi.org/10.1242/DEV.051250.

Bossing, Torsten, Gerald Udolph, Chris Q. Doe, and Gerhard M. Technau. "The Embryonic Central Nervous System Lineages of Drosophila Melanogaster. I. Neuroblast Lineages Derived from the Ventral Half of the Neuroectoderm." *Developmental Biology* 179, no. 1 (October 10, 1996): 41–64. https://doi.org/10.1006/DBIO.1996.0240.

Briscoe J, Pierani A, Jessell TM, Ericson J. A Homeodomain Protein Code Specifies Progenitor Cell Identity and Neuronal Fate in the Ventral Neural Tube. Cell. 2000;101:435–45.

Broadus, Julie, James B. Skeath, Eric P. Spana, Torsten Bossing, Gerhard Technau, and Chris Q. Doe. "New Neuroblast Markers and the Origin of the ACC/PCC Neurons in the Drosophila Central Nervous System." *Mechanisms of Development* 53, no. 3 (November 1, 1995): 393–402. https://doi.org/10.1016/0925-4773(95)00454-8.

Broihier HT, Kuzin A, Zhu Y, Odenwald W, Skeath JB. Drosophila homeodomain protein Nkx6 coordinates motoneuron subtype identity and axonogenesis. Development. 2004;131:5233–5242.

Cleary MD, Doe CQ. Regulation of neuroblast competence: multiple temporal identity factors specify distinct neuronal fates within a single early competence window. Genes Dev. 2006;20:429–434.

Campos-Ortega, J A. "Mechanisms of Early Neurogenesis in Drosophila Melanogaster." *Journal of Neurobiology* 24, no. 10 (October 1993): 1305–27. https://doi.org/10.1002/neu.480241005.

Chang, F.L., J.G. Steedman, and R.D. Lund. 1986. The lamination and connectivity of embryonic cerebral cortex transplanted into newborn rat cortex. The Journal of comparative neurology. 244:401-411.

Cheesman SE, Layden MJ, Von Ohlen T, Doe CQ, Eisen JS. Zebrafish and fly Nkx6 proteins have similar CNS expression patterns and regulate motoneuron formation. Development. 2004;131:5221–5232.

Cleary, Michael D., and Chris Q. Doe. "Regulation of Neuroblast Competence: Multiple Temporal Identity Factors Specify Distinct Neuronal Fates within a Single Early Competence Window." *Genes & Development* 20, no. 4 (February 15, 2006): 429–34. https://doi.org/10.1101/GAD.1382206.

Contreras, Esteban G., Tomás Palominos, Álvaro Glavic, Andrea H. Brand, Jimena Sierralta, and Carlos Oliva. "The Transcription Factor SoxD Controls Neuronal Guidance in the Drosophila Visual System." *Scientific Reports 2018 8:1* 8, no. 1 (September 6, 2018): 1–12. https://doi.org/10.1038/s41598-018-31654-5.

Cui, X, and C Q Doe. “Ming Is Expressed in Neuroblast Sublineages and Regulates Gene Expression in the Drosophila Central Nervous System.” *Development* 116, no. 4 (December 1, 1992): 943–52. https://doi.org/10.1242/dev.116.4.943.

Delgado RN, Allen DE, Keefe MG, Mancia Leon WR, Ziffra RS, Crouch EE, Alvarez-Buylla A, Nowakowski TJ. Individual human cortical progenitors can produce excitatory and inhibitory neurons. Nature. 2022 Jan;601(7893):397-403. doi: 10.1038/s41586-021-04230-7. Epub 2021 Dec 15. PMID: 34912114.

Delile J, Rayon T, Melchionda M, Edwards A, Briscoe J, Sagner A. Single cell transcriptomics reveals spatial and temporal dynamics of gene expression in the developing mouse spinal cord. Development [Internet]. 2019 [cited 2020 Jan 27];146. Available from: https://dev.biologists.org/content/146/12/dev173807

Doe, Chris Q. “Temporal Patterning in the Drosophila CNS.” *Annual Review of Cell and Developmental Biology* 33, no. June (2017): 219–40. https://doi.org/10.1146/annurev-cellbio-111315-125210.

Doe, C.Q., M.J. Bastiani, and C.S. Goodman. 1986. Guidance of neuronal growth cones in the grasshopper embryo. IV. Temporal delay experiments. The Journal of neuroscience : the official journal of the Society for Neuroscience. 6:3552-3563.

Dolan, M.J., H. Luan, W.C. Shropshire, B. Sutcliffe, B. Cocanougher, R.L. Scott, S. Frechter, M. Zlatic, G. Jefferis, and B.H. White. 2017. Facilitating Neuron-Specific Genetic Manipulations in Drosophila melanogaster Using a Split GAL4 Repressor. Genetics. 206:775-784.

Egger, Boris, Jason Q. Boone, Naomi R. Stevens, Andrea H. Brand, and Chris Q. Doe. “Regulation of Spindle Orientation and Neural Stem Cell Fate in the Drosophila Optic Lobe.” *Neural Development* 2, no. 1 (2007). https://doi.org/10.1186/1749-8104-2-1.

Elliott J, Jolicoeur C, Ramamurthy V, Cayouette M. Ikaros Confers Early Temporal Competence to Mouse Retinal Progenitor Cells. Neuron. 2008;60:26–39.

Enriquez, J., L. Venkatasubramanian, M. Baek, M. Peterson, U. Aghayeva, and R.S. Mann. 2015. Specification of individual adult motor neuron morphologies by combinatorial transcription factor codes. Neuron. 86:955-970.

Erclik, T., X. Li, M. Courgeon, C. Bertet, Z. Chen, R. Baumert, J. Ng, C. Koo, U. Arain, R. Behnia, A. del Valle Rodriguez, L. Senderowicz, N. Negre, K.P. White, and C. Desplan. 2017. Integration of temporal and spatial patterning generates neural diversity. Nature. 541:365-370.

Fradkin, L.G., M. van Schie, R.R. Wouda, A. de Jong, J.T. Kamphorst, M. Radjkoemar-Bansraj, and J.N. Noordermeer. 2004. The Drosophila Wnt5 protein mediates selective axon fasciculation in the embryonic central nervous system. Developmental biology. 272:362-375.

Gerhard, S., I. Andrade, R.D. Fetter, A. Cardona, and C.M. Schneider-Mizell. 2017. Conserved neural circuit structure across Drosophila larval development revealed by comparative connectomics. eLife. 6:e29089.

Grosskortenhaus R, Robinson KJ, Doe CQ. Pdm and Castor specify late-born motor neuron identity in the NB7-1 lineage. Genes Dev. 2006;20:2618–2627.

H, Apitz, and Salecker I. "A Challenge of Numbers and Diversity: Neurogenesis in the Drosophila Optic Lobe." *Journal of Neurogenetics* 28, no. 3–4 (December 1, 2014): 233–49. https://doi.org/10.3109/01677063.2014.922558.

Harris, R., L.M. Sabatelli, and M.A. Seeger. 1996. Guidance cues at the Drosophila CNS midline: identification and characterization of two Drosophila Netrin/UNC-6 homologs. Neuron. 17:217-228.

Hartenstein, V. 1993. Atlas of Drosophila development. Cold Spring HArbor Laboratory Press. 57 pp.

Hartenstein, V., E. Rudloff, and J.A. Campos-Ortega. 1987. The pattern of proliferation of the neuroblasts in the wild-type embryo of Drosophila melanogaster. Roux's archives of developmental biology : the official organ of the EDBO. 196:473-485.

Hartenstein, Volker, Shana Spindler, Wayne Pereanu, and Siaumin Fung. "The Development of the Drosophila Larval Brain." In *Brain Development in Drosophila Melanogaster*, edited by Gerhard M Technau, 1–31. New York, NY: Springer New York, 2008. https://doi.org/10.1007/978-0-387-78261-4_1.

Hartenstein, Volker, Amelia Younossi-Hartenstein, and Arne Lekven. "Delamination and Division in the Drosophila Neurectoderm: Spatiotemporal Pattern, Cytoskeletal Dynamics, and Common Control by Neurogenic and Segment Polarity Genes." *Developmental Biology* 165, no. 2 (October 1, 1994): 480–99. https://doi.org/10.1006/dbio.1994.1269.

Hasegawa, Eri, Masako Kaido, Rie Takayama, and Makoto Sato. "Brain-Specific-Homeobox Is Required for the Specification of Neuronal Types in the Drosophila Optic Lobe." *Developmental Biology* 377, no. 1 (2013): 90–99. https://doi.org/10.1016/j.ydbio.2013.02.012.

Hasegawa, Eri, Yusuke Kitada, Masako Kaido, Rie Takayama, Takeshi Awasaki, Tetsuya Tabata, and Makoto Sato. "Concentric Zones, Cell Migration and Neuronal Circuits in the Drosophila Visual Center." *Development* 138, no. 5 (March 1, 2011): 983–93. https://doi.org/10.1242/DEV.058370.

Hobert, Oliver. “Regulation of Terminal Differentiation Programs in the Nervous System.” *Annual Review of Cell and Developmental Biology* 27, no. 1 (October 10, 2011): 681–96. https://doi.org/10.1146/annurev-cellbio-092910-154226.

Hobert, Oliver. “Terminal Selectors of Neuronal Identity.” *Current Topics in Developmental Biology* 116 (2016): 455–75. https://doi.org/10.1016/bs.ctdb.2015.12.007.

Hofbauer, Alois, and José A Campos-Ortega. “Proliferation Pattern and Early Differentiation of the Optic Lobes in Drosophila Melanogaster.” *Roux’s Archives of Developmental Biology : The Official Organ of the EDBO* 198, no. 5 (February 1990): 264–74. https://doi.org/10.1007/BF00377393.

Holguera I, Desplan C. Neuronal specification in space and time. Science. 2018;362:176–80.

Isshiki, Takako, Bret Pearson, Scott Holbrook, and Chris Q. Doe. “Drosophila Neuroblasts Sequentially Express Transcription Factors Which Specify the Temporal Identity of Their Neuronal Progeny.” *Cell* 106, no. 4 (2001): 511–21. https://doi.org/10.1016/S0092-8674(01)00465-2.

Jankovski, A., F. Rossi, and C. Sotelo. 1996. Neuronal precursors in the postnatal mouse cerebellum are fully committed cells: evidence from heterochronic transplantations. The European journal of neuroscience. 8:2308-2319.

Jefferis, G.S., E.C. Marin, R.F. Stocker, and L. Luo. 2001. Target neuron prespecification in the olfactory map of Drosophila. Nature. 414:204-208.

Kambadur, Ravi, Keita Koizumi, Chad Stivers, James Nagle, Stephen J. Poole, and Ward F. Odenwald. “Regulation of POU Genes by Castor and Hunchback Establishes Layered Compartments in the Drosophila CNS.” *Genes & Development* 12, no. 2 (January 15, 1998): 246. https://doi.org/10.1101/GAD.12.2.246.

Kanai, M.I., M. Okabe, and Y. Hiromi. 2005. seven-up Controls switching of transcription factors that specify temporal identities of Drosophila neuroblasts. Developmental cell. 8:203-213.

Kao, C.F., and T. Lee. 2010. Birth time/order-dependent neuron type specification. Current opinion in neurobiology. 20:14-21.

Kohwi, Minoree, and Chris Q. Doe. “Temporal Fate Specification and Neural Progenitor Competence During Development.” *Nature Reviews. Neuroscience* 14, no. 12 (December 2013): 823. https://doi.org/10.1038/NRN3618.

Kohwi, Minoree, Laurel S Hiebert, and Chris Q Doe. “The Pipsqueak-Domain Proteins Distal Antenna and Distal Antenna-Related Restrict Hunchback Neuroblast Expression and Early-Born Neuronal Identity.” *Development* 138, no. 9 (May 1, 2011): 1727–35. https://doi.org/10.1242/dev.061499.

Kohwi, M., J.R. Lupton, S.L. Lai, M.R. Miller, and C.Q. Doe. 2013. Developmentally regulated subnuclear genome reorganization restricts neural progenitor competence in Drosophila. Cell. 152:97-108.

Konstantinides, Nikolaos, Katarina Kapuralin, Chaimaa Fadil, Luendreo Barboza, Rahul Satija, and Claude Desplan. “Phenotypic Convergence: Distinct Transcription Factors Regulate Common Terminal Features.” *Cell* 174, no. 3 (July 26, 2018): 622-635.e13. https://doi.org/10.1016/j.cell.2018.05.021.

Konstantinides, Nikolaos, Anthony M. Rossi, Aristides Escobar, Liébaut Dudragne, Yen-Chung Chen, Thinh Tran, Azalia Martinez Jaimes, et al. “A Comprehensive Series of Temporal Transcription Factors in the Fly Visual System.” *BioRxiv*, June 14, 2021, 2021.06.13.448242. https://doi.org/10.1101/2021.06.13.448242.

Kulkarni, A., D. Ertekin, C.H. Lee, and T. Hummel. 2016. Birth order dependent growth cone segregation determines synaptic layer identity in the Drosophila visual system. Elife. 5:e13715.

Kurmangaliyev, Yerbol Z., Juyoun Yoo, Samuel A. Locascio, and S. Lawrence Zipursky. “Modular Transcriptional Programs Separately Define Axon and Dendrite Connectivity.” *ELife* 8 (2019): 1–18. https://doi.org/10.7554/eLife.50822.

Lacin, Haluk, and James W. Truman. “Lineage Mapping Identifies Molecular and Architectural Similarities between the Larval and Adult Drosophila Central Nervous System.” *ELife* 5, no. MARCH2016 (March 15, 2016). https://doi.org/10.7554/ELIFE.13399.

Landgraf, M., T. Bossing, G.M. Technau, and M. Bate. 1997. The origin, location, and projections of the embryonic abdominal motorneurons of Drosophila. The Journal of neuroscience : the official journal of the Society for Neuroscience. 17:9642-9655.

Landgraf M, Jeffrey V, Fujioka M, Jaynes JB, Bate M. Embryonic Origins of a Motor System: Motor Dendrites Form a Myotopic Map in Drosophila. PLoS Biol. 2003;1:e1.

Layden MJ, Odden JP, Schmid A, Garces A, Thor S, Doe CQ. Zfh1, a somatic motor neuron transcription factor, regulates axon exit from the CNS. Dev Biol. 2006;291:253–263.

Lee T, Lee A, Luo L. Development of the Drosophila mushroom bodies: sequential generation of three distinct types of neurons from a neuroblast. Development. 1999;126:4065–4076.

Li, X., Z. Chen, and C. Desplan. 2013a. Temporal patterning of neural progenitors in Drosophila. Curr Top Dev Biol. 105:69-96.

Li, Xin, Ted Erclik, Claire Bertet, Zhenqing Chen, Roumen Voutev, Srinidhi Venkatesh, Javier Morante, Arzu Celik, and Claude Desplan. "Temporal Patterning of Drosophila Medulla Neuroblasts Controls Neural Fates." *Nature*, 2013. https://doi.org/10.1038/nature12319.

Lin S, Kao C-F, Yu H-H, Huang Y, Lee T. Lineage analysis of Drosophila lateral antennal lobe neurons reveals notch-dependent binary temporal fate decisions. PLoS Biol. 2012;10:e1001425.

Liu, Z., C.P. Yang, K. Sugino, C.C. Fu, L.Y. Liu, X. Yao, L.P. Lee, and T. Lee. 2015. Opposing intrinsic temporal gradients guide neural stem cell production of varied neuronal fates. Science (New York, N.Y.). 350:317-320.

Mark, Brandon, Sen Lin Lai, Aref Arzan Zarin, Laurina Manning, Heather Q. Pollington, Ashok Litwin-Kumar, Albert Cardona, James W. Truman, and Chris Q. Doe. "A Developmental Framework Linking Neurogenesis and Circuit Formation in the Drosophila Cns." *ELife* 10 (May 1, 2021). https://doi.org/10.7554/ELIFE.67510.

Mason, C.A. 1983. Postnatal maturation of neurons in the cat's lateral geniculate nucleus. The Journal of comparative neurology. 217:458-469.

Mattar P, Ericson J, Blackshaw S, Cayouette M. A Conserved Regulatory Logic Controls Temporal Identity in Mouse Neural Progenitors. Neuron. 2015;85:497–504.

Mattar P, Jolicoeur C, Shah S, Cayouette M. A Casz1 - NuRD complex regulates temporal identity transitions in neural progenitors. bioRxiv. 2020;2020.02.11.944470.

Mauss, A., M. Tripodi, J.F. Evers, and M. Landgraf. 2009. Midline signalling systems direct the formation of a neural map by dendritic targeting in the Drosophila motor system. PLoS Biol. 7:e1000200.

Meissner GW, Grimm JB, Johnston RM, Sutcliffe B, Ng J, Jefferis GSXE, et al. Optimization of fluorophores for chemical tagging and immunohistochemistry of Drosophila neurons. PLOS ONE. 2018;13:e0200759.

McConnell, S.K. 1988. Fates of visual cortical neurons in the ferret after isochronic and heterochronic transplantation. The Journal of neuroscience : the official journal of the Society for Neuroscience. 8:945-974.

Meng, Julia L., Zarion D. Marshall, Meike Lobb-Rabe, and Ellie S. Heckscher. "How Prolonged Expression of Hunchback, a Temporal Transcription Factor, Re-Wires Locomotor Circuits." *ELife* 8 (2019): 1–30. https://doi.org/10.7554/eLife.46089.

Meng, Julia L., Yupu Wang, Robert A. Carrillo, and Ellie S. Heckscher. “Temporal Transcription Factors Determine Circuit Membership by Permanently Altering Motor Neuron-to-Muscle Synaptic Partnerships.” *ELife* 9 (May 1, 2020): 1–23. https://doi.org/10.7554/ELIFE.56898.

Mitchell, K.J., J.L. Doyle, T. Serafini, T.E. Kennedy, M. Tessier-Lavigne, C.S. Goodman, and B.J. Dickson. 1996. Genetic analysis of Netrin genes in Drosophila: Netrins guide CNS commissural axons and peripheral motor axons. Neuron. 17:203-215.

Miyares RL, Lee T. Temporal control of Drosophila central nervous system development. Curr Opin Neurobiol. 2019;56:24–32.Morante, Javier, and Claude Desplan. “The Color Vision Circuit in the Medulla of Drosophila.” *Current Biology : CB* 18, no. 8 (April 22, 2008): 553. https://doi.org/10.1016/J.CUB.2008.02.075.

Morante, Javier, Ted Erclik, and Claude Desplan. “Cell Migration in Drosophila Optic Lobe Neurons Is Controlled by Eyeless/Pax6.” *Journal of Cell Science* 124 (February 15, 2011): e1–e1. https://doi.org/10.1242/jcs.086975.

Monastirioti M, Giagtzoglou N, Koumbanakis KA, Zacharioudaki E, Deligiannaki M, Wech I, et al. Drosophila Hey is a target of Notch in asymmetric divisions during embryonic and larval neurogenesis. Development. Oxford University Press for The Company of Biologists Limited; 2010;137:191–201.

Mora, Oliva C, Fiers M, Ejsmont R, Soldano A, Zhang TT, Yan J, Claeys A, De Geest N, and Hassan BA. “A Temporal Transcriptional Switch Governs Stem Cell Division, Neuronal Numbers, and Maintenance of Differentiation.” *Developmental Cell* 45, no. 1 (April 9, 2018): 53-66.e5. https://doi.org/10.1016/J.DEVCEL.2018.02.023.

Moris-Sanz, M., A. Estacio-Gomez, E. Sanchez-Herrero, and F.J. Diaz-Benjumea. 2015. The study of the Bithorax-complex genes in patterning CCAP neurons reveals a temporal control of neuronal differentiation by Abd-B. Biol Open. 4:1132-1142.

Mumm, J.S., P.R. Williams, L. Godinho, A. Koerber, A.J. Pittman, T. Roeser, C.B. Chien, H. Baier, and R.O. Wong. 2006. In vivo imaging reveals dendritic targeting of laminated afferents by zebrafish retinal ganglion cells. Neuron. 52:609-621.

Naidu, Vamsikrishna G., Yu Zhang, Scott Lowe, Alokananda Ray, Hailun Zhu, and Xin Li. “Temporal Progression of Drosophila Medulla Neuroblasts Generates the Transcription Factor Combination to Control T1 Neuron Morphogenesis.” *Developmental Biology* 464, no. 1 (August 1, 2020): 35–44. https://doi.org/10.1016/J.YDBIO.2020.05.005.

Nériec, Nathalie, and Claude Desplan. “From The Eye To The Brain: Development Of The Drosophila Visual System.” *Current Topics in Developmental Biology* 116 (2016): 247. https://doi.org/10.1016/BS.CTDB.2015.11.032.

Nern, A., B.D. Pfeiffer, and G.M. Rubin. 2015. Optimized tools for multicolor stochastic labeling reveal diverse stereotyped cell arrangements in the fly visual system. Proceedings of the National Academy of Sciences of the United States of America. 112:E2967-2976.

Ngo, Kathy T., Jay Wang, Markus Junker, Steve Kriz, Gloria Vo, Bobby Asem, John M. Olson, Utpal Banerjee, and Volker Hartenstein. "Concomitant Requirement for Notch and Jak/Stat Signaling during Neuro-Epithelial Differentiation in the Drosophila Optic Lobe." *Developmental Biology* 346, no. 2 (October 15, 2010): 284–95. https://doi.org/10.1016/J.YDBIO.2010.07.036.

Novotny, Tanja, Regina Eiselt, and Joachim Urban. "Hunchback Is Required for the Specification of the Early Sublineage of Neuroblast 7-3 in the Drosophila Central Nervous System." *Development* 129, no. 4 (February 15, 2002): 1027–36. https://doi.org/10.1242/dev.129.4.1027.

Ohyama, T., C.M. Schneider-Mizell, R.D. Fetter, J.V. Aleman, R. Franconville, M. Rivera-Alba, B.D. Mensh, K.M. Branson, J.H. Simpson, J.W. Truman, A. Cardona, and M. Zlatic. 2015. A multilevel multimodal circuit enhances action selection in Drosophila. Nature. 520:633-639.

O'Leary, D.D., and B.B. Stanfield. 1989. Selective elimination of axons extended by developing cortical neurons is dependent on regional locale: experiments utilizing fetal cortical transplants. The Journal of neuroscience : the official journal of the Society for Neuroscience. 9:2230-2246.

Oliva, Carlos, Ching-Man Choi, Laura J J Nicolai, Natalia Mora, Natalie De Geest, and Bassem A Hassan. "Proper Connectivity of Drosophila Motion Detector Neurons Requires Atonal Function in Progenitor Cells." *Neural Development 2014 9:1* 9, no. 1 (February 26, 2014): 1–8. https://doi.org/10.1186/1749-8104-9-4.

Olsson-Carter, K., and F.J. Slack. 2010. A developmental timing switch promotes axon outgrowth independent of known guidance receptors. PLoS Genet. 6:pii: e1001054.

Özel, Mehmet Neset, Félix Simon, Shadi Jafari, Isabel Holguera, Yen Chung Chen, Najate Benhra, Rana Naja El-Danaf, et al. "Neuronal Diversity and Convergence in a Visual System Developmental Atlas." *Nature* 589, no. 7840 (January 7, 2021): 88–95. https://doi.org/10.1038/S41586-020-2879-3.

Pearson, Bret J., and Chris Q. Doe. "Regulation of Neuroblast Competence in Drosophila." *Nature 2003 425:6958* 425, no. 6958 (October 9, 2003): 624–28. https://doi.org/10.1038/nature01910.

Pearson, Bret J., and Chris Q. Doe. "Specification of Temporal Identity in the Developing Nervous System." *Annual Review of Cell and Developmental Biology* 20, no. 1 (2004): 619–47. https://doi.org/10.1146/annurev.cellbio.19.111301.115142.

Peters, A., and M.L. Feldman. 1976. The projection of the lateral geniculate nucleus to area 17 of the rat cerebral cortex. I. General description. Journal of neurocytology. 5:63-84.

Petrovic, M., and T. Hummel. 2008. Temporal identity in axonal target layer recognition. Nature. 456:800-803.

Pfeiffer, B.D., A. Jenett, A.S. Hammonds, T.T. Ngo, S. Misra, C. Murphy, A. Scully, J.W. Carlson, K.H. Wan, T.R. Laverty, C. Mungall, R. Svirskas, J.T. Kadonaga, C.Q. Doe, M.B. Eisen, S.E. Celniker, and G.M. Rubin. 2008. Tools for neuroanatomy and neurogenetics in Drosophila. Proceedings of the National Academy of Sciences of the United States of America. 105:9715-9720.

Ramon y Cajal, S. 1909. Histology of the Nervous System of Man and Vertebrates. Maloine, Paris, France.

Rees, C.L., K. Moradi, and G.A. Ascoli. 2017. Weighing the Evidence in Peters' Rule: Does Neuronal Morphology Predict Connectivity? Trends in neurosciences. 40:63-71.

Ren, Q., C.P. Yang, Z. Liu, K. Sugino, K. Mok, Y. He, M. Ito, A. Nern, H. Otsuna, and T. Lee. 2017. Stem Cell-Intrinsic, Seven-up-Triggered Temporal Factor Gradients Diversify Intermediate Neural Progenitors. Current biology : CB. 27:1303-1313.

Rossi, A.M., V.M. Fernandes, and C. Desplan. 2016. Timing temporal transitions during brain development. Current opinion in neurobiology. 42:84-92.

Rothberg, J.M., D.A. Hartley, Z. Walther, and S. Artavanis-Tsakonas. 1988. slit: an EGF-homologous locus of D. melanogaster involved in the development of the embryonic central nervous system. Cell. 55:1047-1059.

Sagner A, Briscoe J. Establishing neuronal diversity in the spinal cord: a time and a place. Development [Internet]. 2019 [cited 2020 Jan 27];146. Available from: https://dev.biologists.org/content/146/22/dev182154

Sanchez-Soriano, N., and A. Prokop. 2005. The influence of pioneer neurons on a growing motor nerve in Drosophila requires the neural cell adhesion molecule homolog FasciclinII. The Journal of neuroscience : the official journal of the Society for Neuroscience. 25:78-87.

Sander M, Paydar S, Ericson J, Briscoe J, Berber E, German M, et al. Ventral neural patterning by Nkx homeobox genes: Nkx6.1 controls somatic motor neuron and ventral interneuron fates. Genes Dev. 2000;14:2134–9.

Satija R. Integrative single-cell analysis. Nat Rev Genet. 2019;20:257–72.

Schilling, Tabea, Aicha H. Ali, Aljoscha Leonhardt, Alexander Borst, and Jesús Pujol-Martí. “Transcriptional Control of Morphological Properties of Direction-Selective T4/T5 Neurons in Drosophila.” *Development (Cambridge)* 146, no. 2 (2019). https://doi.org/10.1242/dev.169763.

Schlaggar, B.L., and D.D. O'Leary. 1991. Potential of visual cortex to develop an array of functional units unique to somatosensory cortex. Science (New York, N.Y.). 252:1556-1560.

Schmid, Aloisia, Akira Chiba, and Chris Q. Doe. "Clonal Analysis of Drosophila Embryonic Neuroblasts: Neural Cell Types, Axon Projections and Muscle Targets." *Development* 126, no. 21 (November 1, 1999): 4653–89. https://doi.org/10.1242/DEV.126.21.4653.

Schmidt, Hartmut, Christof Rickert, Torsten Bossing, Olaf Vef, Joachim Urban, and Gerhard M. Technau. "The Embryonic Central Nervous System Lineages OfDrosophila Melanogaster." *Developmental Biology* 189, no. 2 (September 15, 1997): 186–204. https://doi.org/10.1006/DBIO.1997.8660.

Sen, Sonia Q., Sachin Chanchani, Tony D. Southall, and Chris Q. Doe. "Neuroblast-Specific Open Chromatin Allows the Temporal Transcription Factor, Hunchback, to Bind Neuroblast-Specific Loci." *ELife* 8 (2019): 1–26. https://doi.org/10.7554/eLife.44036.

Seroka, Austin Q., and Chris Q. Doe. "The Hunchback Temporal Transcription Factor Determines Motor Neuron Axon and Dendrite Targeting in Drosophila." *Development (Cambridge)* 146, no. 7 (2019): 1–11. https://doi.org/10.1242/dev.175570.

Seroka, Austin, Rita M. Yazejian, Sen Lin Lai, and Chris Q. Doe. "A Novel Temporal Identity Window Generates Alternating Cardinal Motor Neuron Subtypes in a Single Progenitor Lineage." *BioRxiv*, January 1, 2020, 2020.02.12.946442. https://doi.org/10.1101/2020.02.12.946442.

Skeath JB, Doe CQ. Sanpodo and Notch act in opposition to Numb to distinguish sibling neuron fates in the Drosophila CNS. Development. 1998;125:1857–1865.

Skeath, James B., and Stefan Thor. "Genetic Control of Drosophila Nerve Cord Development." *Current Opinion in Neurobiology* 13, no. 1 (February 1, 2003): 8–15. https://doi.org/10.1016/S0959-4388(03)00007-2.

Sockanathan S, Jessell TM. Motor Neuron–Derived Retinoid Signaling Specifies the Subtype Identity of Spinal Motor Neurons. Cell. 1998;94:503–14.

Sullivan, Luis F., Timothy L. Warren, and Chris Q. Doe. "Temporal Identity Establishes Columnar Neuron Morphology, Connectivity, and Function in a Drosophila Navigation Circuit." *ELife* 8 (2019): 1–24. https://doi.org/10.7554/eLife.43482.

Stam FJ, Hendricks TJ, Zhang J, Geiman EJ, Francius C, Labosky PA, et al. Renshaw cell interneuron specialization is controlled by a temporally restricted transcription factor program. Development. 2011;139:179–190.

Stanfield, B.B., and D.D. O'Leary. 1985. Fetal occipital cortical neurones transplanted to the rostral cortex can extend and maintain a pyramidal tract axon. Nature. 313:135-137.

Stepanyants, A., and D.B. Chklovskii. 2005. Neurogeometry and potential synaptic connectivity. Trends in neurosciences. 28:387-394.

Sullivan, L.F., T.L. Warren, and C.Q. Doe. 2019. Temporal identity establishes columnar neuron morphology, connectivity, and function in a Drosophila navigation circuit. Elife. 8.

Suzuki, Kaido M, Takayama R, and Sato M. "A Temporal Mechanism That Produces Neuronal Diversity in the Drosophila Visual Center." *Developmental Biology* 380, no. 1 (August 1, 2013): 12–24. https://doi.org/10.1016/J.YDBIO.2013.05.002.

Syed, M.H., B. Mark, and C.Q. Doe. 2017. Steroid hormone induction of temporal gene expression in Drosophila brain neuroblasts generates neuronal and glial diversity. Elife. 6:eLife.26287.

Tran, K.D., and C.Q. Doe. 2008. Pdm and Castor close successive temporal identity windows in the NB3-1 lineage. Development (Cambridge, England). 135:3491-3499.

Tran, K.D., M.R. Miller, and C.Q. Doe. 2010. Recombineering Hunchback identifies two conserved domains required to maintain neuroblast competence and specify early-born neuronal identity. Development (Cambridge, England). 137:1421-1430.

Ulvklo C, MacDonald R, Bivik C, Baumgardt M, Karlsson D, Thor S. Control of neuronal cell fate and number by integration of distinct daughter cell proliferation modes with temporal progression. Development. 2012;139:678–89.

Wreden, Christopher C., Julia L. Meng, Weidong Feng, Wanhao Chi, Zarion D. Marshall, and Ellie S. Heckscher. "Temporal Cohorts of Lineage-Related Neurons Perform Analogous Functions in Distinct Sensorimotor Circuits." *Current Biology* 27, no. 10 (2017): 1521-1528.e4. https://doi.org/10.1016/j.cub.2017.04.024.

Wu, Z., L.B. Sweeney, J.C. Ayoob, K. Chak, B.J. Andreone, T. Ohyama, R. Kerr, L. Luo, M. Zlatic, and A.L. Kolodkin. 2011. A combinatorial semaphorin code instructs the initial steps of sensory circuit assembly in the Drosophila CNS. Neuron. 70:281-298.

Yasugi, Tetsuo, Daiki Umetsu, Satoshi Murakami, Makoto Sato, and Tetsuya Tabata. "Drosophila Optic Lobe Neuroblasts Triggered by a Wave of Proneural Gene Expression That Is Negatively Regulated by JAK/STAT." *Development* 135, no. 8 (April 15, 2008): 1471–80. https://doi.org/10.1242/DEV.019117.

Yoshikawa, S., H. Long, and J.B. Thomas. 2016. A subset of interneurons required for Drosophila larval locomotion. Mol Cell Neurosci. 70:22-29.

Yoshikawa, S., R.D. McKinnon, M. Kokel, and J.B. Thomas. 2003. Wnt-mediated axon guidance via the Drosophila Derailed receptor. Nature. 422:583-588.

Zarin AA, Mark B, Cardona A, Litwin-Kumar A, Doe CQ. A multilayer circuit architecture for the generation of distinct locomotor behaviors in Drosophila. Scott K, editor. eLife. 2019;8:e51781.

Zhu, S., S. Lin, C.F. Kao, T. Awasaki, A.S. Chiang, and T. Lee. 2006. Gradients of the Drosophila Chinmo BTB-zinc finger protein govern neuronal temporal identity. Cell. 127:409-422.

Zlatic, M., M. Landgraf, and M. Bate. 2003. Genetic specification of axonal arbors: atonal regulates robo3 to position terminal branches in the Drosophila nervous system. Neuron. 37:41-51.

Zlatic, M., F. Li, M. Strigini, W. Grueber, and M. Bate. 2009. Positional cues in the Drosophila nerve cord: semaphorins pattern the dorso-ventral axis. PLoS Biol. 7:e1000135.